Fermilab FERMILAB-Pub-03/186-A July 2003

arXiv:astro-ph/0305202 v1 12 May 2003

Version 7.0, Last modified 05-May-2003

A MERGED CATALOG OF CLUSTERS OF GALAXIES FROM EARLY SDSS DATA

Neta A. Bahcall[1], Timothy A. McKay[2], James Annis[3], Rita S.J. Kim[4], Feng Dong[1], Sarah Hansen[2], Tomo Goto[5], James E. Gunn[1], Chris Miller[5], R. C. Nichol[5], Marc Postman[6], Don Schneider[7], Josh Schroeder[1], Wolfgang Voges[8], Jon Brinkmann[9], Masataka Fukugita[10]

ABSTRACT

We present a catalog of 799 clusters of galaxies in the redshift range z_{est} = 0.05 - 0.3 selected from ∼400 deg^2 of early SDSS commissioning data along the celestial equator. The catalog is based on merging two independent selection methods – a color-magnitude red-sequence maxBCG technique (B), and a Hybrid Matched-Filter method (H). The BH catalog includes clusters with richness $\Lambda \geq$ 40 (Matched-Filter) and $N_{gal} \geq$ 13 (maxBCG), corresponding to typical velocity dispersion of $\sigma_v \gtrsim$ 400 km s^{-1} and mass (within 0.6 h^{-1} Mpc radius) $\gtrsim 5 \times 10^{13}\ h^{-1}$ M$_\odot$. This threshold is below Abell richness class 0 clusters. The average space density of these clusters is $2 \times 10^{-5}\ h^3$ Mpc^{-3}. All NORAS X-ray clusters and 53 of the 58 Abell clusters in the survey region are detected in the catalog; the 5 additional Abell clusters are detected below the BH catalog cuts. The cluster richness

[1]Princeton University Observatory, Princeton, NJ 08544

[2]University of Michigan, Department of Physics, 500 East University, Ann Arbor, MI 48109

[3]Fermi National Accelerator Laboratory, P.O. Box 500, Batavia, IL 60510

[4]Department of Physics and Astronomy, The Johns Hopkins University, Baltimore, MD 21218

[5]Dept. of Physics, Carnegie Mellon University, 5000 Forbes Ave., Pittsburgh, PA-15232

[6]Space Telescope Science Institute, Baltimore, MD 21218

[7]Department of Astronomy and Astrophysics, The Pennsylvania State University, University Park, PA 16802

[8]Max-Planck-Institut für Extraterrestrische Physik, D-85740 Garching, Germany

[9]Apache Point Observatory, 2001 Apache Point Road, P.O. Box 59, Sunspot, NM 88349-0059

[10]Institute for Cosmic Ray Research, University of Tokyo, Midori, Tanashi, Tokyo 188-8502, Japan

function is determined and found to exhibit a steeply decreasing cluster abundance with increasing richness. We derive observational scaling relations between cluster richness and observed cluster luminosity and cluster velocity dispersion; these scaling relations provide important physical calibrations for the clusters. The catalog can be used for studies of individual clusters, for comparisons with other sources such as X-ray clusters and AGNs, and, with proper correction for the relevant selection functions, also for statistical analyses of clusters.

Subject headings: galaxies:clusters:general–large-scale structure of universe–cosmology:observations–cosmology:theory

1. Introduction

Clusters of galaxies, the largest virialized systems known, provide one of the most powerful tools in studying the structure and evolution of the Universe. Clusters highlight the large scale structure of the universe (Abell 1958; Bahcall & Soneira 1983, 1984; Klypin & Kopylov 1983; Bahcall 1988; Huchra, Geller, Henry, & Postman 1990; Postman, Huchra, & Geller 1992; Croft et al. 1997); they trace the evolution of structure with time (Henry et al. 1992; Eke, Cole, & Frenk 1996; Bahcall, Fan, & Cen 1997; Carlberg et al. 1997; Bahcall & Fan 1998; Donahue & Voit 1999; Henry 2000; Rosati, Borgani, & Norman 2002); they constrain the amount and distribution of dark and baryonic matter (Zwicky 1957; Abell 1958; Bahcall 1977; White, Navarro, Evrard, & Frenk 1993; Bahcall, Lubin, & Dorman 1995; Fischer & Tyson 1997; Carlberg et al. 1997; Carlstrom et al. 2001); they reveal important clues about the formation and evolution of galaxies (Dressler 1984; Gunn & Dressler 1988); and they place critical constraints on cosmology (Bahcall & Cen 1992; White, Efstathiou, & Frenk 1993; Eke, Cole, & Frenk 1996; Carlberg et al. 1997; Bahcall & Fan 1998; Bahcall, Ostriker, Perlmutter, & Steinhardt 1999). In fact, clusters of galaxies place some of the most powerful constraints on cosmological parameters such as the mass density of the Universe and the amplitude of mass fluctuations. In spite of their great value and their tremendous impact on understanding the Universe, systematic studies of clusters of galaxies are currently limited by the lack of large area, accurate, complete, and objectively selected catalogs of optical clusters, and by the limited photometric and redshift information for those that do exist.

The first comprehensive catalog of clusters of galaxies ever produced, the Abell Catalog of Rich Clusters (Abell 1958; Abell, Corwin, & Olowin 1989), was a pioneering project that provided a seminal contribution to the study of extragalactic astronomy and to the field of clusters of galaxies. While galaxy clustering had been recognized before Abell, the data were fragmentary and not well understood. Both Abell's catalog, as well as Zwicky's

(Zwicky, Herzog, & Wild 1968) independent catalog, were obtained by visual inspection of the Palomar Observatory Sky Survey plates. These catalogs have served the astronomical community for nearly half a century and were the basis for many of the important advances in cluster science (see references above; also Abell's Centennial paper, Bahcall 1999). At the beginning of the new century, the need for a new comprehensive catalog of optical clusters – one that is automated, precise, and objectively selected, with redshifts that extend beyond the $z \lesssim 0.2$ limit of the Abell catalog – has become apparent.

There have been recent advances in this direction, including large area catalogs selected by objective algorithms from digitized photographic plates (Shectman 1985 for the Lick Catalog; Lumsden, Nichol, Collins, & Guzzo 1992 for the EDCC Catalog; Dalton, Efstathiou, Maddox, & Sutherland 1994 and Croft et al. 1997 for the APM catalog), as well as small area, deep digital surveys of distant clusters (e.g., the 5 deg^2 Palomar Distant Cluster Survey, Postman et al. 1996; 100 deg^2 Red-Sequence Cluster Survey, Gladders & Yee 2000; and 16 deg^2 KPNO Deeprange Survey, Postman et al. 2002). A particularly important advance for optical surveys has been the inclusion of accurate CCD-based color information for galaxy selection. The inclusion of color in cluster selection greatly reduces the problems of density projection which have long plagued optical selection of clusters. Good examples of color-based optical selection include the 100 deg^2 Red-Sequence Cluster Survey (Gladders & Yee 2000) and the SDSS selection described in this work.

Surveys of X-ray clusters and observations of the Sunyaev-Zeldovich effect in clusters have and will continue to provide important data that is complementary to the optical observations of clusters of galaxies. These methods identify rich systems that have developed an extensive hot intracluster medium. While excellent for selection of massive, well developed clusters, these methods have thresholds which are sensitive to the evolution of the hot intracluster medium, both with cosmic time and with the richness of the objects. In this sense, optical selection has the important complementary advantage of being able to identify galaxy clustering across a wide range of system richness and time evolution.

The Sloan Digital Sky Survey (SDSS; York et al. 2000) will provide a comprehensive digital imaging survey of 10^4 deg^2 of the North Galactic Cap (and a smaller, deeper area in the South) in five bands (u, g, r, i, z), followed by a spectroscopic multi-fiber survey of the brightest one million galaxies (§2). With high photometric precession in 5 colors and a large area coverage (comparable to the Abell catalog), the SDSS survey will enable state-of-the-art cluster selection using automated cluster selection methods. Nearby clusters (to $z \lesssim 0.05$ - 0.1) can be selected directly in 3-dimensions using redshifts from the spectroscopic survey. The imaging survey will enable cluster selection to $z \sim 0.5$ and beyond using the 5 color bands of the survey. In the range $z \sim 0.05$ - 0.3, the 2D cluster selection algorithms

work well, with only small effects due to selection function (for the richest clusters). In the nearest part of this range, z$\sim$0.05 - 0.15, the SDSS spectroscopic data can also be useful for cluster confirmation and for redshift determination. Even poor clusters can be detected with high efficiency in this redshift range. For z$\sim$0.3 - 0.5, 2D selection works well, but selection function effects become important, especially for poorer clusters.

Several cluster selection algorithms have recently been applied to $\sim$400 deg^2 of early SDSS imaging commissioning data in a test of various 2D cluster selection techniques. These methods, outlined in §2, include the Matched-Filter method (Postman et al. 1996; Kepner et al. 1999; Kim et al. 2002), and the red-sequence color-magnitude method, maxBCG (Annis et al. 2003a), as well as a Cut and Enhance method (Goto et al. 2002) and a multicolor technique (C4; Miller et al. 2003). Each method can identify clusters of galaxies in SDSS data to z$\sim$0.5, with richness thresholds that range from small groups to rich clusters, and with different selection functions. Since each algorithm uses different selection criteria that emphasize different aspects of clusters, the lists of clusters found by different techniques will not be identical.

In this paper we present a catalog of 799 clusters of galaxies in the redshift range z = 0.05 - 0.3 from 379 deg^2 of SDSS imaging data. The catalog was constructed by merging lists of clusters found by two independent 2D cluster selection methods: Hybrid Matched Filter and maxBCG. We compare the results from the two techniques and investigate the nature of clusters they select. We derive scaling relations between cluster richness and observed cluster luminosity and cluster velocity dispersion. We use the scaling relations to combine appropriate subsamples of these lists to produce a conservative merged catalog; the catalog is limited to a richness threshold specified in §5; the threshold corresponds to clusters with a typical velocity dispersion of $\sigma_v \gtrsim 400$ km s^{-1}. The average space density of the clusters is $\sim 2 \times 10^{-5} h^3$ Mpc^{-3}. A flat LCDM cosmology with Ω_m= 0.3 and a Hubble constant of $H_0 = 100\ h$ km s^{-1} Mpc^{-1} with $h = 1$ is used throughout. The current work represents preliminary tests of selection algorithms on early SDSS commissioning data. The results will improve as more extensive SDSS data become available.

2. Cluster Selection from SDSS Commissioning Data

The SDSS imaging survey is carried out in drift-scan mode in five filters, u, g, r, i, z, to a limiting magnitude of r <23 (Fukugita et al. 1996; Gunn et al. 1998; Lupton et al. 2001; Hogg et al. 2001). The spectroscopic survey will target nearly one million galaxies to approximately r <17.7, with a median redshift of z$\sim$0.1 (Strauss, et al. 2002), and a small, deeper sample of $\sim 10^5$ Luminous Red Galaxies to r $\sim$19 and z$\sim$0.5 (Eisenstein, et al. 2001).

For more details of the SDSS survey see York et al. (2000), Blanton et al. (2002), Pier et al. (2002), Smith et al. (2002) and Stoughton et al. (2002).

Cluster selection was performed on 379 deg^2 of SDSS commissioning data, covering the area $\alpha(2000)$ = 355° to 56°, $\delta(2000)$ = -1.25° to 1.25°; and $\alpha(2000)$ = 145.3° to 236.0°, $\delta(2000)$= -1.25° to 1.25° (runs 94/125 and 752/756). The limiting magnitude of galaxies used in the cluster selection algorithms was conservatively selected to be r <21 (where r is the SDSS Petrosian magnitude). At this magnitude limit, star-galaxy separation is excellent (Scranton et al. 2002). The clusters of galaxies studied in this paper were selected from these imaging data using a Matched Filter method (Kim et al. 2002, 2003) and an independent color-magnitude maximum-likelihood Brightest Cluster Galaxy method (maxBCG; Annis et al. 2003a). These methods are briefly described below.

The Matched Filter method HMF (Hybrid Matched Filter; Kim et al. 2002) is a Hybrid of the Matched Filter (Postman et al. 1996) and the Adaptive Matched Filter techniques (Kepner et al. 1999). This method identifies clusters in imaging data by finding peaks in a cluster likelihood map generated by convolving the galaxy survey with a filter based on a model of the cluster and field galaxy distributions. The cluster filter is composed of a projected density profile model for the galaxy distribution (a Plummer law profile is used here), and a luminosity function filter (Schechter function). The filters use the typical parameters observed for galaxy clusters (e.g., core radius R_c = 0.1 h^{-1} Mpc, cutoff radius R_{max}=1 h^{-1} Mpc, and luminosity function parameters $M_r^* = -20.93$ and $\alpha = -1.1$ for h = 1). The HMF method identifies the highest likelihood clusters in the imaging data (r-band) and determines their estimated redshift (z_{est}) and richness (Λ); the richness Λ is derived from the best-fit cluster model that satisfies $L_{cl}(< 1\ h^{-1}$ Mpc) = ΛL^*, where L_{cl} is the total cluster luminosity within 1 h^{-1} Mpc radius (at z_{est}), and $L^* \sim 10^{10} h^{-2} L_\odot$. A relatively high threshold has been applied to the cluster selection (σ >5.2, Kim et al. 2002); the selected clusters have richnesses $\Lambda \gtrsim$ 20 - 30 (i.e., $L_{cl}(< 1h^{-1}$ Mpc) $\gtrsim 2 \times 10^{11} h^{-2} L_\odot$). This threshold is below the typical Abell richness class 0.

The maxBCG method (Annis et al. 2003a) is based on the fact that the brightest cluster galaxy (BCG) generally lies in a narrowly defined space in luminosity and color (see, e.g, Hoessel & Schneider 1985; Gladders & Yee 2000). For each SDSS galaxy, a "BCG likelihood" is calculated based on the galaxy color ($g - r$ and $r - i$) and magnitude (M_i, in i-band). The BCG likelihood is then weighted by the number of nearby galaxies located within the color-magnitude region of the appropriate E/S0 ridgeline; this count includes all galaxies within 1 h^{-1} Mpc projected separation that are fainter than M_i and brighter than the magnitude limit M_i(lim) = -20.25, and are located within 2-σ of the mean observed color scatter around the E/S0 ridgeline (i.e., $\pm^{0.1^m}_{0.15^m}$). The combined likelihood is used for

cluster identification. The likelihood is calculated for every redshift from z = 0 to 0.5, at 0.01 intervals; the redshift that maximizes the cluster likelihood is adopted as the cluster redshift. Since BCG and elliptical galaxies in the red ridgeline possess very specific colors and luminosities, their observed magnitude and colors provide excellent photometric redshift estimates for the parent clusters. The richness estimator, N_{gal}, is defined as the number of red E/S0 ridgeline galaxies (within the 2-σ color scatter as discussed above) that are brighter than M_i(lim) = -20.25 (i.e., 1 mag fainter than L^* in the i-band; $h = 1$), and are located within a 1 h^{-1} Mpc projected radius of the BCG.

The HMF and maxBCG methods focus on different properties of galaxy clusters: HMF finds clusters with approximately Plummer density profiles and a Schechter luminosity function, while maxBCG selects groups and clusters dominated by red $\sim L^*$ galaxies. We compare the results of these cluster selection algorithms in the following sections and merge the clusters into a single complementary self-consistent catalog.

3. Comparison of the HMF and maxBCG Clusters

When comparing different catalogs, uncertainties in cluster estimated redshift, position, richness, and selection function, in addition to the different nature of each cluster selection algorithm, render the comparisons difficult. Even selecting the richest clusters from each catalog will not provide a perfect match, mostly due to the noisy estimate of richness and its sharp threshold. In this section we briefly summarize the main comparisons of the cluster redshift, position, and richness estimators for the HMF and maxBCG methods.

The accuracy of cluster redshift estimates for each method was determined using comparisons with measured redshifts from the SDSS spectroscopic data. A comparison of the estimated and spectroscopic redshifts for HMF and maxBCG clusters with z_{est} = 0.05 - 0.3 and richnesses $\Lambda \geq 40$ (HMF) and $N_{gal} \geq 13$ (maxBCG) is shown in Figures 1 and 2. A spectroscopic match is considered if the spectroscopic galaxy is located at the position of the BCG. For these relatively high richness clusters we find a redshift uncertainty of $\sigma_z = 0.014$ for maxBCG (from 382 cluster matches) and $\sigma_z = 0.033$ for HMF (from 237 cluster matches; there are fewer HMF matches since a spectroscopic match is defined at the BCG position so as to minimize noise). A direct comparison between the HMF and maxBCG estimated cluster redshifts, using a positional matching criterion defined below, is shown in Figure 3.

The positional accuracy of cluster centers is determined by comparing HMF-maxBCG cluster pairs (in the above z = 0.05 - 0.3 sample) with pairs in random catalogs. The comparison shows significant excess of cluster matches over random for projected cluster

separations of $\lesssim 0.5\ h^{-1}$ Mpc, with a tail to $\sim 1\ h^{-1}$ Mpc (Figure 4). These excess pairs represent real cluster matches; their distribution provides a measure of the typical offset between the cluster centers determined in the two methods. The offsets follow a Gaussian distribution with a dispersion of $0.175\ h^{-1}$ Mpc (Figure 4).

Comparison of clusters identified by different selection methods depends not only on the positional and redshift uncertainties discussed above, and on the different selection function inherent to each catalog, but also on the uncertainties in the richness estimates. The difference in selection functions and the uncertainties in richness estimates are the main cause of the relatively low matching rates among different samples (see §5). The richness scatter is important because each cluster sample is cut at a specific richness threshold; since the observed richness function is steep and the richness scatter is significant, a richness threshold causes many clusters to scatter across the threshold. This scatter has a strong effect on cluster sample comparisons. We illustrate the effect by Monte Carlo simulations of two identical cluster samples with different noisy richness estimators (Figure 5). Placing a richness threshold on each sample, we obtain richness limited subsamples. For an intrinsic richness function of $N_{cl} \propto (\mathrm{richness})^{-4}$ (see §7), and a 30 % scatter in richness, the overlap of the two samples is only 54 %. Any difference in selection functions, which can be nearly a factor of $\sim$2 in the two methods used here, will further reduce the apparent overlap. This simple model provides an estimate for how large we might expect the overlap between two otherwise identical cluster samples to be. It is important to bear this in mind as we make direct comparisons of cluster catalogs in subsequent sections.

How do the HMF and maxBCG cluster richness estimates compare with each other? Cluster richness estimates describe, in one form or another, how populated or luminous a cluster is: either by counting galaxy members within a given radius and luminosity range, or by estimating total cluster luminosity. In general, this measure also reflects the mass of the cluster, its velocity dispersion, and temperature. While richness correlates well on average with other parameters (e.g., rich clusters are more luminous and more massive than poor clusters), individual cluster richness estimates exhibit large scatter. This scatter is due to the sharp luminosity threshold in the richness galaxy count, uncertainties in the background corrections, uncertainties in the estimated redshift and center of the cluster, sub-structure in clusters, and other effects. Still, optical richness estimators provide a basic measure of a cluster population; richnesses have been determined for all clusters in the above catalogs. The two richness estimates obtained by the cluster selection algorithms described above are N_{gal} for maxBCG and Λ for HMF (§2). N_{gal} is the number of red (E/S0) ridgeline galaxies located within $1\ h^{-1}$ Mpc of the BCG galaxy and are brighter then $M_i(\mathrm{lim}) = -20.25$. The richness Λ is determined by the HMF fine likelihood for each cluster and reflects the best-fit cluster model luminosity within $1\ h^{-1}$ Mpc radius, $L_{cl}(< 1h^{-1}\ \mathrm{Mpc}) = \Lambda\ L^*$ (§2; see Kepner

et al. 1999 and Kim et al. 2002). In comparing these richnesses, differences in the estimated redshifts and cluster centers introduce additional scatter on top of any intrinsic variations.

Figure 6 presents the observed relation between Λ and N_{gal} for clusters with $z_{est} = 0.05$ - 0.3 and $N_{gal} \geq 13$. While the scatter is large, as expected from the Monte Carlo simulations (Figure 5), a clear correlation between the mean richnesses is observed. The best-fit relation between N_{gal} (as determined for the maxBCG clusters with $N_{gal} \geq 13$) and the mean Λ (for the matching HMF clusters) is:

$$\Lambda = (11.1 \pm 0.8)\ N_{gal}^{(0.50 \pm 0.03)} \tag{1}$$

The error-bars reflect uncertainties on the mean best-fit. (This relation differs somewhat if both richnesses are determined at the maxBCG-selected cluster positions and redshifts or at the HMF-selected clusters; see, e.g., Annis et al. 2003b). The ratio Λ/N_{gal} decreases somewhat with N_{gal}; we find $\Lambda/N_{gal} \simeq 2$ for $N_{gal} \gtrsim 20$, increasing to $\Lambda/N_{gal} \sim 3$ for lower richnesses.

A comparison of the richness estimates Λ and N_{gal} with directly observed cluster luminosities and velocity dispersions is discussed in the following section.

4. Cluster Scaling Relations: Richness, Luminosity, and Velocity Dispersion

We derive preliminary scaling relations between cluster richness estimates and directly observed mean cluster luminosity and cluster velocity dispersion. This enables a direct physical comparison between the independent catalogs and allows proper merging of the two samples. It also provides a physical calibration of the cluster richness estimates in terms of their mean luminosity, velocity dispersion, and hence mass.

4.1. Cluster Luminosity

The observed cluster luminosities can be directly obtained from the SDSS imaging data using population subtraction. By comparing the galaxy population in regions around cluster centers to that in random locations we can determine the properties of galaxies in and around the clusters as well as the cluster luminosities. Since the redshifts of the SDSS clusters are relatively accurate, we can determine cluster luminosities in physical units — i.e., in solar luminosities within a metric aperture. The multi-color SDSS data also allow us to apply accurate k-corrections to cluster galaxy magnitudes.

We determine the luminosity of a cluster by measuring the total luminosity of all galaxies

within 0.6 h^{-1} Mpc of the cluster center. We use all HMF and maxBCG clusters in the redshift range 0.05 $\leq$ z $\leq$ 0.3 with richness $\Lambda \geq$ 30 (HMF) and $N_{gal} \geq$ 10 (maxBCG). For each cluster, we extract all galaxies within a projected radius of 0.6 h^{-1} Mpc of the cluster center, and compute a k-corrected absolute magnitude for each galaxy according to its type (following Fukugita et al. 1996). We then sum the total luminosity (r-band) within the absolute magnitude range of -23.0$\leq M_r \leq$-19.8. We determine the background contribution to this total luminosity by selecting five random locations away from the cluster area (within the same SDSS stripe), each with the same angular extent; we extract galaxies within these regions, k-correct them as if they were at the cluster redshift, and subtract the resulting mean luminosity (within the same magnitude range) from that of the cluster. This process allows a determination of the variance in the background correction and yields an estimate of cluster luminosity within a radius of 0.6 h^{-1} Mpc and within the luminosity range -23.0$\leq M_r \leq$-19.8 (corresponding to approximately 1.3 mag below HMF's L_r^*). We denote this luminosity $L_{0.6}^r$. A Hubble constant of $h = 1$ and a flat LCDM cosmology with Ω_m= 0.3 are used to determine cluster distances and luminosities. Details of this analysis, along with tests and a variety of related population subtraction results, will be presented in a forthcoming paper (Hansen et al. 2003).

For greater accuracy, and to minimize the spread due to redshift uncertainty, all clusters with a given richness are stacked and their mean luminosity $L_{0.6}^r$ determined. These stacked luminosities are presented as a function of cluster richness in Figures 7 and 8 for the HMF and maxBCG clusters. A strong correlation between richness and mean luminosity is observed; this is of course expected, since both N_{gal} and Λ represent cluster richnesses which broadly relate to luminosity (§3). The best-fit power-law relations to the binned mean luminosities are:

$$L_{0.6}^r(10^{10}L_\odot) = (1.6 \pm 0.4)\ N_{gal}^{1\pm0.07} \quad (maxBCG; N_{gal} \simeq 10-33) \tag{2}$$

$$L_{0.6}^r(10^{10}L_\odot) = (0.013 \pm 0.004)\ \Lambda^{1.98\pm0.08} \quad (HMF; \Lambda \simeq 30-80) \tag{3}$$

The few highest richness points ($\Lambda >$ 80, $N_{gal} >$ 33) exhibit large scatter due to their small numbers. Inclusion of these points does not change the fits; we find $L_{0.6}^r = 1.6\ N_{gal}$ (for maxBCG, $N_{gal} \geq$10) and $L_{0.6}^r = 0.015\ \Lambda^{1.95}$ (for HMF, $\Lambda \geq$ 30). The non-linearity observed in the L-Λ relation at high Λ reflects the fact that the measured cluster luminosity L corrects for an underestimate in Λ at high richness seen in simulations (Kim et al. 2002); the luminosity L measures the true cluster luminosity, independent of any uncertainty in cluster richness estimates.

The luminosity $L_{0.6}^r$ is the cluster luminosity down to a magnitude of -19.8. To convert this luminosity to a total cluster luminosity, we integrate the cluster luminosity function from -19.8^m down to the faintest luminosities. The luminosity function of HMF clusters (within

R = 0.6 h^{-1} Mpc) is observed to have Schechter function parameters of $\alpha = -1.08 \pm 0.01$ and $M_r^* = -21.1 \pm 0.02$, and maxBCG has $\alpha = -1.05 \pm 0.01$ and $M_r^* = -21.25 \pm 0.02$ ($h = 1$; Hansen et al. 2003). Integrating these luminosity functions from -19.8 down to zero luminosity yields correction factors of 1.42 (for HMF) and 1.34 (for maxBCG) for the added contribution of faint galaxies to the total cluster luminosity. The total mean cluster luminosities are therefore given by Equations 2 and 3 multiplied by these correction factors, yielding

$$L_{0.6}^{r,tot}(10^{10}L_\odot) = (2.1 \pm 0.5)\ N_{gal}^{1\pm0.07} \quad (maxBCG) \tag{4}$$

$$L_{0.6}^{r,tot}(10^{10}L_\odot) = (0.018 \pm 0.005)\ \Lambda^{1.98\pm0.08} \quad (HMF) \tag{5}$$

4.2. Velocity Dispersion

The SDSS spectroscopic survey includes spectra of galaxies brighter than $r = 17.7$ (Strauss, et al. 2002), with a median redshift of z = 0.1, as well as spectra of the 'luminous red galaxy' (LRG) sample that reaches to r $\simeq$ 19 and z $\sim$ 0.5 (Eisenstein, et al. 2001). For some rich clusters at low redshift, it is possible within the SDSS spectroscopic data to directly measure the cluster velocity dispersion. Here we compare these velocity dispersions, together with velocity dispersions available from the literature (for some of the Abell clusters within the current sample; §6), to cluster richnesses; this provides an independent physical calibration of richness.

The correlation between the observed cluster velocity dispersion and cluster richness is presented in Figure 9. We use cluster velocity dispersions of 20 clusters determined from the SDSS spectroscopic survey (for clusters with ~30 to 160 redshifts) using a Gaussian fit method, as well as from several Abell clusters available in the literature (Abell 168, 295, 957, 1238, 1367, 2644; Mazure et al. 1996; Slinglend et al. 1998). Even though the number of clusters with measured velocity dispersion is not large and the scatter is considerable, a clear correlation between median velocity dispersion and richness is observed, as expected (Figure 9). The best-fit relations are:

$$\sigma_v(km/s) = (10.2\pm^{13}_{6})\ \Lambda^{1\pm0.2} \quad (HMF; \Lambda \simeq 30-70) \tag{6}$$

$$\sigma_v(km/s) = (93\pm^{45}_{30})\ N_{gal}^{0.56\pm0.14} \quad (maxBCG; N_{gal} \simeq 8-40) \tag{7}$$

Also shown in Figure 9, for comparison, are all stacked SDSS spectroscopic data for the galaxy velocity differences in the clusters (relative to the BCG velocity), subtracted for the mean observed background, as a function of richness. These are obtained using the best

Gaussian fit to the stacked velocity data, after background subtraction. The results are consistent with the directly observed σ-Λ and σ-N_{gal} relations discussed above.

The velocity scaling relations (Equations 6 and 7) provide an important calibration of cluster richness versus mean cluster velocity dispersion (and thus mass). Also shown in the figures, for comparison, are the σ_v-richness relations derived from the observed mean $L_{0.6}$-Λ and $L_{0.6}$-N_{gal} correlations (Section §4.1, Figures 7 - 8). Here the luminosity $L_{0.6}^{tot}$ is converted to mass, $M_{0.6}$, using the typical observed M/L ratio relevant for these clusters and the observed relation between $M_{0.6}$ and σ_v based on calibration using gravitational lensing observations (see Bahcall et al. 2003 for details). Good agreement exists between these independent scaling relations. Larger samples, when available, will further improve this important calibration.

4.3. Consistency of Scaling Relations

The independent scaling relations discussed above are consistent with each other. The directly observed mean Λ-N_{gal} relation (Equation 1) is in agreement with the observed luminosity-richness relations, $L_{0.6}^{r,tot}$-Λ and $L_{0.6}^{r,tot}$-N_{gal} (Equations 4 and 5). Both relations — the luminosity-richness relations and the Λ-N_{gal} relation — yield, independently, $\Lambda \simeq 11\ N_{gal}^{0.5}$, and reproduce the observed total luminosity relations discussed above. This consistency is illustrated by the solid and dashed lines in Figure 6 which represent, respectively, the observed mean Λ-N_{gal} relation and the one obtained from the mean luminosty-richness relations ($L_{0.6}^{r,tot}$-Λ and $L_{0.6}^{r,tot}$-N_{gal}).

The third independent relation, velocity dispersion versus richness (Equations 6 and 7), is also consistent with the above results; this is illustrated by the dotted curve in Figure 6.

The non-linearity observed in the $L(\Lambda) \sim \Lambda^2$ relation (Equation 3 and discussion below it; Figure 7), and the similar non-linearity observed in the $\Lambda \sim {N_{gal}}^{0.5}$ relation (i.e., $N_{gal} \sim \Lambda^2$; Equation 1; Figure 6), are consistent with the velocity scaling relation, $\sigma = 10.2\ \Lambda$ (Equation 6), since the latter implies that cluster mass (within a fixed radius) is M $\sim \sigma^2 \sim \Lambda^2$; this is consistent with the observed $L \sim \Lambda^2$. The maxBCG relations are also self-consistent, with a linear $L \sim N_{gal}$, $\sigma \sim {N_{gal}}^{0.56}$, and hence M $\sim \sigma^2 \sim N_{gal}^{1.1}$. In both cases, M/L is nearly constant — in fact, slightly increasing with L as expected (e.g., Bahcall et al. 2000).

The consistency of the scaling relations is illustrated in Figure 6. A summary of the mean quantitative scaling relations betweem Λ, N_{gal}, velocity dispersion, luminosity, and mass (within 0.6 h^{-1} Mpc) is presented in Table 1.

5. A Merged Cluster Catalog

We use the scaling relations derived above (§4) to define a conservative merged catalog of clusters of galaxies from the early SDSS commissioning data based on the maxBCG and the Hybrid Matched-Filter samples. The merged BH catalog is limited to clusters within the redshift range z_{est} = 0.05 - 0.3 and richness above the threshold listed below, over the 379 deg^2 area (§2). A total of 799 clusters are listed in the catalog.

The clusters are selected using the following criteria:

1. z_{est} = 0.05 - 0.3
2. Richness threshold of $\Lambda \geq 40$ (for HMF clusters) and $N_{gal} \geq 13$ (for maxBCG clusters). These thresholds are comparable to each other and correspond to a mean cluster velocity dispersion of $\sigma_r \gtrsim 400$ km s^{-1} and luminosity $L_{0.6}^{r,tot} \gtrsim 3 \times 10^{11}\ h^{-2}\ L_\odot$; the related mass is approximately $M_{0.6} \gtrsim 5 \times 10^{13}\ h^{-1}\ M_\odot$(see Table 1).

Clusters that overlap between the two methods are considered as single clusters if they are separated by $\leq 1\ h^{-1}$ Mpc (projected) and ≤ 0.08 in estimated redshift (2.5-σ_z). Overlap clusters are listed as a single cluster, on a single line, but include the relevant parameters from both the HMF and maxBCG selection (position, redshift, richness). This is done in order to provide complete information about the clusters and allow their proper use with the independent HMF and maxBCG selection functions. For each cataloged cluster (HMF with $\Lambda \geq 40$ or maxBCG with $N_{gal} \geq 13$) we include cluster matches (i.e., overlaps with separations as defined above) that reach beyond the richness or redshift thresholds of the catalog. For example, an HMF cluster with $\Lambda \geq 40$ and z = 0.30 may list as a match a maxBCG cluster with $N_{gal} < 13$ and/or z = 0.22 to 0.38 (i.e., $\Delta z \leq 0.08$). A lower limit of $N_{gal} \geq 6$ is set for all matches. While not part of the $\Lambda \geq 40$, $N_{gal} \geq 13$ catalog, such matches with $N_{gal} < 13$ and $\Lambda < 40$ clusters are listed in order to provide full information of possible matches, considering the large uncertainty in the richness parameter. (If there is more than one match per cluster, we select the one with the closest separation). Some of the matches, especially at low richness ($N_{gal} \lesssim 10$) and large separation ($\sim 1\ h^{-1}$ Mpc or $\Delta z \sim 0.08$), may be coincidental. Clusters that do not overlap are listed as separate clusters and are so noted.

The catalog is presented in Table 2. Listed in the catalog, in order of increasing right-ascension, are the following: SDSS cluster number (column 1), method of detection (H for HMF, B for maxBCG; lower case (h, b) represents cluster matches that are outside the catalog richness or redshift thresholds, i.e., $\Lambda < 40$, $N_{gal} < 13$, z>0.3; column 2), HMF α and δ (in degrees 2000; column 3 - 4), HMF estimated redshift (column 5), HMF cluster richness

Λ (column 6). Columns 7 - 10 provide similar information for the maxBCG detection, if the cluster so detected: α and δ (2000; column 7 - 8), maxBCG redshift estimate (column 9), and richness estimate N_{gal} (column 10). An SDSS spectroscopic redshift that matches the cluster, if available, is listed in column 11 (mainly for the BCG galaxy). Column 12 lists matches with Abell and X-ray clusters. All the NORAS X-ray clusters and 53 of the 58 Abell clusters in this area are identified in the catalog; the additional five Abell clusters are identified by the combined HMF and maxBCG techniques but are below the catalog richness threshold (see §6).

The catalog contains 436 HMF clusters ($\Lambda \geq 40$), 524 maxBCG clusters ($N_{gal} \geq 13$), and a total merged catalog (as defined above) of 799 clusters (at $z_{est} = 0.05$ - 0.3). Some clusters are false-positive detections (i.e., not real clusters); the false-positive rate is discussed below. The overlap between the independent HMF and maxBCG clusters within the above redshift range is 81% (of the HMF clusters, accounting for all matches to $N_{gal} \geq 6$). This overlap rate is consistent with expectations based on the selection functions and false-positive rates for the HMF and maxBCG clusters (see below) and the effects of redshift and positional uncertainties. The overlap rate increases to $\gtrsim 90\%$ with more liberal matching criteria (e.g., separation larger than 1 h^{-1} Mpc and/or larger than 0.08 in redshift). The overlap rate drops, as expected, when the richness restriction of the matching sample is tightened (e.g., the matching rate is 37% if only $N_{gal} \geq 13$ matches are considered for $\Lambda \geq 40$ HMF clusters; this is consistent with expectations based on Monte Carlo richness simulations, §3). The richest clusters, HMF with $\Lambda \geq 52$, are matched at a higher rate, as expected: 90% match with $N_{gal} \geq 6$ maxBCG clusters and 61% match with $N_{gal} \geq 13$ clusters. A summary of the catalog cluster distribution by redshift and richness is presented in Table 3.

Selection functions for the independent HMF and maxBCG clusters have been determined from simulations and are presented as a function of redshift and richness in Figure 10 (for HMF; Kim et al. 2002) and Figure 11 (for maxBCG; Annis et al. 2003a) (see above refereneces for more details). The richest clusters are nearly complete and volume limited to z $\lesssim$ 0.3, while the $\Lambda \sim 40$ HMF clusters are only $\sim$40% complete at z $\sim$ 0.3. The selection functions need to be properly accounted for in any statistical analysis of the current samples.

Some systems are false-positive detections (i.e., non-real clusters). The false-positive detection rates for the clusters have been estimated from simulations (Kim et al. 2002; Annis et al. 2003a) as well as from visual inspection. The false-positive rate is found to be small ($\lesssim$10%) for the $N_{gal} \geq 13$ maxBCG and $\Lambda \geq 40$ HMF clusters (z = 0.05 - 0.3). All detections are included in the catalog, including false-positive detections, in order to avoid unquantitative visual selection.

Some maxBCG systems are found to be small clumps of red galaxies in the outskirts of

richer HMF clusters. Some un-matched HMF and maxBCG systems are in fact parts of the same larger cluster split into separate listings because of the Δz $\leq$0.08 and the 1 h^{-1} Mpc separation cutoff. This can result from uncertainties in z_{est} and from the different definitions of cluster center (i.e., HMF clusters typically center on a mean high density region, while maxBCG clusters center on a likely BCG galaxy). The splittings may also represent sub-structure in clusters. Occasionally, a single HMF or maxBCG cluster may be split by the selection algorithm into two separate systems, which may represent sub-clustering. Some systems may be part of an extended galaxy overdensity region rather than true condensed virialized clusters; this is less likely for the richer systems.

The scaling relations between richness, luminosity and velocity dispersion (§4) suggest that $\Lambda \gtrsim 40$ and $N_{gal} \gtrsim 13$ clusters correspond to approximately $\sigma_v \gtrsim 400$ km s^{-1}, and $\Lambda \gtrsim 60$ and $N_{gal} \gtrsim 30$ clusters correspond to $\sigma_v \gtrsim 600$ km s^{-1}, i.e., rich clusters. The mean calibrations are summarized in Table 1.

The distribution of clusters on the sky is mapped for the catalog clusters in Figure 12. All clusters with $0.05 \leq z \leq 0.3$, richness $\Lambda \geq 40$ (for HMF) and $N_{gal} \geq 13$ (for maxBCG), and their matching clusters are shown. The Abell clusters located in the survey area are also shown (see §6). A 1 h^{-1} Mpc radius circle is presented around the center of each cluster; this helps visualize possible matches that may be offset in their center position due to uncertainties in cluster centers and the different definition of "center" (§3), or may represent sub-structure within more extended regions.

Images of a sample of cataloged clusters representing a wide range of redshift (z$\simeq$0.05-0.3) and richness ($\Lambda \gtrsim 40$, $N_{gal} \gtrsim 13$) are presented as examples in Figure 13.

6. Comparison with Abell and X-Ray clusters

A total of 58 Abell clusters (Abell 1958; Abell, Corwin, & Olowin 1989) are located in the current survey region. The SDSS BH catalog includes 53 (91%) of these clusters (listed in the last column of Table 2), using the matching requirement of a projected separation of less than 1 h^{-1} Mpc. (Since many of Abell clusters have no measured redshifts, no redshift information is used.) Most matches are at separations typically $\lesssim 0.2$ h^{-1}. The five additional Abell clusters not listed in the catalog are all detected by the combined HMF and maxBCG methods, but are below the catalog threshold; these are A116 (Λ= 29, N_{gal}= 9), A237 (Λ= 35, N_{gal}= 7), A295 (N_{gal}= 11), A2051 (N_{gal}= 11), A2696 (N_{gal}= 11). This matching rate is consistent with the expected selection function of the HMF and maxBCG methods.

Eight clusters from the NORAS X-ray cluster catalog (Böhringer et al. 2000) lie in the SDSS BH area and redshift region. All eight X-ray clusters are detected and included in our catalog; maxBCG detects all eight clusters (with 2 below the threshold of N_{gal}= 13), and HMF detects seven of the clusters (all within the catalog threshold of $\Lambda \geq 40$). Details of the comparison are given in Table 4.

7. Cluster Abundance and Richness Function

The observed distribution of cluster abundance as a function of richness — the cluster richness function — is presented in Figure 14. The observed cluster counts are corrected for the relevant HMF and maxBCG selection functions. Here each cluster is corrected by the selection function appropriate for its richness and redshift (for each method; see Figures 10, 11) and by the false-positive expectation rate (§5). The corrected count is divided by the sample volume to produce a volume-limited cluster abundance as a function of richness. Smaller corrections for richness and redshift uncertainties are not included; these will reduce the cluster abundances by $\sim 10\%$ to $\sim 30\%$ for $\Lambda \sim 40$ to ~ 60 (see Bahcall et al. 2003).

The results show a steeply declining richness function with increasing richness, as expected. The richness function of the HMF-selected and maxBCG-selected clusters are consistent with each other when properly corrected for the different selection functions and scaled by the richness scaling relation. The richness function indicates a cluster abundance of $2 \times 10^{-5}\ h^3\ \mathrm{Mpc}^{-3}$ for $\Lambda \gtrsim 40$ and $N_{gal} \gtrsim 13$ clusters ($\sigma \gtrsim 400\ km\ s^{-1}$). These abundances are in general good agreement with Abell clusters and with other richness or temperature function observations when properly scaled by the relevant richness scaling relations (e.g., Bahcall & Cen 1992; Ikebe et al. 2002).

The mass function of SDSS clusters was recently determined by Bahcall et al. (2003) (for z = 0.1-0.2, using an extension of the current catalog to slightly lower richnesses), yielding consistent results for the HMF and maxBCG subsamples. The mass function was used by Bahcall et al. (2003) to place strong cosmological constraints on the mass density parameter of the universe, Ω_m, and the amplitude of mass fluctuations, σ_8: $\Omega_m = 0.19\ \pm^{0.08}_{0.07}$ and $\sigma_8 = 0.9\ \pm^{0.3}_{0.2}$.

8. Summary

We compare two independent cluster selection methods used on 379 deg^2 of early SDSS commissioning data: Matched-Filter (HMF) and the color-magnitude maxBCG. We clarify

the relation between the methods and the nature of clusters they select. HMF selects clusters that follow a typical density profile and luminosity function, while maxBCG selects clusters dominated by bright red galaxies — quite different selection criteria. We determine scaling relations between the observed cluster richness, luminosity, and velocity dispersion. We use the above scaling relations to combine appropriate subsamples of the HMF and maxBCG clusters and produce a conservative merged catalog of 799 clusters of galaxies at $z_{est} = 0.05$ - 0.3 above richness threshold of $\Lambda \geq 40$ (HMF) and $N_{gal} \geq 13$ (maxBCG) (§5). This threshold corresponds to clusters with a typical mean velocity dispersion of $\sigma_v \gtrsim 400$ km s^{-1}, total r-band luminosity $L_{0.6}^{tot} \gtrsim 3 \times 10^{11} h^{-2}$ $L_\odot$ and mass $M_{0.6} \gtrsim 5 \times 10^{13} h^{-1}$ $M_\odot$ (within a radius of 0.6 h^{-1} Mpc). This threshold reflects clusters that are poorer than Abell richness class 0. The average space density of the clusters is 2×10^{-5} h^3 clusters/Mpc^3. Using the relevant selection functions, we determine the cluster richness function; we find it to be a steeply declining function of cluster abundance with increasing richness. We compare the cataloged clusters with the Abell and X-ray clusters located in the survey region; they are all detected (with 5 of the 58 Abell clusters below the above merged richness cuts).

The relevant selection functions for the catalog clusters are provided. The catalog can be used for studies of individual clusters, for comparisons with other objects (e.g., X-ray clusters, SZ clusters, AGNs), and in statistical analyses (when properly corrected for the relevant selection functions).

As an example, we determined the mass function of clusters (see Bahcall et al. 2003) and used it to place powerful constarints on the mass-density parameter of the universe and the amplitude of mass fluctuations; we find $\Omega_m = 0.19 \pm^{0.08}_{0.07}$ and $\sigma_8 = 0.9 \pm^{0.3}_{0.2}$.

The current work represents preliminary results from early SDSS commissioning data (4% of the ultimate SDSS survey). The results will greatly improve as more extensive SDSS data become available.

The SDSS is a joint project of The University of Chicago, Fermilab, the Institute for Advanced Study, the Japan Participation Group, The Johns Hopkins University, Los Alamos National Laboratory, the Max-Planck-Institute for Astronomy (MPIA), the Max-Planck-Institute for Astrophysics (MPA), New Mexico State University, University of Pittsburgh, Princeton University, the United States Naval Observatory, and the University of Washington.

Funding for the creation and distribution of the SDSS Archive has been provided by the Alfred P. Sloan Foundation, the Participating Institutions, the National Aeronautics and Space Administration, the National Science Foundation, the U.S. Department of Energy, the Japanese Monbukagakusho, and the Max Planck Society. The SDSS Web site is

http://www.sdss.org/. Tim McKay acknowledges support from NSF PECASE grant AST 9708232.

REFERENCES

Abell, G. O. 1958, ApJS, 3, 211

Abell, G. O., Corwin, H. G., & Olowin, R. P. 1989, ApJS, 70, 1

Annis, J., et al. 2003a, in preparation.

Annis, J., et al. 2003b, in preparation.

Bahcall, N. A. 1977, ARA&A, 15, 505

Bahcall, N. A. & Soneira, R. M. 1983, ApJ, 270, 20

Bahcall, N. A. & Soneira, R. M. 1984, ApJ, 277, 27

Bahcall, N. A. 1988, ARA&A, 26, 631

Bahcall, N. A. & Cen, R. 1992, ApJ, 398, L81

Bahcall, N. A., Lubin, L. M., & Dorman, V. 1995, ApJ, 447, L81

Bahcall, N. A., Fan, X., & Cen, R. 1997, ApJ, 485, L53

Bahcall, N. A. & Fan, X. 1998, ApJ, 504, 1

Bahcall, N. A., Ostriker, J. P., Perlmutter, S., & Steinhardt, P. J. 1999, Science, 284, 1481

Bahcall, N. A. 1999, ApJ, 525, C873

Bahcall, N. A., Cen, R., Davé, R., Ostriker, J. P., & Yu, Q. 2000, ApJ, 541, 1

Bahcall, N. A. et. al. 2003, ApJ, vol.585, in press

Blanton, M. R., Lupton, R .H., Maley, F .M., Young, N., Zehavi, I., & Loveday, J. 2002, AJ, in press, astro-ph/0105535

Böhringer, H. et al. 2000, ApJS, 129, 435

Carlberg, R. G. et al. 1997, ApJ, 485, L13

Carlstrom, J. et al. 2001, IAP Conference 2000, Constructing the Universe with Clusters of Galaxies, edt. F. Durret and D. Gerbal (astro-ph/0103480)

Connolly, A. J., Csabai, I., Szalay, A. S., Koo, D. C., Kron, R. G., & Munn, J. A. 1995, AJ, 110, 2655

Croft, R. A. C., Dalton, G. B., Efstathiou, G., Sutherland, W. J., & Maddox, S. J. 1997, MNRAS, 291, 305

Csabai, I., Connolly, A. J., Szalay, A. S., & Budavári, T. 2000, AJ, 119, 69

Dalton, G. B., Efstathiou, G., Maddox, S. J., & Sutherland, W. J. 1994, MNRAS, 269, 151

Dressler, A. 1984, ARA&A, 22, 185

Donahue, M. & Voit, G. M. 1999, ApJ, 523, L137

Ebeling, H., Voges, W., Bohringer, H., Edge, A. C., Huchra, J. P., & Briel, U. G. 1996, MNRAS, 281, 799

Eisenstein, D., et al. 2001, AJ, 122, 2267

Eke, V. R., Cole, S., & Frenk, C. S. 1996, MNRAS, 282, 263

Fischer, P. & Tyson, J. A. 1997, AJ, 114, 14

Fukugita, M., Ichikawa, T., Gunn, J. E., Doi, M., Shimasaku, K., & Schneider, D. P. 1996, AJ, 111, 1748

Gladders, M. D. & Yee, H. K. C. 2000, AJ, 120, 2148

Goto, T., et al. 2002, AJ, 123, 1807

Gunn, J. E. & Dressler, A. 1988, ASSL Vol. 141: Towards Understanding Galaxies at Large Redshift , 227

Gunn, J. E. et al. 1998, AJ, 116, 3040

Hansen, S., et al. 2003, in preparation (Senior Thesis, Univ. of Michigan, 2003)

Henry, J. P., Gioia, I. M., Maccacaro, T., Morris, S. L., Stocke, J. T., & Wolter, A. 1992, ApJ, 386, 408

Henry, J. P. 2000, ApJ, 534, 565

Hoessel, J. G., & Schneider, D. P. 1985, AJ, 90, 1648

Hogg, D. W. et al. 1998, AJ, 115, 1418

Hogg, D. W. et al. 2001, AJ, 122, 2129

Huchra, J. P., Geller, M. J., Henry, J. P., & Postman, M. 1990, ApJ, 365, 66

Ikebe, Y., Reiprich, T. H., Böhringer, H., Tanaka, Y. & Kitayama, T. 2002, A&A, 383, 773

Joffre, M. et al. 2000, ApJ, 534, L131

Kepner, J., Fan, X., Bahcall, N., Gunn, J., Lupton, R., & Xu, G. 1999, ApJ, 517, 78

Kim, R., et al. 2002, AJ123, 20.

Kim, R., et al. 2003, in preparation

Klypin, A. A. & Kopylov, A. I. 1983, Soviet Astronomy Letters, 9, 41

Lumsden, S. L., Nichol, R. C., Collins, C. A., & Guzzo, L. 1992, MNRAS, 258, 1

Lupton, R., et al. 2001, in preparation

Mazure, A., et al. 1996, A&A, 310, 31

Miller, C., et al. 2003, in preparation

Pier, J. R. et al. 2002, AJ, in press, astro-ph/0211375

Postman, M., Huchra, J. P., & Geller, M. J. 1992, ApJ, 384, 404

Postman, M., Lubin, L. M., Gunn, J. E., Oke, J. B., Hoessel, J. G., Schneider, D. P., & Christensen, J. A. 1996, AJ, 111, 615

Postman, M., Lauer, T. R., Oegerle, W., Donahue, M. 2002, submitted to ApJ

Rosati, P., Stanford, S. A., Eisenhardt, P. R., Elston, R., Spinrad, H., Stern, D., & Dey, A. 1999, AJ, 118, 76

Rosati, P., Borgani, S., & Norman, C. 2002, ARA&A, 40, 539

Scranton, R., et al. 2002, ApJ, 579, 48

Shectman, S. A. 1985, ApJS, 57, 77

Sheldon, E. S. et al. 2001, ApJ, 554, 881

Slinglend, K., Batuski, D., Miller, C., Haase, S., Michaud, K., Hill, J. M., 1998, ApJS, 115, 1S

Smail, I., Ellis, R. S., Dressler, A., Couch, W. J., Oemler, A. J., Sharples, R. M., & Butcher, H. 1997, ApJ, 479, 70

Smith, J. A. et al. 2002, AJ, 123, 2121

Squires, G. & Kaiser, N. 1996, ApJ, 473, 65

Stoughton, C., et al. 2002, AJ, 123, 485

Strauss, M., et al. 2002, AJ, 124, 1810

Trumper, J. 1983, Mitteilungen der Astronomischen Gesellschaft Hamburg, 60, 255

Voges, W. et al. 1999, A&A, 349, 389

Voges, W. et al. 2000, IAU Circ., 7432, 1

White, S. D. M., Navarro, J. F., Evrard, A. E., & Frenk, C. S. 1993, Nature, 366, 429

White, S. D. M., Efstathiou, G., & Frenk, C. S. 1993, MNRAS, 262, 1023

York, D. G. et al. 2000, AJ, 120, 1579

Zwicky, F. 1957, Berlin: Springer, 1957

Zwicky, F., Herzog, E., & Wild, P. 1968, Pasadena: California Institute of Technology (CIT), 1961-1968

This preprint was prepared with the AAS LaTeX macros v5.0.

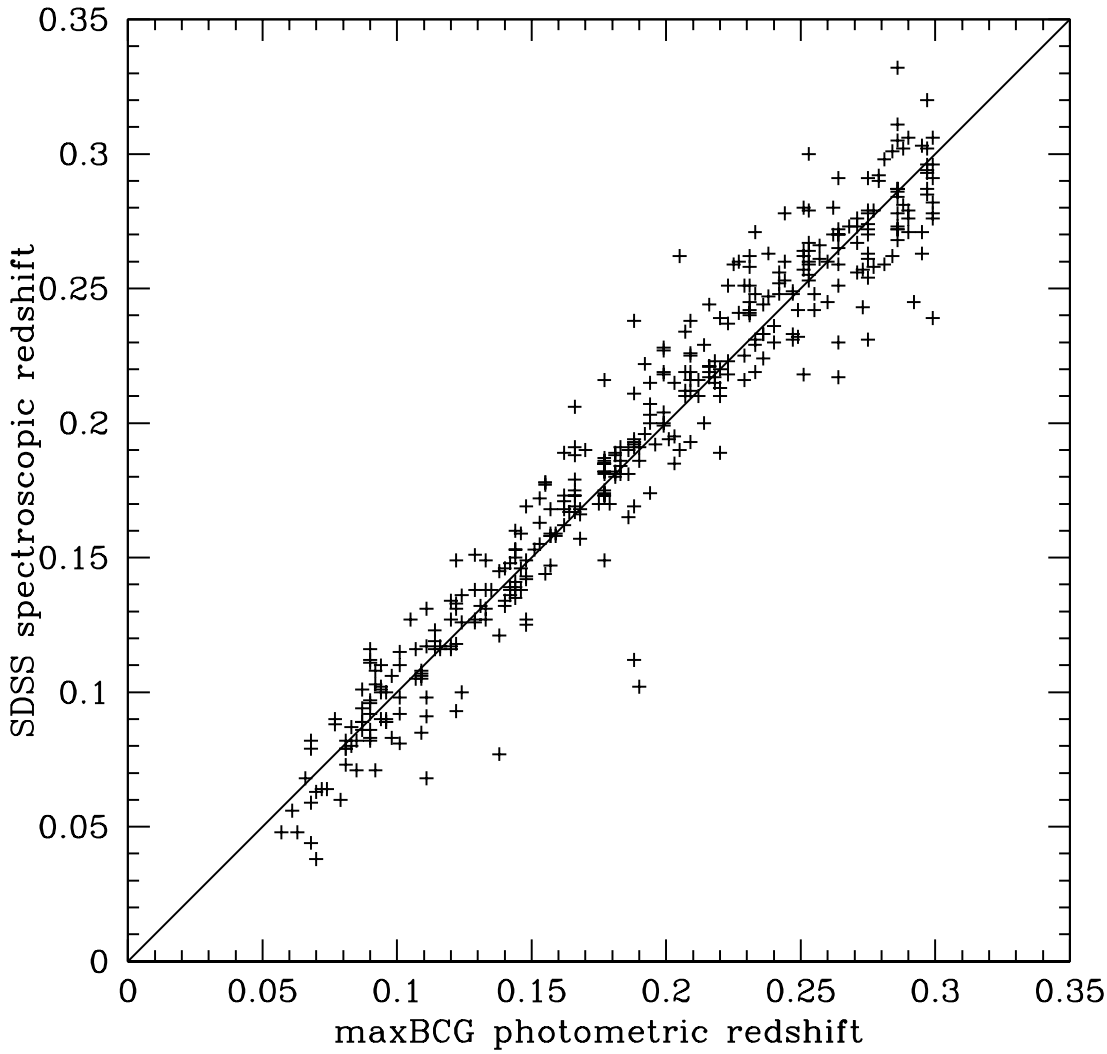

Fig. 1.— Comparison of measured SDSS spectroscopic redshifts with photometric redshifts estimated by the maxBCG method for 382 maxBCG clusters ($N_{gal}\geq 13$, z_{est} = 0.05-0.3). The dispersion in the estimated redshifts is $\sigma_z = 0.014$.

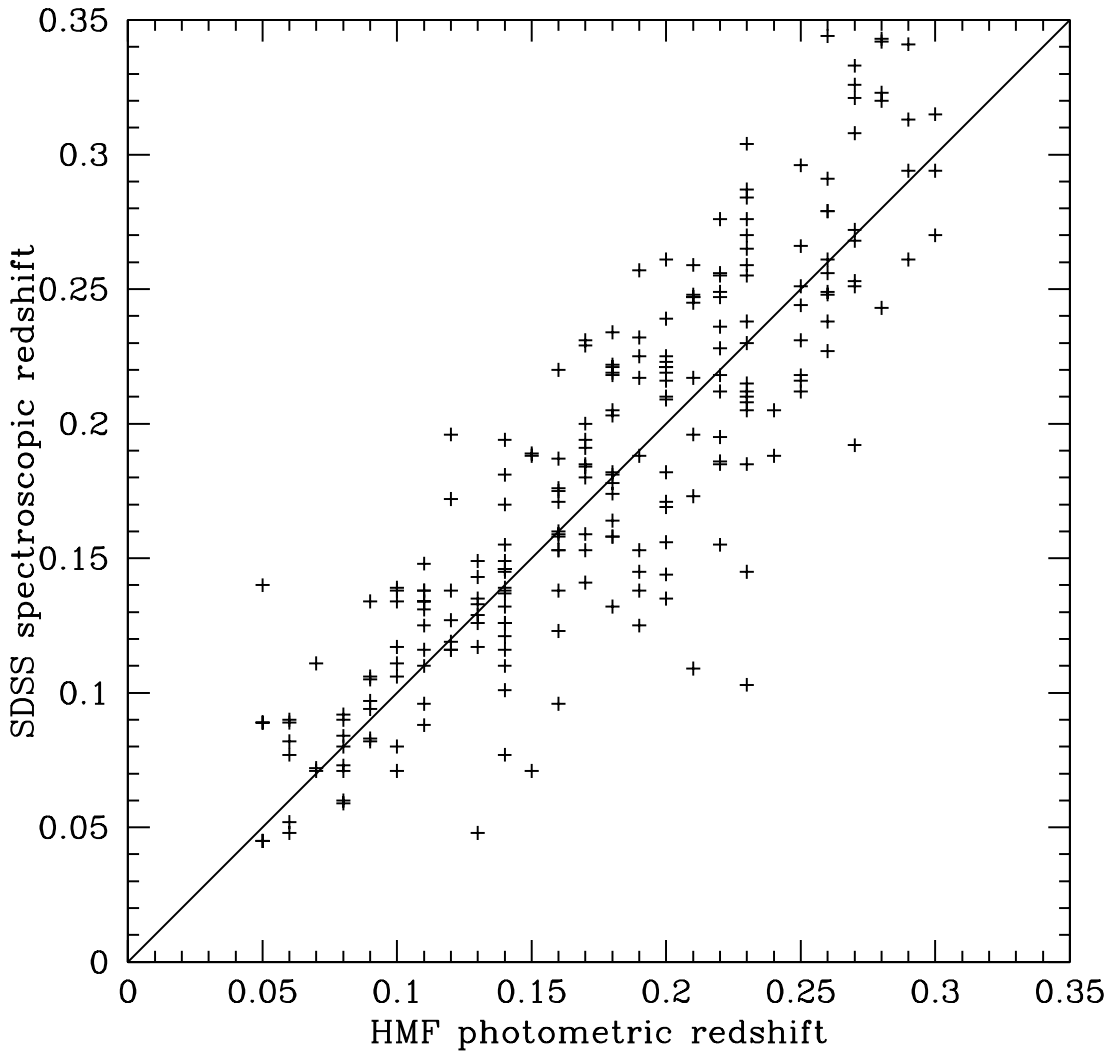

Fig. 2.— Comparison of measured SDSS spectroscopic redshifts with photometric redshifts estimated by the HMF method for 237 HMF clusters ($\Lambda \geq 40$, $z_{est} = 0.05$-0.3). The dispersion in the estimated redshifts is $\sigma_z = 0.033$.

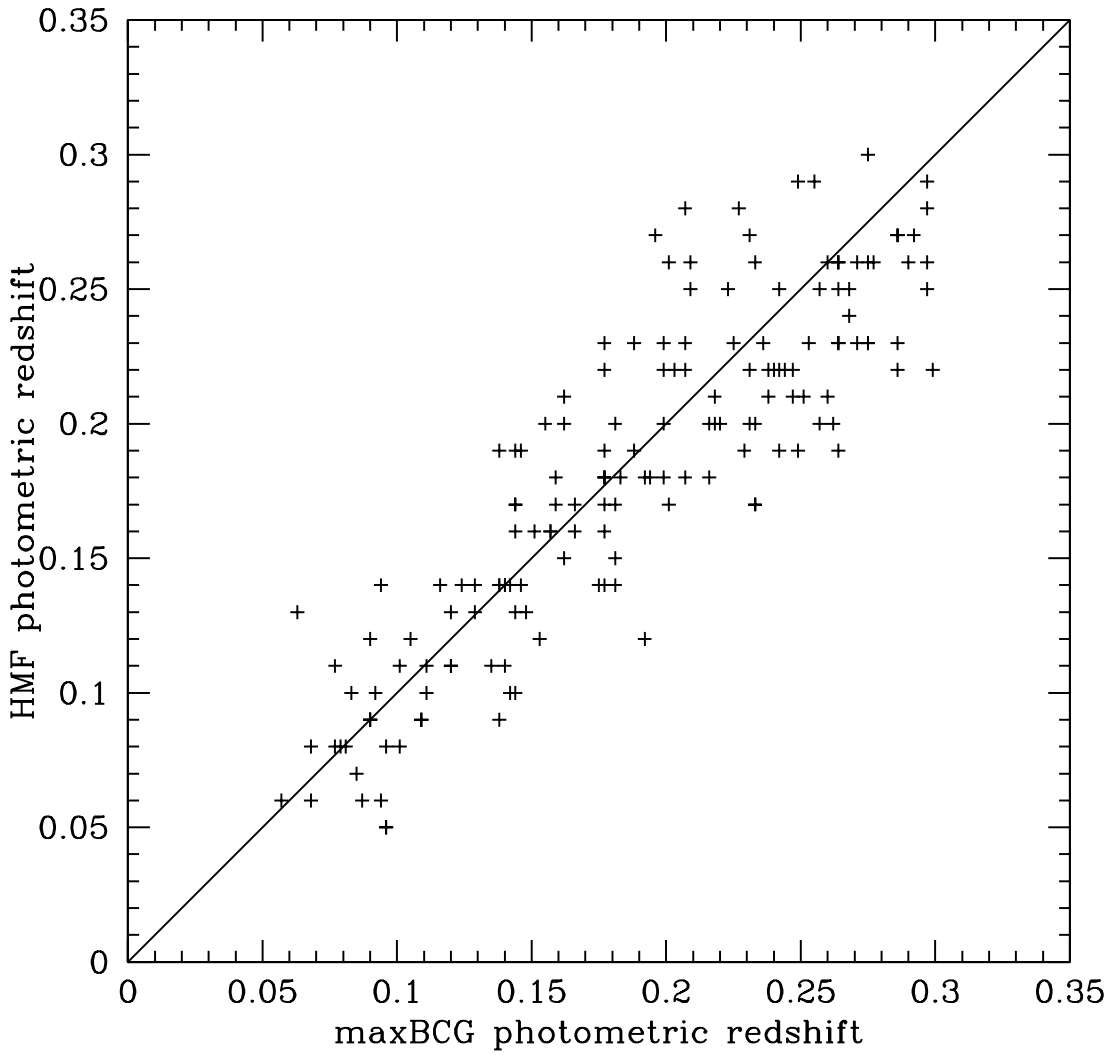

Fig. 3.— Comparison of HMF and maxBCG estimated redshifts for 161 cluster pairs ($\Lambda \geq 40$, $N_{gal} \geq 13$, z_{est} = 0.05-0.3). The cluster pairs are separated by $\leq 1h^{-1}$ Mpc (projected) and $\Delta z_{est} \leq 0.08$ in estimated redshift.

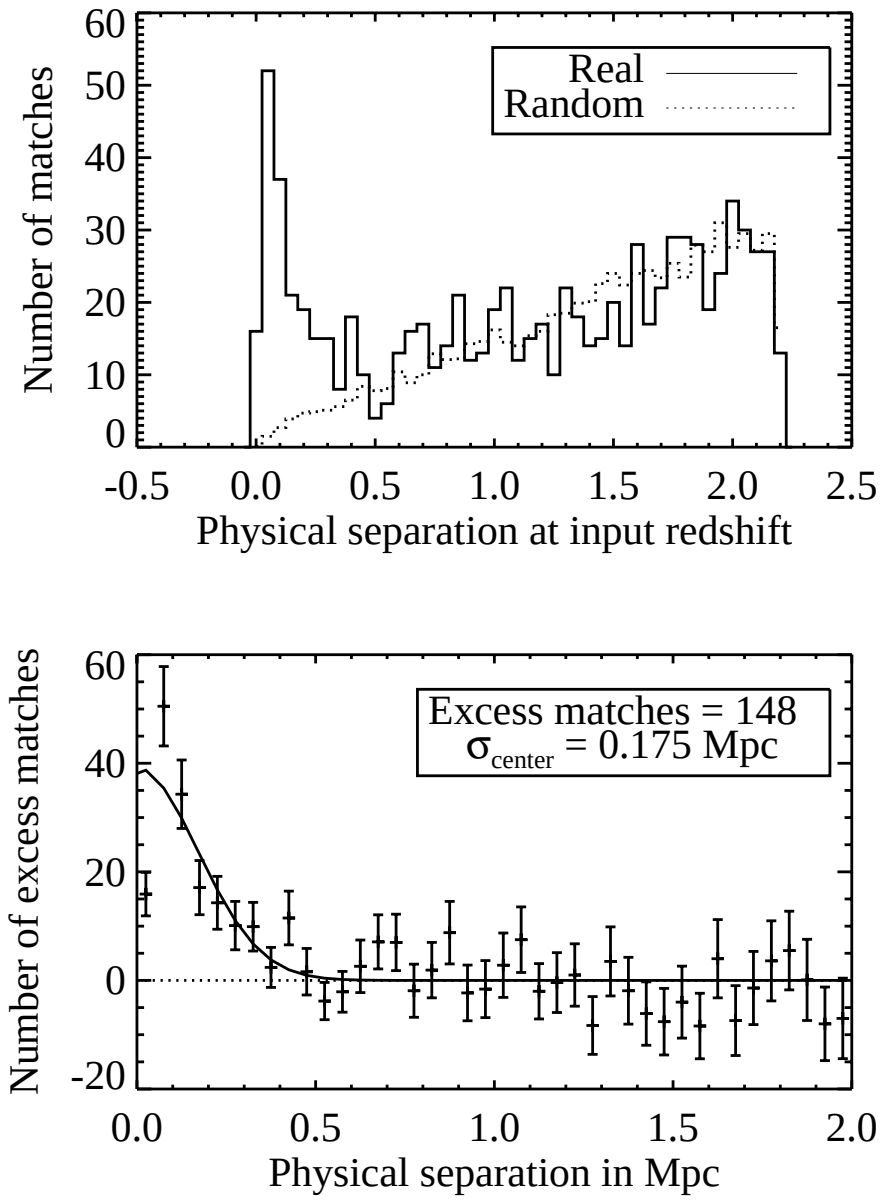

Fig. 4.— Top panel is the histogram of the number of matches between HMF and maxBCG clusters (z = 0.05 - 0.3) as a function of physical projected separation in Mpc (calculated at the maxBCG estimated redshift). The solid line represents the data (real matches); the dashed line results from matching the clusters with random positions (thus representing chance contribution to matches). Lower panel shows the difference between these two (all matches minus random matches). The excess pairs are concentrated at small separations ($\lesssim$ 0.5 h^{-1} Mpc) and represent real matches.

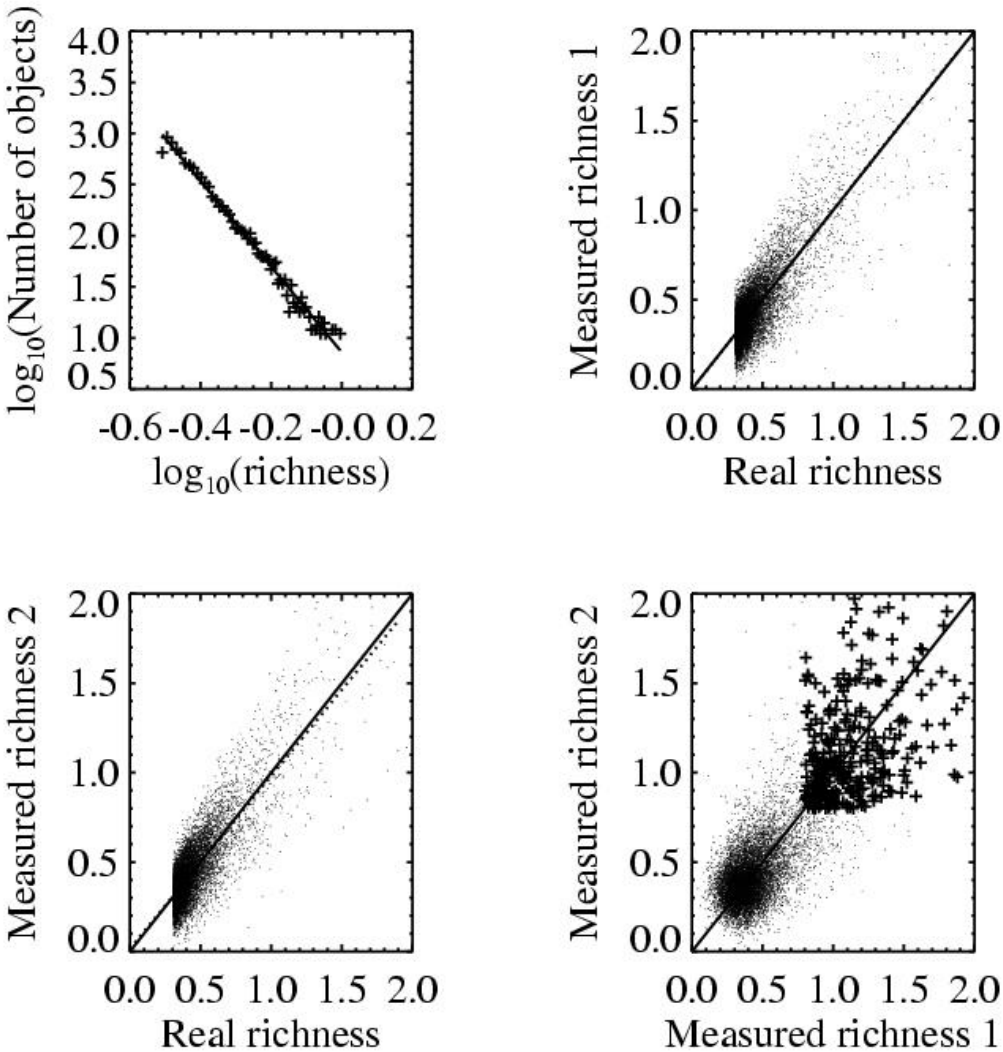

Fig. 5.— Monte Carlo simulations showing the effect of uncertainty in richness estimates on comparison of catalogs drawn from a steeply declining richness function. The top left panel shows the model richness function ($N_{cl} \sim \mathrm{Richness}^{-4}$). The top right and bottom left panels compare measured to actual richness measures for two realizations of richness measurements with 30% measurement uncertainties. The bottom right panel compares the richness measurements of the two Monte Carlo realizations of the data, illustrating that only 54% of the clusters passing one richness threshold will also pass the other.

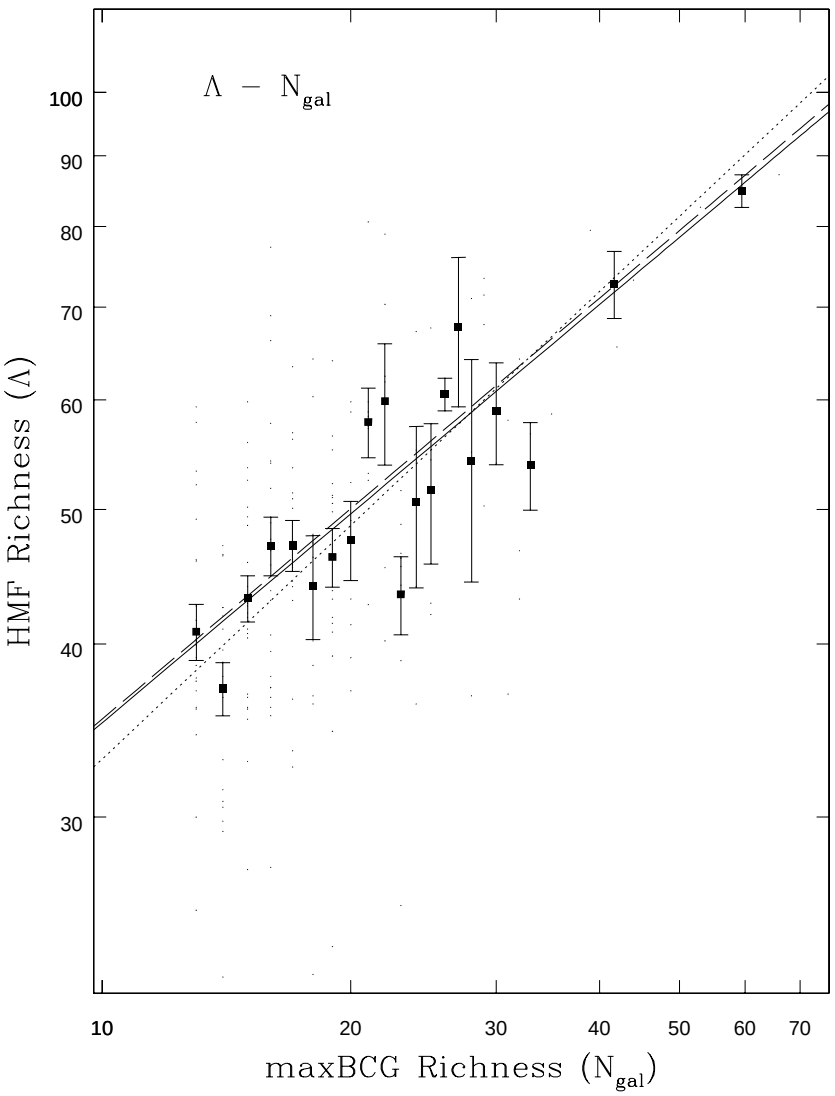

Fig. 6.— Comparison of HMF and maxBCG richnesses. The HMF richness Λ (determined for HMF clusters) is compared with the maxBCG richness N_{gal} (determined for maxBCG clusters with $N_{gal} \geq 13$) for matched cluster pairs (HMF clusters that match maxBCG clusters within 1 h^{-1} Mpc projected separation and $\Delta z \leq 0.05$). Individual Λ-N_{gal} matches are shown by the faint points; the mean richness Λ as a function of N_{gal} is presented by the solid squares, with rms error-bars on the means. The best-fit relation, $\Lambda = (11.1 \pm 0.8)\ {N_{gal}}^{0.5 \pm 0.03}$, is shown by the solid line. The dashed line represents the independent correlation obtained using the observed luminosity-richness relations for HMF and maxBCG clusters (§4, figures 7 and 8). The dotted line represents another independent relation implied from the observed velocity dispersion versus richness correlations (§4, figure 9). All three independent methods yield consistent results.

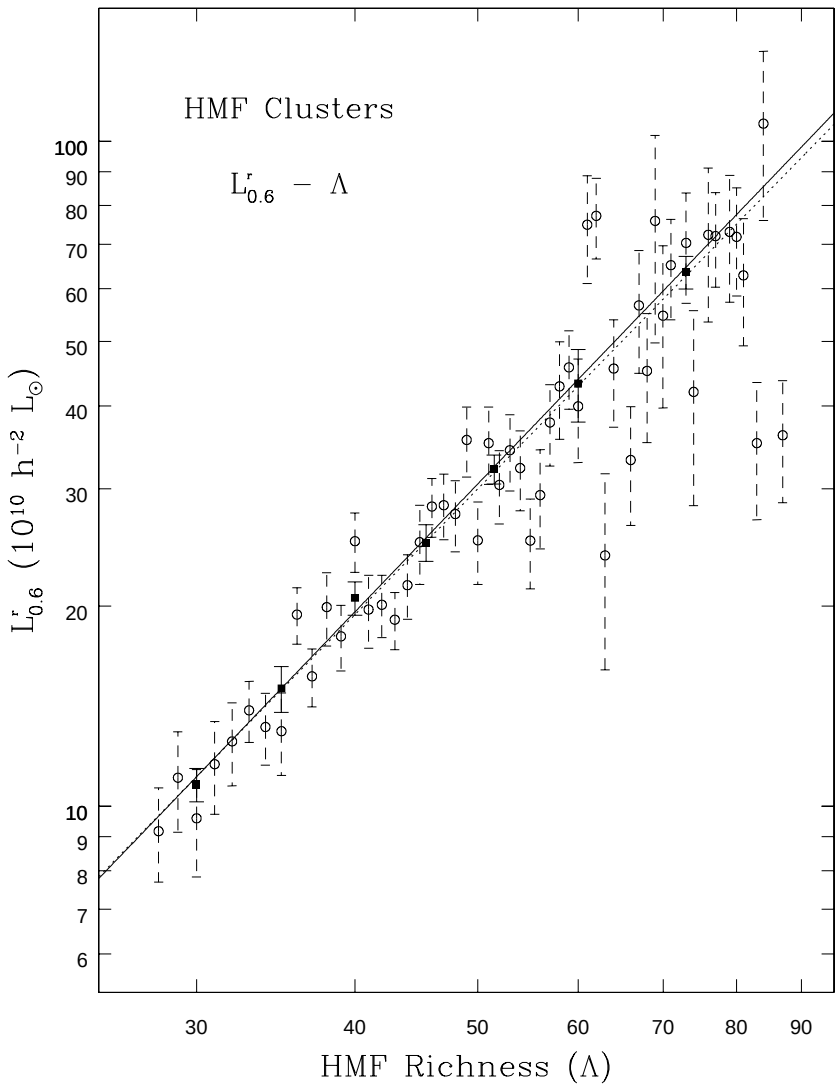

Fig. 7.— Observed cluster luminosity versus richness for HMF clusters. Cluster luminosity is observed in the r-band, within a radius of 0.6 h^{-1} Mpc, for stacked clusters at a given richness. The luminosities are k-corrected, background subtracted, and integrated down to $M_r = -19.8$. Dark squares represent binned data (in richness bins) of the stacked clusters. The solid line is the best-fit power-law relation (for the range $\Lambda \simeq$ 30 - 80): $L^r_{0.6}(10^{10} L_\odot) = 0.013\ \Lambda^{1.98}$ (Equation 3). (The dotted line is the best-fit when the Λ>80 higher scatter clusters are added). The contribution of galaxies fainter than -19.8 adds a correction factor of 1.42 to the above luminosities (§4).

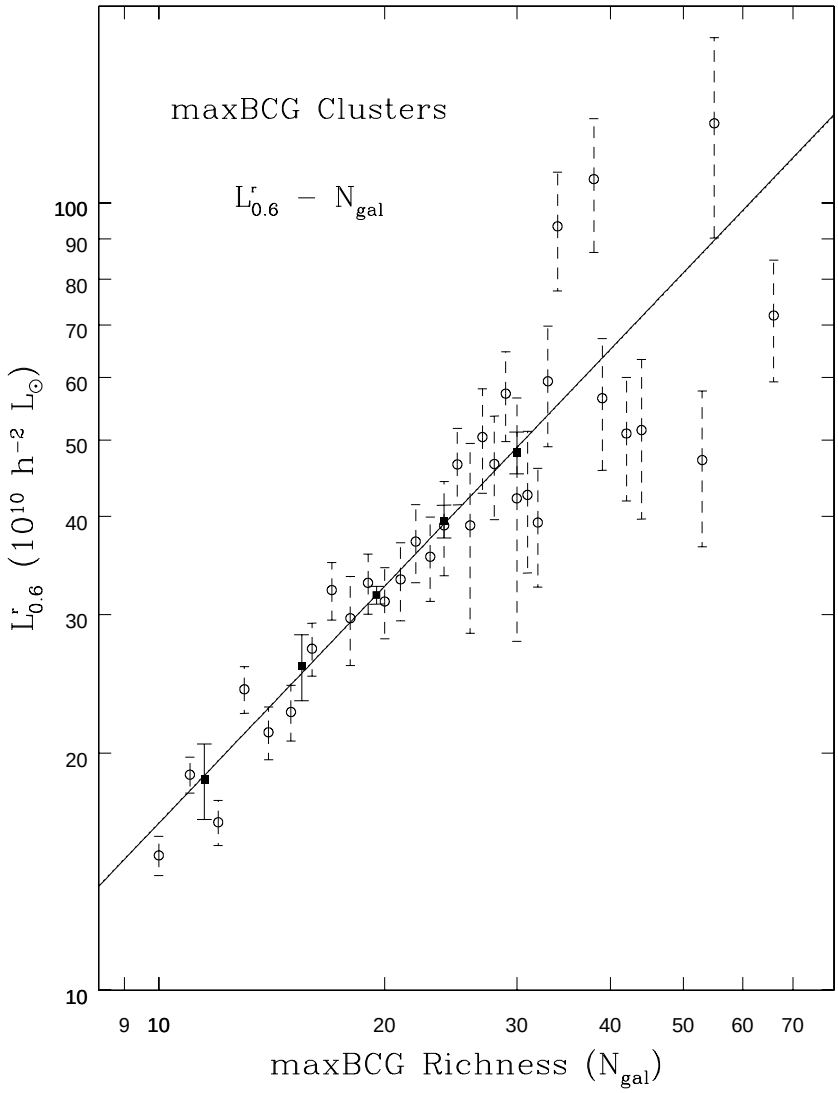

Fig. 8.— Observed cluster luminosity versus richness for maxBCG clusters. Cluster luminosity is observed in the r-band, within a radius of 0.6 h^{-1} Mpc, for stacked clusters at a given richness. The luminosities are k-corrected, background subtracted, and integrated down to $M_r = -19.8$. Dark squares represent binned data (in richness bins) of the stacked clusters. The solid line is the best-fit power-law relation (for the range $N_{gal} \simeq$ 10 - 33): $L^r_{0.6}(10^{10} L_\odot) = 1.6\ N_{gal}$ (Equation 2). (A similar relation is obtained when the N_{gal}>33 higher scatter clusters are added, shown by the dotted line which overlaps the solid line). The contribution of galaxies fainter than -19.8 adds a correction factor of 1.34 to the above luminosities (§4).

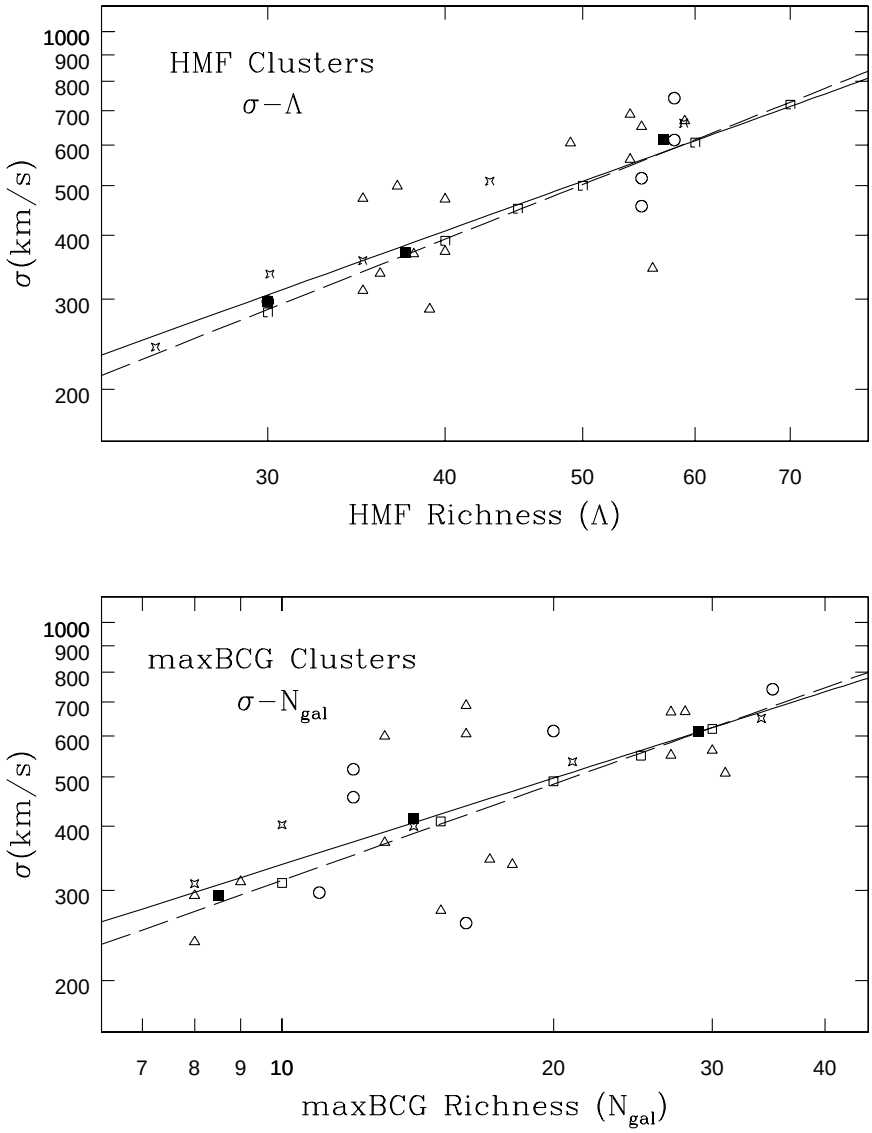

Fig. 9.— Relation between observed cluster velocity dispersion σ and cluster richness. Triangles are SDSS observed velocity dispersions, circles are Abell clusters, dark squares are medians, and the solid line is the best fit to the velocity data. Stars represent SDSS observations of Gaussian σ from stacked galaxy velocity differences (relative to the BCG velocity) in all clusters with available data (shown for comparison only). Typical uncertainties in the velocity dispersion measurements and the richness estimates are $\sim$20% (1-σ). The dashed line represents the expected relation based on the observed luminosity-richness relations (Figures 7 and 8) [followed by a conversion of luminosity to mass using mean M/L ratios and a conversion of mass to velocity dispersion using observed gravitational lensing calibration; see Bahcall et al. 2003].

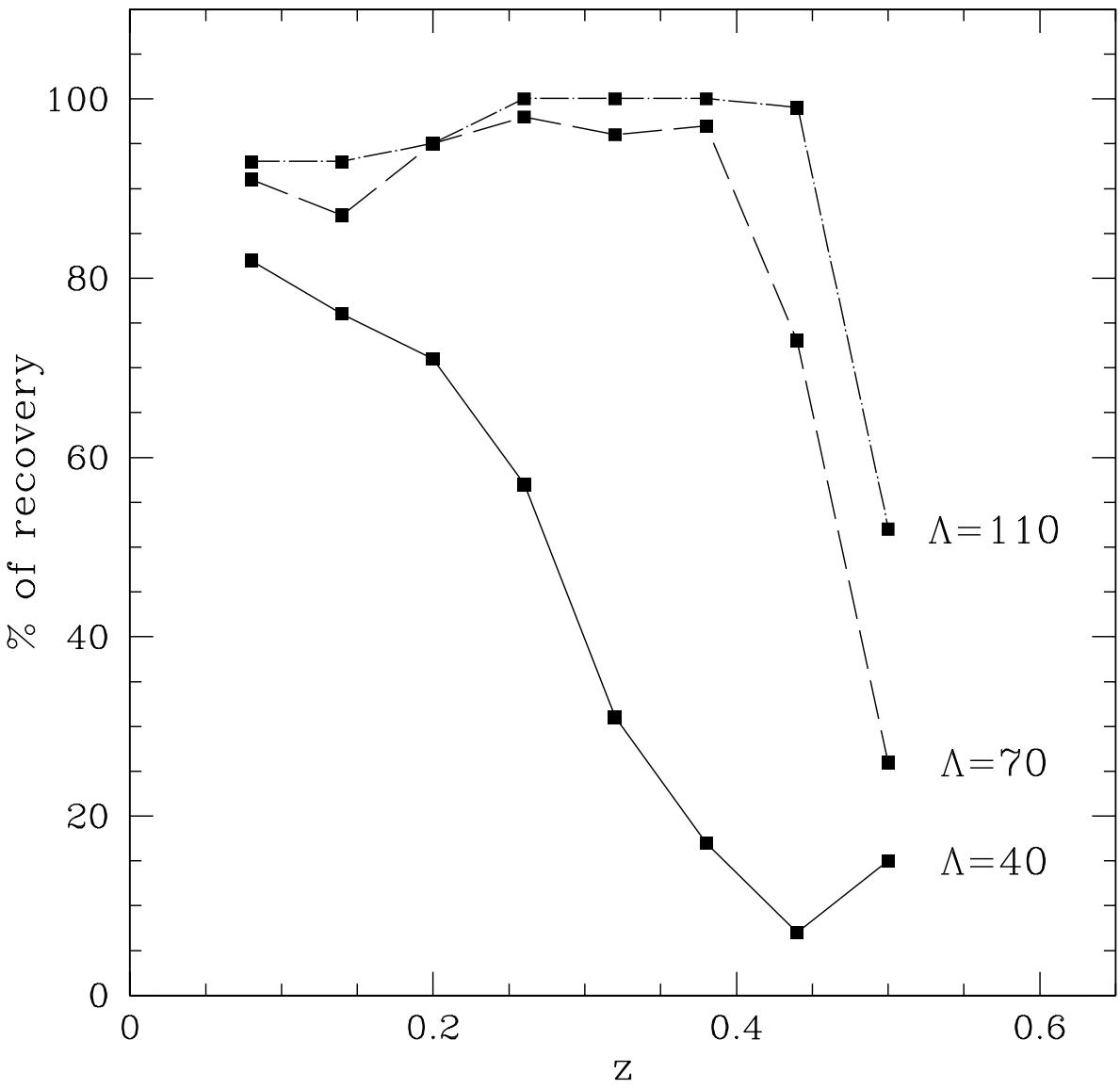

Fig. 10.— Selection function for HMF clusters as a function of redshift and richness; determined from cluster simulations (Kim et al. 2002).

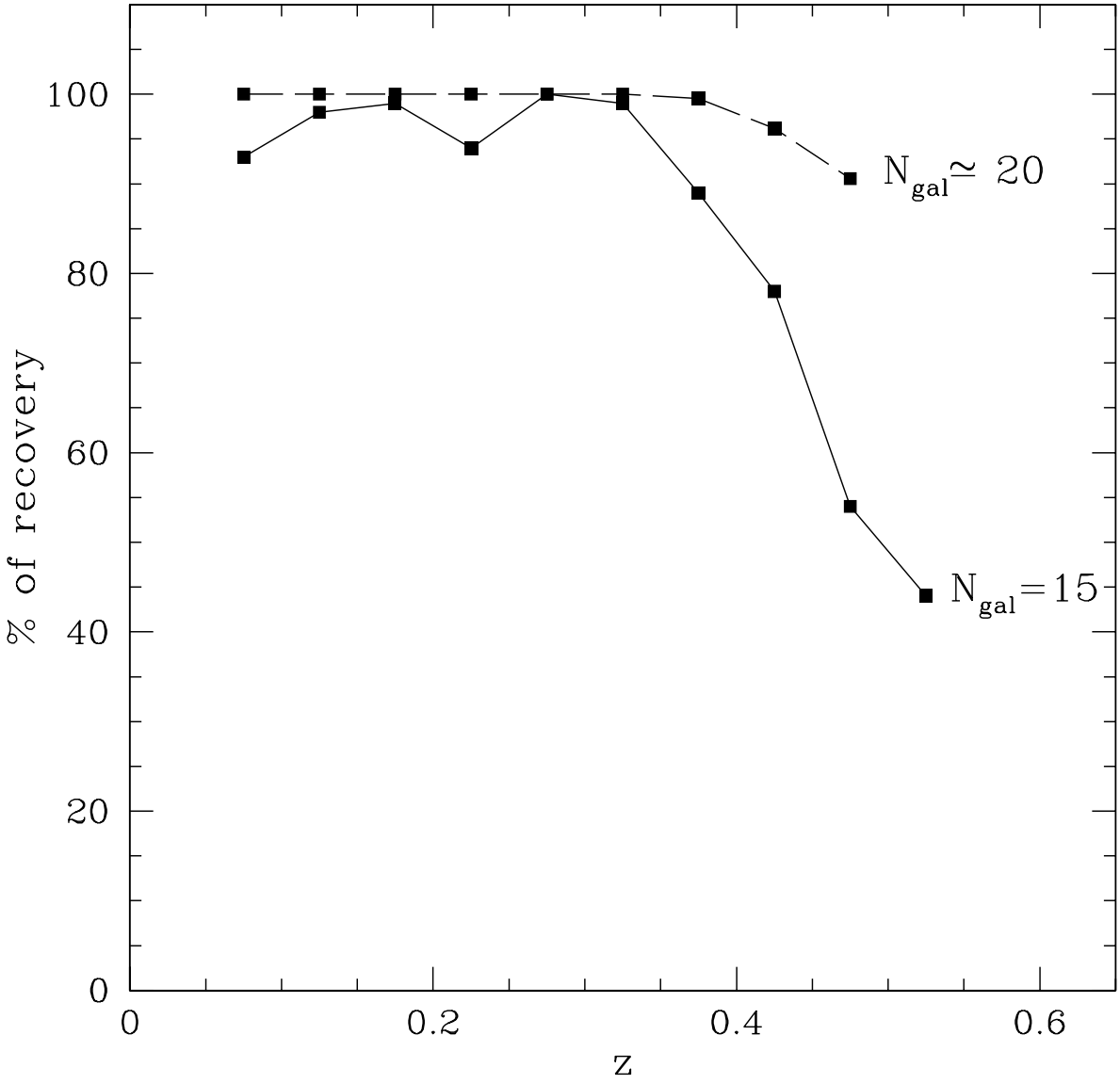

Fig. 11.— Selection function for maxBCG clusters, determined from simulations (Annis et al. 2003a).

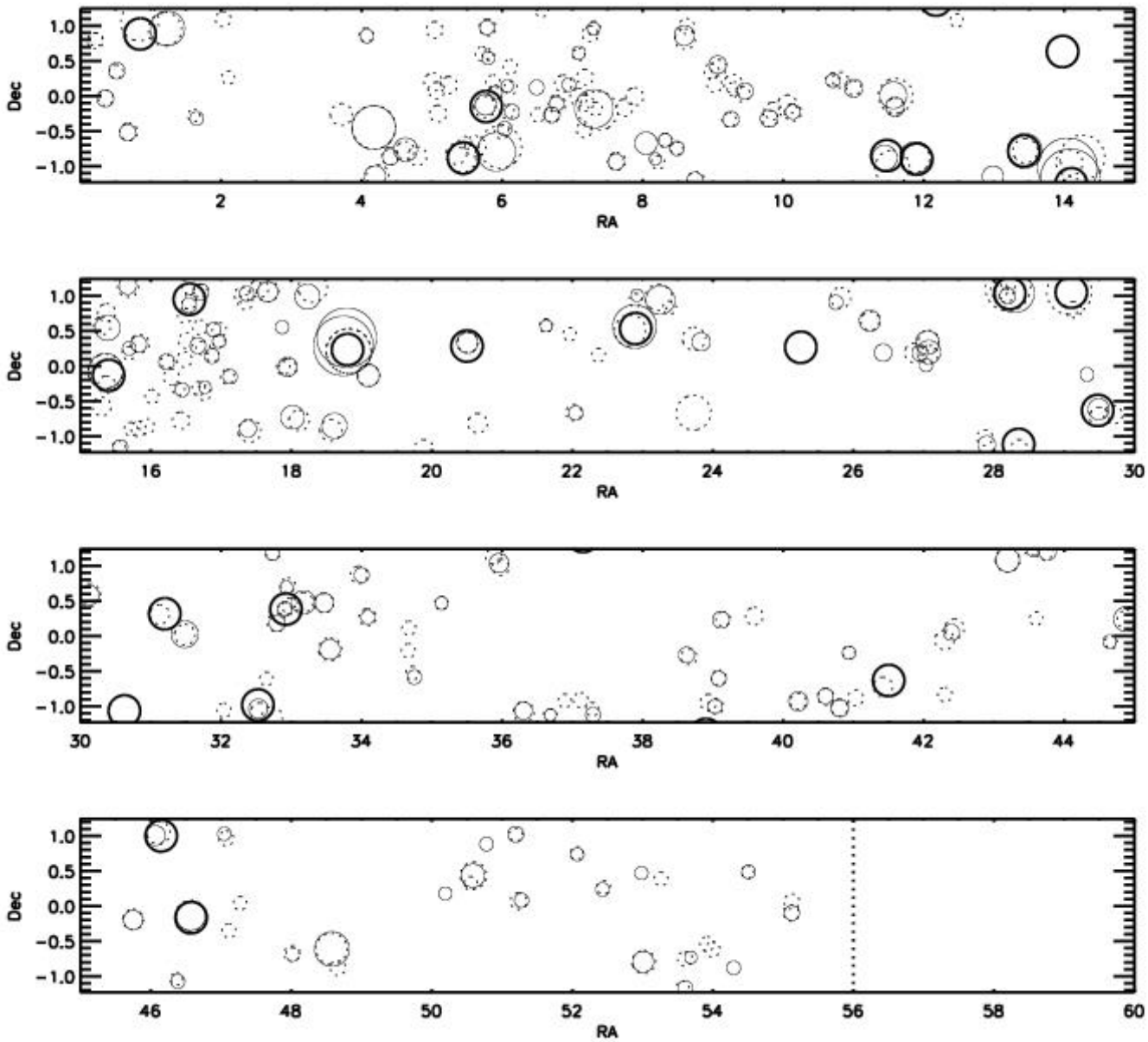

Fig. 12.— Overlay map of clusters in the merged catalog [z_{est} = 0.05 - 0.3, $\Lambda \geq 40$ (HMF), $N_{gal} \geq 13$ (maxBCG), and their matches]. Dotted circles are maxBCG clusters, solid circles are HMF clusters, and bold solid circles are Abell clusters in the survey area. All circles have a radius of 1 h^{-1} Mpc at the cluster redshift. (A redshift of 0.1 is assumed for the Abell clusters, many of which have no measured redshift.)

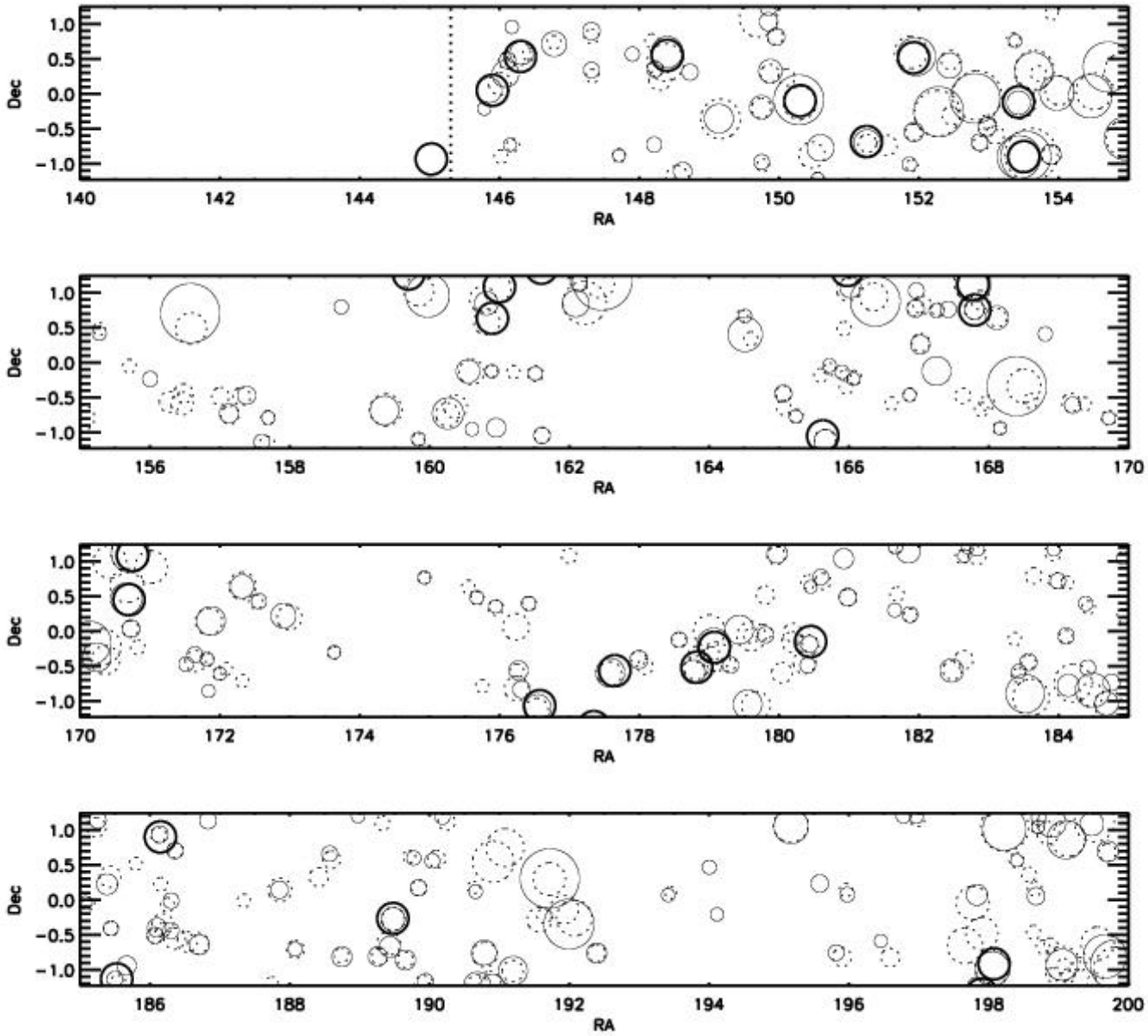

Fig. 12.— Continued

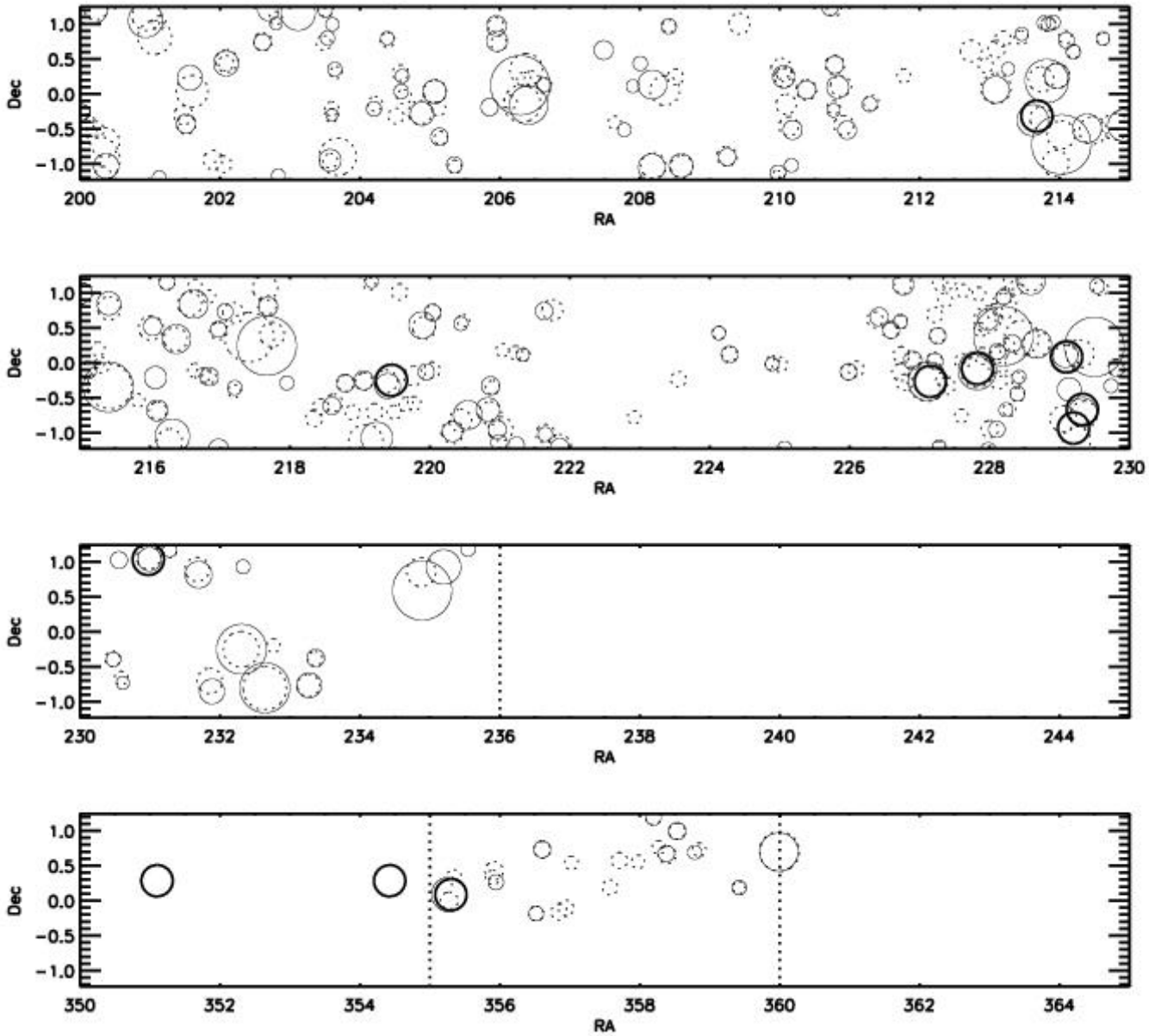

Fig. 12.— Continued

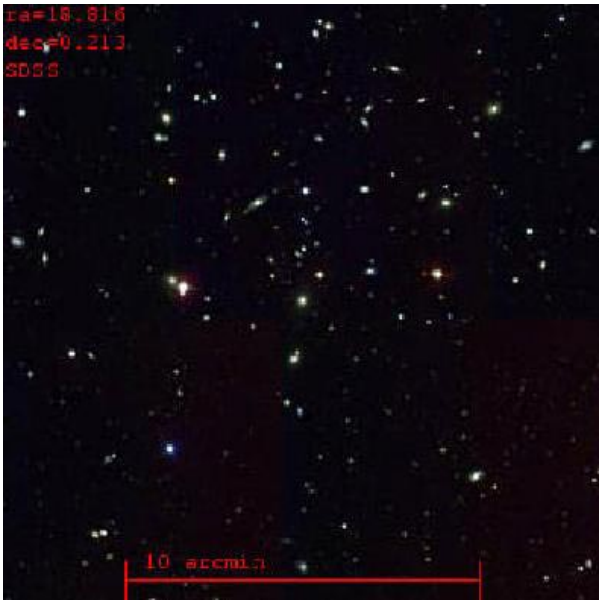

BH148 (z=0.045; H,b; Λ=55.1; N_{gal}=12; A168; RXC0114.9)

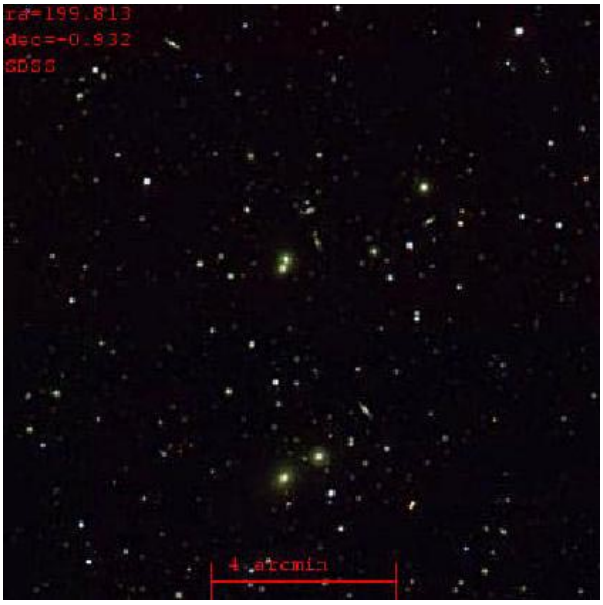

BH563 (z=0.082; H,B; Λ=59.3; N_{gal}=27)

BH1 (z=0.090; H; Λ=45.1; A2644; [RXC2341.1])

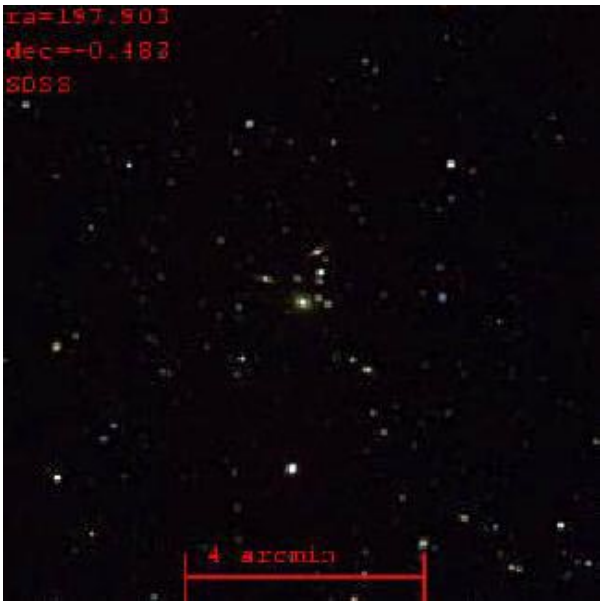

BH541 (z=0.090; B; N_{gal}=13)

Fig. 13.— Images of a sample of cataloged clusters in the redshift range z $\simeq$ 0.05 - 0.3. The clusters are ordered by increasing redshift.

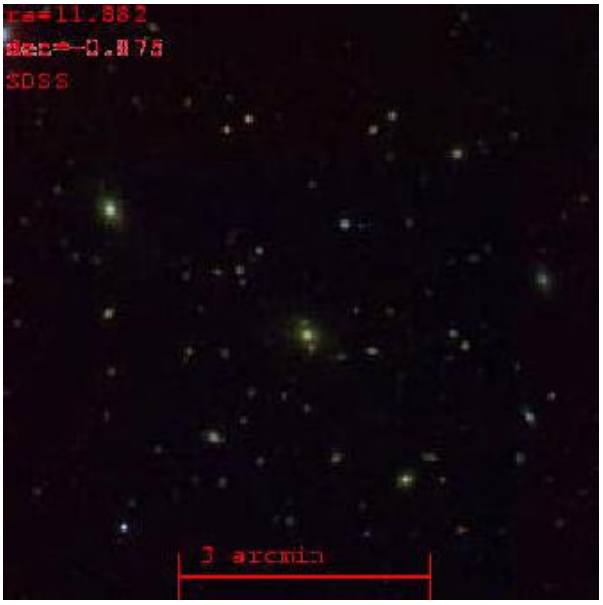

BH100 (z=0.117; H,B; Λ=43.0; N_{gal}=17; A101)

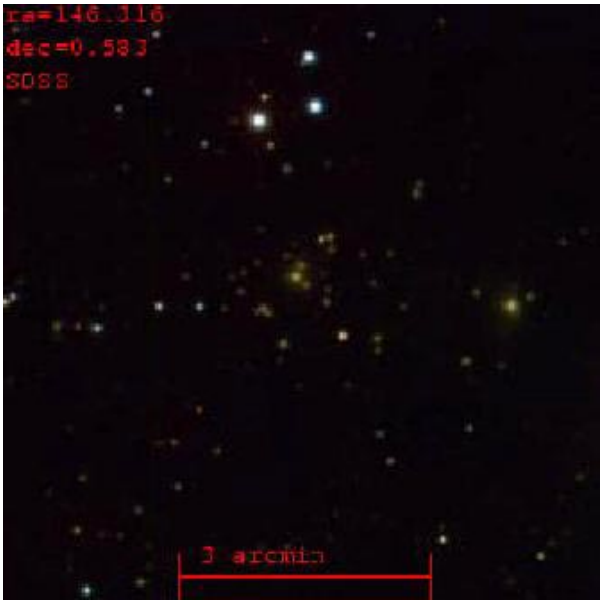

BH269 (z=0.121; H,B; Λ=55.2; N_{gal}=19; A867)

BH645 (z=0.127; H,B; Λ=52.5; N_{gal}=15)

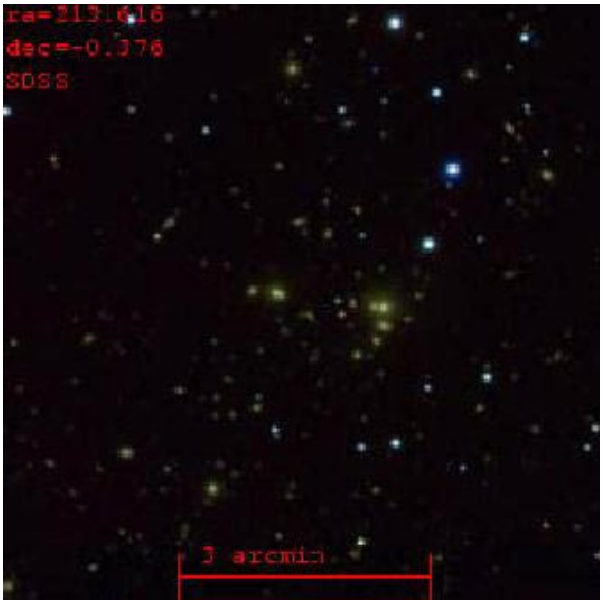

BH650 (z=0.139; H,B; Λ=87.2; N_{gal}=66; A1882)

Fig. 13.— Continued

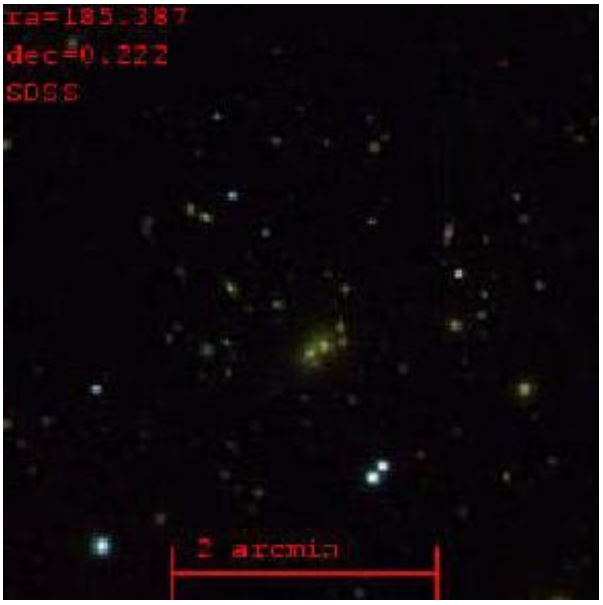

BH479 (z=0.157; H,B; Λ=67.6; N_{gal}=25)

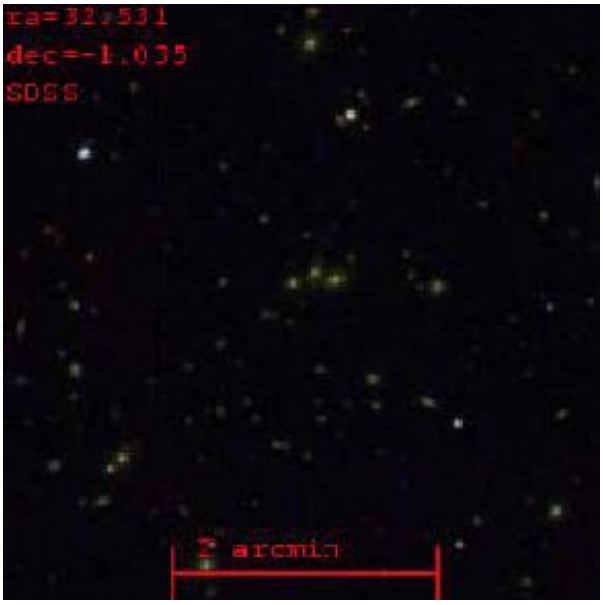

BH187 (z=0.174; H,B; Λ=67.2; N_{gal}=24; A315)

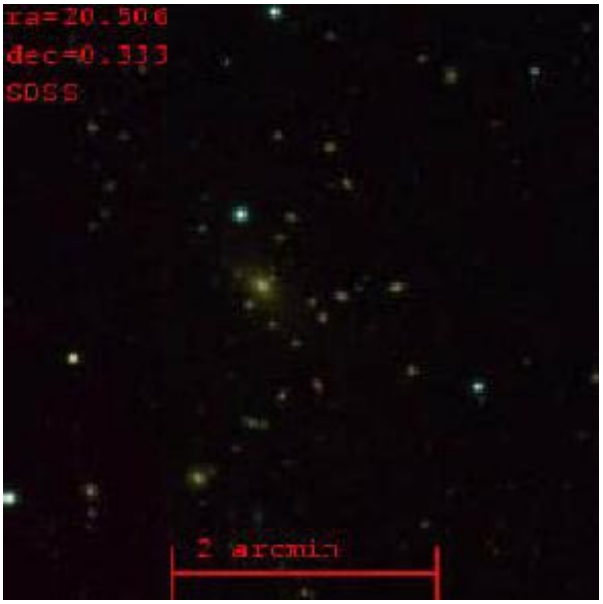

BH152 (z=0.175; H,B; Λ=46.7; N_{gal}=32; A181; RXC0121.9)

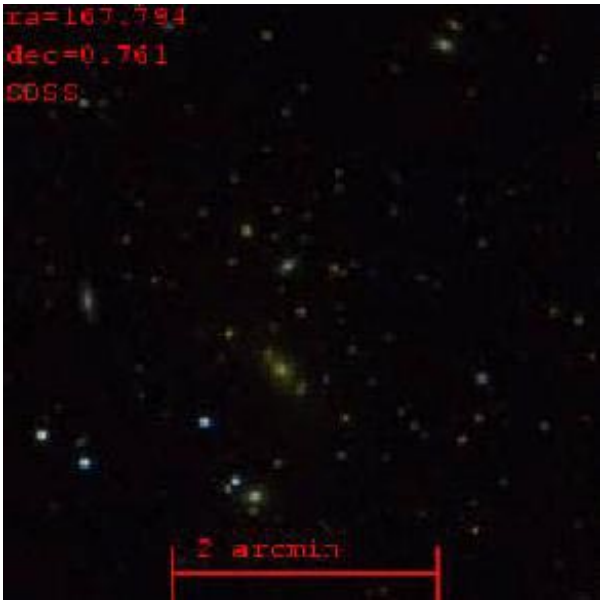

BH379 (z=0.185; H,B; Λ=76.0; N_{gal}=27; A1191)

Fig. 13.— Continued

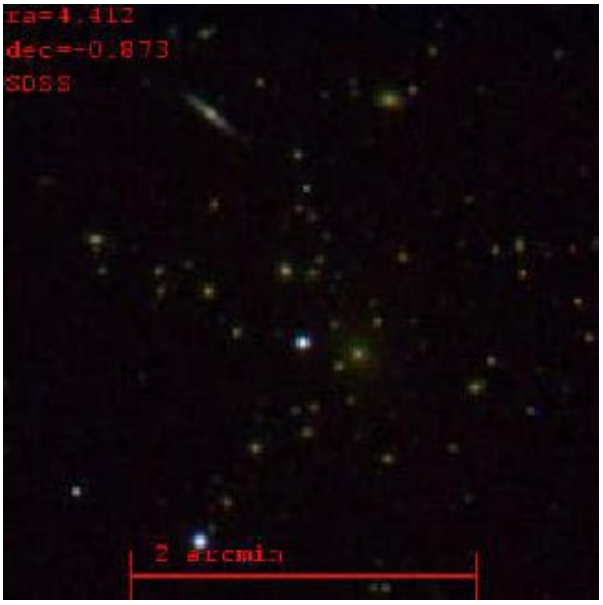

BH35 (z=0.210; H,B; Λ=62.2; N_{gal}=26)

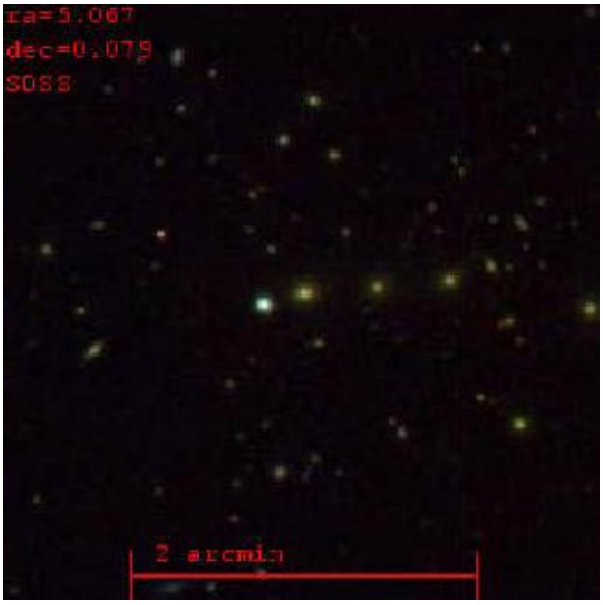

BH40 (z=0.210; B; N_{gal}=33; RXC0020.1)

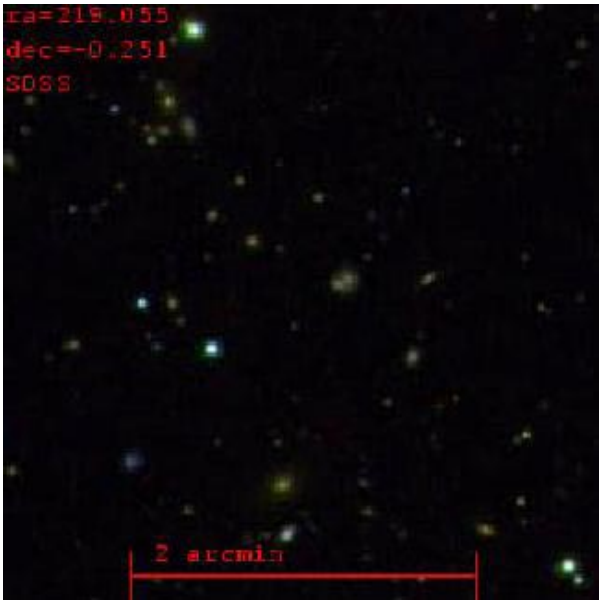

BH695 (z=0.219; H,B; Λ=66.2; N_{gal}=16)

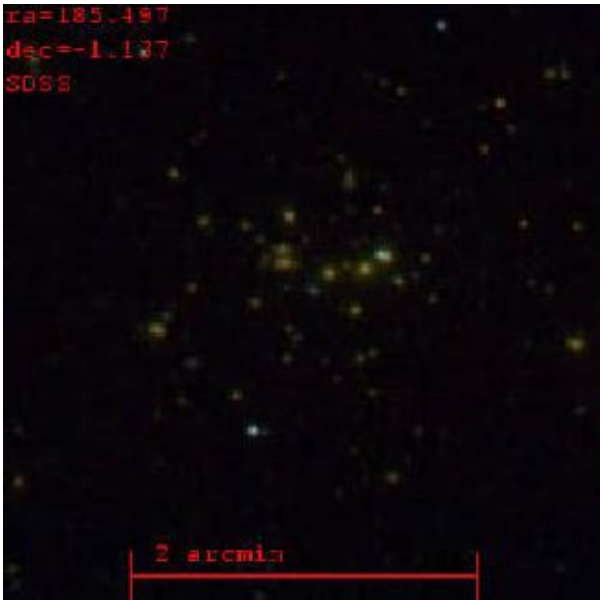

BH481 (z=0.225; H,B; Λ=79.0; N_{gal}=22; A1525)

Fig. 13.— Continued

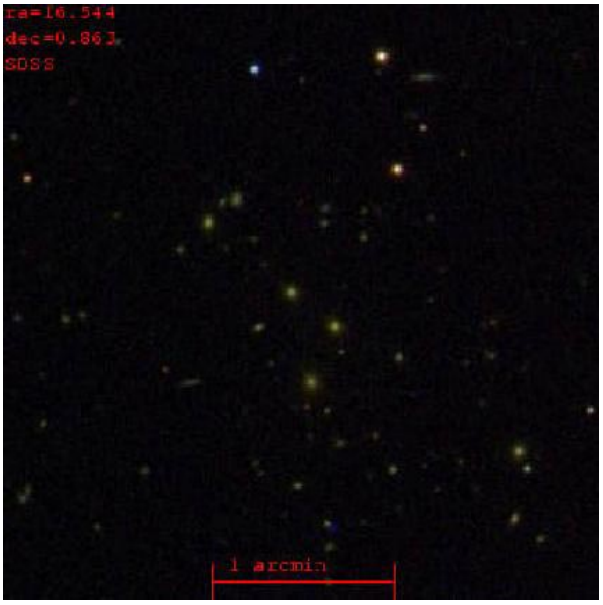

BH126 (z=0.264; H,B; Λ=61.8; N_{gal}=22; A142)

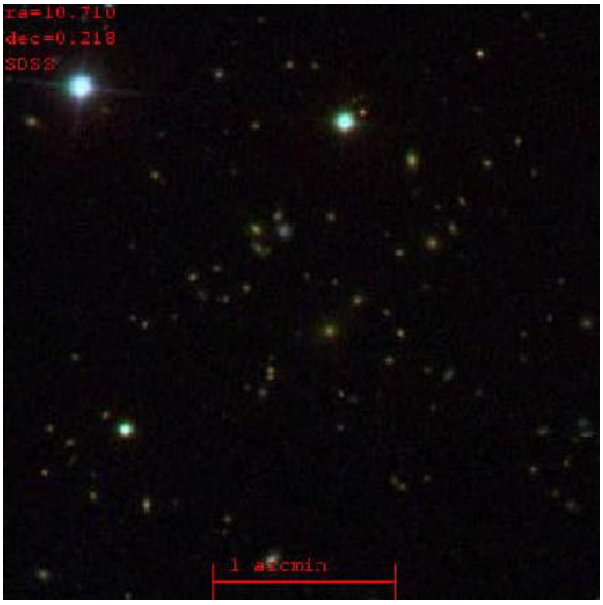

BH94 (z=0.268; H,B; Λ=69.0; N_{gal}=16)

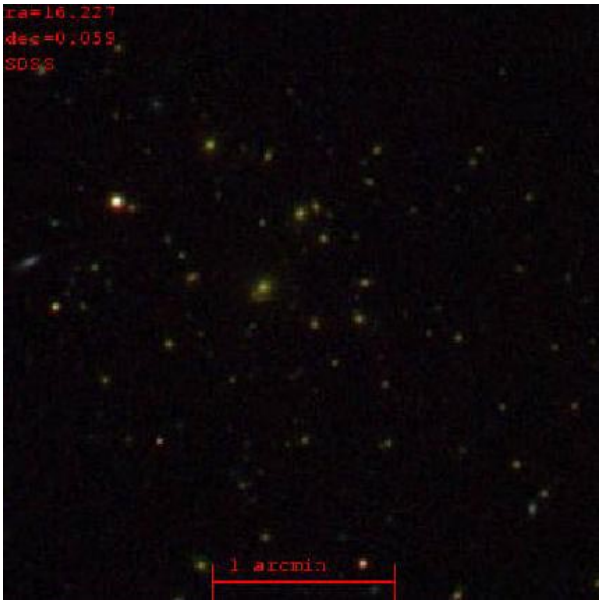

BH119 (z=0.276; H,b; Λ=77.4; N_{gal}=35)

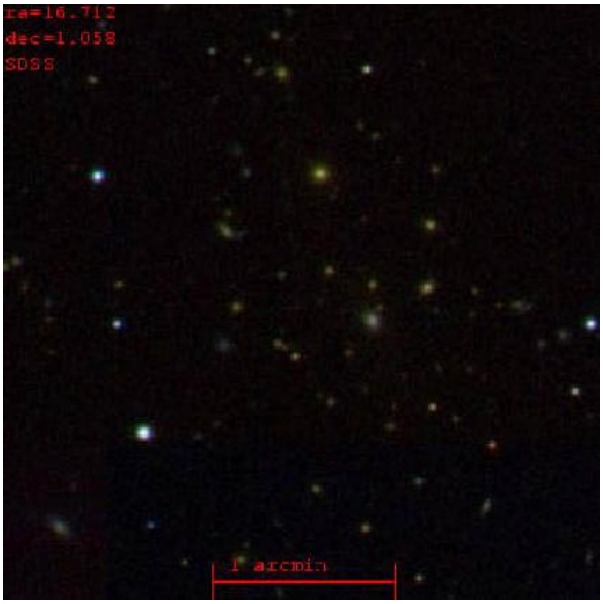

BH131 (z=0.286; H,B; Λ=50.9; N_{gal}=25; RXC0106.8)

Fig. 13.— Continued

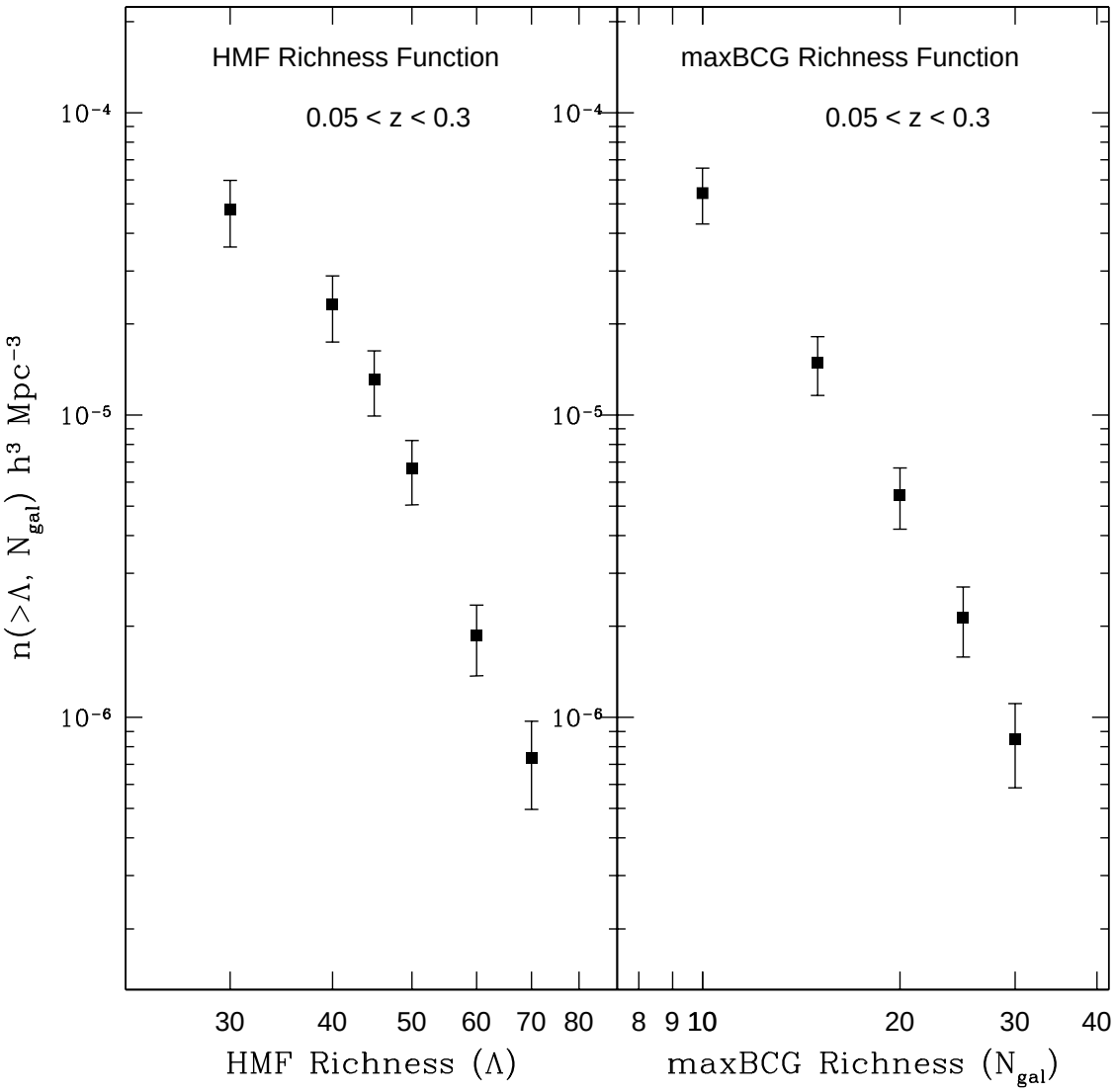

Fig. 14.— The richness function of HMF and maxBCG clusters. The function represents the abundance of z_{est} = 0.05 - 0.3 clusters above a given richness as a function of richness. The observed number of clusters has been corrected by the relevant selection function and the false-positive correction factor for each method. A flat cosmology with Ω_m= 0.3 is used for the volume determination.

Table 1. Cluster Mean Scaling Relations

Λ	N_{gal}	σ_v $(km\ s^{-1})$	$L_{0.6}^{tot}$ $(10^{11}h^{-2}L_\odot)$	$M_{0.6}$ $(10^{14}h^{-1}M_\odot)$
30	8	300	1.6	0.3
40	13	400	2.8	0.5
50	20	500	4.4	0.9
60	29	610	6.3	1.4
70	40	720	8.5	2.0

N_{gal}	Λ	σ_v $(km\ s^{-1})$	$L_{0.6}^{tot}$ $(10^{11}h^{-2}L_\odot)$	$M_{0.6}$ $(10^{14}h^{-1}M_\odot)$
10	35	350	2.1	0.35
15	43	430	3.2	0.6
20	50	500	4.4	0.9
25	56	560	5.5	1.2
30	61	620	6.6	1.5
40	70	730	8.7	2.2

Table 2. BH SDSS Cluster Catalog*

BH #	Method	α(H) (2000)	δ(H) (2000)	z_{hmf}	Λ	α(B) (2000)	δ(B) (2000)	z_{bcg}	N_{gal}	z_{spec}	Comments
1	H	355.271	0.088	0.09	45.1	0.000	0.000	0.000	0	0.000	A2644, (RXC 2341.1)
2	B	0.000	0.000	0.00	0.0	355.277	-0.002	0.205	16	0.190	
3	B	0.000	0.000	0.00	0.0	355.342	0.333	0.244	16	0.278	
4	B	0.000	0.000	0.00	0.0	355.916	0.424	0.190	13	0.186	
5	H,B	355.945	0.263	0.24	64.4	355.899	0.331	0.268	38	0.000	
6	H,B	356.518	-0.185	0.25	46.0	356.520	-0.186	0.257	17	0.266	
7	H,B	356.604	0.732	0.21	49.1	356.607	0.728	0.218	20	0.000	
8	B	0.000	0.000	0.00	0.0	356.847	-0.164	0.227	19	0.000	
9	B	0.000	0.000	0.00	0.0	356.944	-0.106	0.238	20	0.263	
10	B	0.000	0.000	0.00	0.0	357.021	0.540	0.281	14	0.000	
11	B	0.000	0.000	0.00	0.0	357.574	0.188	0.242	13	0.000	
12	B	0.000	0.000	0.00	0.0	357.709	0.573	0.225	13	0.000	
13	B	0.000	0.000	0.00	0.0	357.977	0.553	0.295	13	0.271	
14	H,b	358.195	1.187	0.24	42.6	358.194	1.193	0.238	11	0.000	
15	B	0.000	0.000	0.00	0.0	358.272	0.761	0.284	13	0.000	
16	H,B	358.381	0.673	0.22	40.2	358.391	0.651	0.199	18	0.228	
17	h,B	358.535	0.993	0.20	34.4	358.531	0.992	0.227	13	0.241	
18	H,B	358.784	0.690	0.27	42.8	358.849	0.727	0.286	14	0.272	
19	H,b	359.419	0.184	0.26	45.8	359.417	0.184	0.325	6	0.000	
20	H,b	359.988	0.696	0.08	41.0	359.995	0.702	0.077	10	0.084	
21	B	0.000	0.000	0.00	0.0	0.211	0.785	0.229	13	0.000	
22	B	0.000	0.000	0.00	0.0	0.219	0.804	0.286	17	0.000	
23	H,B	0.354	-0.036	0.21	44.0	0.360	-0.029	0.247	24	0.248	
24	h,B	0.516	0.359	0.22	36.5	0.508	0.347	0.284	13	0.301	
25	H,B	0.671	-0.521	0.22	40.4	0.686	-0.510	0.203	15	0.195	
26	B	0.000	0.000	0.00	0.0	0.844	1.058	0.081	13	0.079	
27	h,B	1.239	0.963	0.09	32.6	1.204	0.951	0.094	17	0.100	
28	H,b	1.655	-0.320	0.28	40.3	1.614	-0.277	0.329	7	0.000	
29	B	0.000	0.000	0.00	0.0	2.030	1.094	0.242	14	0.000	
30	B	0.000	0.000	0.00	0.0	2.102	0.261	0.299	13	0.000	
31	B	0.000	0.000	0.00	0.0	3.715	-0.264	0.153	13	0.155	
32	H,b	4.076	0.852	0.28	43.8	4.067	0.871	0.275	11	0.000	
33	h,B	4.172	-0.451	0.07	37.8	4.177	-0.445	0.070	13	0.063	
34	H,B	4.191	-1.142	0.16	43.7	4.228	-1.133	0.151	19	0.153	
35	H,B	4.412	-0.873	0.23	62.2	4.404	-0.854	0.207	26	0.210	
36	h,B	4.627	-0.764	0.14	36.7	4.622	-0.778	0.190	18	0.191	
37	B	0.000	0.000	0.00	0.0	4.792	-0.856	0.183	15	0.191	
38	B	0.000	0.000	0.00	0.0	5.019	0.200	0.194	20	0.207	
39	B	0.000	0.000	0.00	0.0	5.041	0.941	0.220	15	0.213	
40	B	0.000	0.000	0.00	0.0	5.067	0.079	0.220	33	0.210	RXC 0020.1
41	B	0.000	0.000	0.00	0.0	5.089	-0.253	0.212	17	0.210	
42	B	0.000	0.000	0.00	0.0	5.241	0.155	0.212	29	0.216	
43	B	0.000	0.000	0.00	0.0	5.348	-0.826	0.168	22	0.168	
44	B	0.000	0.000	0.00	0.0	5.427	-0.876	0.107	27	0.105	A23

Table 2—Continued

BH #	Method	α(H) (2000)	δ(H) (2000)	z_{hmf}	Λ	α(B) (2000)	δ(B) (2000)	z_{bcg}	N_{gal}	z_{spec}	Comments
45	B	0.000	0.000	0.00	0.0	5.471	-0.670	0.299	13	0.239	
46	B	0.000	0.000	0.00	0.0	5.622	-0.719	0.162	13	0.162	
47	B	0.000	0.000	0.00	0.0	5.723	0.601	0.262	13	0.000	
48	H,B	5.767	-0.123	0.16	68.0	5.752	-0.155	0.157	29	0.158	A25
49	H,b	5.784	0.975	0.26	42.2	5.794	0.976	0.216	9	0.227	
50	H,b	5.803	0.540	0.30	49.6	5.799	0.589	0.368	7	0.000	
51	B	0.000	0.000	0.00	0.0	5.872	0.199	0.268	20	0.000	
52	H,b	5.908	0.049	0.29	47.7	5.902	0.048	0.249	8	0.000	
53	h,B	5.915	-0.795	0.08	31.4	5.976	-0.725	0.072	14	0.064	
54	H,B	6.038	-0.466	0.26	45.6	5.996	-0.511	0.271	17	0.000	
55	B	0.000	0.000	0.00	0.0	6.114	0.414	0.260	15	0.260	
56	h,B	6.071	0.141	0.32	53.6	6.124	0.121	0.295	15	0.000	
57	H,b	6.144	-0.226	0.25	47.0	6.076	-0.223	0.275	12	0.231	
58	H	6.492	0.122	0.25	53.2	0.000	0.000	0.000	0	0.000	
59	B	0.000	0.000	0.00	0.0	6.511	-0.271	0.275	14	0.231	
60	B	0.000	0.000	0.00	0.0	6.565	1.221	0.290	17	0.000	
61	h,B	6.707	-0.266	0.23	38.9	6.703	-0.269	0.247	23	0.231	
62	H,B	6.774	-0.113	0.26	42.4	6.778	-0.115	0.201	17	0.000	
63	H,B	6.951	0.162	0.28	52.1	6.871	0.175	0.207	17	0.000	
64	B	0.000	0.000	0.00	0.0	7.088	-0.017	0.209	24	0.216	
65	H,b	7.092	0.616	0.29	44.5	7.091	0.589	0.336	13	0.000	
66	B	0.000	0.000	0.00	0.0	7.168	-0.483	0.240	13	0.230	
67	B	0.000	0.000	0.00	0.0	7.179	0.269	0.223	15	0.223	
68	B	0.000	0.000	0.00	0.0	7.185	-0.096	0.216	24	0.217	
69	B	0.000	0.000	0.00	0.0	7.254	0.882	0.229	18	0.000	
70	h,B	7.301	0.961	0.32	64.2	7.303	0.962	0.281	18	0.000	
71	H,B	7.309	-0.181	0.08	56.2	7.368	-0.213	0.079	17	0.060	
72	B	0.000	0.000	0.00	0.0	7.328	-0.182	0.281	13	0.000	
73	H,B	7.622	-0.940	0.23	44.0	7.631	-0.931	0.199	15	0.000	
74	B	0.000	0.000	0.00	0.0	7.737	-0.169	0.209	16	0.225	
75	B	0.000	0.000	0.00	0.0	7.887	-0.008	0.199	15	0.219	
76	H	8.048	-0.673	0.15	40.6	0.000	0.000	0.000	0	0.000	
77	h,B	8.182	-0.897	0.33	45.9	8.220	-0.945	0.286	13	0.000	
78	H,b	8.320	-0.631	0.29	50.0	8.321	-0.633	0.275	10	0.261	
79	H,b	8.488	-0.747	0.26	50.8	8.488	-0.744	0.329	10	0.000	
80	H,B	8.593	0.863	0.17	46.1	8.604	0.810	0.166	23	0.191	
81	B	0.000	0.000	0.00	0.0	8.625	0.994	0.242	13	0.000	
82	H,b	8.744	-1.199	0.23	44.3	8.757	-1.205	0.199	7	0.212	
83	B	0.000	0.000	0.00	0.0	8.980	0.356	0.253	20	0.259	
84	B	0.000	0.000	0.00	0.0	9.022	0.158	0.253	23	0.000	
85	h,B	9.068	0.445	0.20	39.1	9.083	0.405	0.231	20	0.258	
86	H,B	9.258	-0.334	0.23	41.9	9.231	-0.342	0.264	14	0.265	
87	B	0.000	0.000	0.00	0.0	9.287	0.174	0.188	13	0.194	
88	B	0.000	0.000	0.00	0.0	9.299	0.096	0.264	14	0.259	

Table 2—Continued

BH #	Method	α(H) (2000)	δ(H) (2000)	z_{hmf}	Λ	α(B) (2000)	δ(B) (2000)	z_{bcg}	N_{gal}	z_{spec}	Comments
89	H,B	9.457	0.069	0.22	52.3	9.418	0.028	0.242	20	0.256	
90	H,b	9.800	-0.322	0.20	42.4	9.811	-0.324	0.231	11	0.216	
91	B	0.000	0.000	0.00	0.0	9.852	-0.214	0.209	19	0.219	
92	B	0.000	0.000	0.00	0.0	10.061	-0.123	0.177	14	0.216	
93	H,B	10.137	-0.227	0.26	53.6	10.138	-0.233	0.209	16	0.238	
94	H,B	10.710	0.218	0.27	69.0	10.700	0.231	0.286	16	0.268	
95	B	0.000	0.000	0.00	0.0	10.814	0.229	0.231	14	0.000	
96	H,B	11.001	0.112	0.19	52.6	11.005	0.113	0.264	13	0.217	
97	h,B	11.444	-0.881	0.13	33.5	11.553	-1.020	0.090	17	0.111	A95
98	H,B	11.567	0.010	0.12	52.2	11.601	0.002	0.090	19	0.116	
99	H,B	11.594	-0.154	0.18	46.7	11.593	-0.155	0.199	16	0.218	
100	H,B	11.882	-0.875	0.10	43.0	11.881	-0.882	0.111	17	0.117	A101
101	B	0.000	0.000	0.00	0.0	12.469	1.077	0.297	22	0.302	
102	H	12.986	-1.146	0.16	46.3	0.000	0.000	0.000	0	0.000	
103	h,B	13.436	-0.781	0.09	36.2	13.443	-0.780	0.133	24	0.138	A112
104	H,b	14.086	-1.178	0.05	40.3	14.071	-0.953	0.122	10	0.140	A119
105	h,B	14.048	-1.023	0.05	36.7	14.259	-0.875	0.068	28	0.044	A119
106	B	0.000	0.000	0.00	0.0	15.303	-0.578	0.188	13	0.192	
107	h,B	15.387	0.542	0.13	33.2	15.308	0.574	0.199	14	0.199	
108	h,B	15.356	-0.068	0.09	39.1	15.359	-0.078	0.090	13	0.112	A130
109	B	0.000	0.000	0.00	0.0	15.371	-0.262	0.209	13	0.193	
110	B	0.000	0.000	0.00	0.0	15.372	0.760	0.199	14	0.200	
111	H,b	15.569	-1.152	0.26	40.2	15.546	-1.165	0.286	6	0.000	
112	H,B	15.672	1.145	0.20	57.7	15.679	1.136	0.155	16	0.144	
113	H,b	15.694	0.250	0.28	53.8	15.689	0.183	0.286	9	0.000	
114	B	0.000	0.000	0.00	0.0	15.718	-0.900	0.286	18	0.000	
115	B	0.000	0.000	0.00	0.0	15.827	-0.897	0.253	14	0.000	
116	H,B	15.831	0.312	0.23	45.6	15.847	0.319	0.188	16	0.238	
117	B	0.000	0.000	0.00	0.0	15.943	-0.860	0.242	14	0.000	
118	B	0.000	0.000	0.00	0.0	16.018	-0.435	0.275	30	0.279	
119	H,b	16.227	0.059	0.23	77.4	16.231	0.060	0.308	35	0.276	
120	B	0.000	0.000	0.00	0.0	16.293	-0.160	0.231	15	0.262	
121	B	0.000	0.000	0.00	0.0	16.430	-0.777	0.209	13	0.000	
122	H,b	16.447	-0.340	0.27	60.8	16.396	-0.331	0.340	16	0.326	
123	B	0.000	0.000	0.00	0.0	16.479	0.093	0.242	22	0.248	
124	B	0.000	0.000	0.00	0.0	16.484	0.715	0.264	16	0.251	
125	B	0.000	0.000	0.00	0.0	16.506	0.361	0.242	13	0.252	
126	H,B	16.544	0.863	0.25	61.8	16.549	0.914	0.264	22	0.000	A142
127	B	0.000	0.000	0.00	0.0	16.552	1.139	0.220	14	0.189	
128	H,B	16.671	0.290	0.23	48.0	16.748	0.255	0.275	15	0.270	
129	B	0.000	0.000	0.00	0.0	16.678	-0.324	0.286	15	0.278	
130	B	0.000	0.000	0.00	0.0	16.703	0.550	0.253	13	0.000	
131	H,B	16.712	1.058	0.22	50.9	16.711	1.070	0.286	25	0.000	RXC 0106.8

Table 2—Continued

BH #	Method	α(H) (2000)	δ(H) (2000)	z_{hmf}	Λ	α(B) (2000)	δ(B) (2000)	z_{bcg}	N_{gal}	z_{spec}	Comments
132	h,B	16.772	-0.304	0.33	49.0	16.758	-0.382	0.253	25	0.000	
133	H,B	16.871	0.142	0.25	42.8	16.878	0.156	0.297	15	0.296	
134	H,B	16.897	0.517	0.26	42.4	16.976	0.515	0.264	15	0.000	
135	H,b	16.972	0.351	0.29	50.0	16.968	0.357	0.329	17	0.313	
136	H,B	17.129	-0.153	0.26	41.0	17.087	-0.155	0.264	15	0.291	
137	B	0.000	0.000	0.00	0.0	17.346	0.908	0.253	15	0.264	
138	H,B	17.367	1.029	0.25	41.6	17.299	1.013	0.242	13	0.000	
139	H,b	17.384	-0.893	0.21	49.1	17.407	-0.922	0.144	8	0.109	
140	B	0.000	0.000	0.00	0.0	17.545	1.105	0.188	14	0.000	
141	h,B	17.664	1.056	0.17	34.6	17.666	1.067	0.155	19	0.178	
142	H	17.871	0.553	0.29	52.7	0.000	0.000	0.000	0	0.000	
143	B	0.000	0.000	0.00	0.0	17.885	-0.027	0.286	18	0.000	
144	H,b	17.948	-0.012	0.18	44.4	17.953	-0.018	0.209	10	0.178	
145	h,B	18.019	-0.730	0.14	36.5	18.112	-0.777	0.166	17	0.179	
146	H,b	18.230	0.988	0.13	42.0	18.306	1.109	0.111	9	0.133	(large spiral)
147	h,B	18.613	-0.851	0.13	37.2	18.562	-0.913	0.155	16	0.000	
148	H,b	18.742	0.287	0.05	55.1	18.816	0.213	0.068	12	0.045	A168, RXC 0114.9
149	H,b	18.787	0.404	0.05	42.6	18.816	0.213	0.068	12	0.045	A168, RXC 0114.9
150	h,B	19.098	-0.134	0.15	36.0	19.102	-0.133	0.155	16	0.177	
151	B	0.000	0.000	0.00	0.0	19.885	-1.185	0.177	15	0.186	
152	H,B	20.506	0.333	0.16	46.7	20.511	0.335	0.166	32	0.175	A181, RXC 0121.9
153	B	0.000	0.000	0.00	0.0	20.652	-0.814	0.177	22	0.173	
154	h,B	21.629	0.571	0.34	66.8	21.624	0.573	0.286	16	0.000	
155	B	0.000	0.000	0.00	0.0	21.962	0.453	0.297	14	0.287	
156	H,b	22.049	-0.671	0.26	42.0	22.020	-0.665	0.231	10	0.256	
157	B	0.000	0.000	0.00	0.0	22.371	0.154	0.286	16	0.286	
158	h,B	22.886	0.561	0.07	36.6	22.823	0.505	0.101	15	0.081	A208
159	h,B	22.920	1.007	0.32	43.6	22.899	0.936	0.297	15	0.293	
160	h,B	23.251	0.938	0.11	35.3	23.228	0.976	0.122	15	0.133	
161	B	0.000	0.000	0.00	0.0	23.379	0.830	0.297	18	0.000	
162	B	0.000	0.000	0.00	0.0	23.724	-0.665	0.090	14	0.086	
163	H,B	23.833	0.343	0.19	40.0	23.731	0.388	0.144	13	0.153	
164	H	25.749	0.906	0.26	41.0	0.000	0.000	0.000	0	0.000	
165	B	0.000	0.000	0.00	0.0	25.819	0.973	0.166	14	0.167	
166	h,B	26.233	0.643	0.16	33.0	26.237	0.642	0.188	14	0.211	
167	H	26.423	0.189	0.20	43.1	0.000	0.000	0.000	0	0.000	
168	H,B	26.944	0.186	0.23	41.4	26.867	0.187	0.177	13	0.185	
169	H	27.035	0.009	0.30	41.3	0.000	0.000	0.000	0	0.000	
170	h,B	27.051	0.333	0.14	27.6	27.069	0.358	0.166	16	0.206	
171	h,B	27.073	0.196	0.14	24.1	27.078	0.166	0.199	16	0.204	
172	H,b	27.895	-1.119	0.20	42.7	27.869	-1.018	0.231	6	0.000	
173	B	0.000	0.000	0.00	0.0	28.075	1.083	0.209	19	0.226	
174	H,B	28.195	0.997	0.23	73.4	28.175	1.007	0.264	29	0.230	A267, RXC 0152.7
175	B	0.000	0.000	0.00	0.0	28.210	1.212	0.199	13	0.227	

Table 2—Continued

BH #	Method	α(H) (2000)	δ(H) (2000)	z_{hmf}	Λ	α(B) (2000)	δ(B) (2000)	z_{bcg}	N_{gal}	z_{spec}	Comments
176	H,B	28.299	1.035	0.08	47.6	28.197	1.105	0.068	16	0.059	
177	B	0.000	0.000	0.00	0.0	28.357	-1.160	0.231	34	0.242	A268
178	B	0.000	0.000	0.00	0.0	29.071	1.051	0.068	19	0.079	A279
179	B	0.000	0.000	0.00	0.0	29.129	0.803	0.220	27	0.220	
180	H	29.324	-0.122	0.28	50.0	0.000	0.000	0.000	0	0.000	
181	H,B	29.488	-0.614	0.16	50.3	29.497	-0.724	0.177	29	0.187	A284
182	B	0.000	0.000	0.00	0.0	29.695	-0.695	0.188	18	0.191	
183	H,b	30.129	0.581	0.18	56.9	30.126	0.582	0.144	12	0.164	
184	B	0.000	0.000	0.00	0.0	31.126	0.305	0.177	15	0.173	A299
185	h,B	31.484	0.025	0.12	27.5	31.486	0.019	0.166	15	0.173	
186	B	0.000	0.000	0.00	0.0	32.040	-1.059	0.264	13	0.000	
187	H,B	32.531	-1.035	0.18	67.2	32.556	-1.090	0.177	24	0.174	A315
188	B	0.000	0.000	0.00	0.0	32.646	-0.609	0.286	23	0.284	
189	B	0.000	0.000	0.00	0.0	32.727	-1.157	0.166	24	0.173	
190	H,b	32.735	1.178	0.26	49.7	32.736	1.168	0.308	15	0.000	
191	h,B	32.799	0.180	0.23	37.6	32.794	0.192	0.188	13	0.112	
192	H,B	32.908	0.386	0.26	46.3	32.906	0.387	0.297	14	0.000	A321
193	H,b	32.931	0.691	0.30	48.4	32.951	0.722	0.253	9	0.000	
194	B	0.000	0.000	0.00	0.0	32.986	0.426	0.220	14	0.000	
195	H,B	33.174	0.480	0.14	42.6	33.175	0.475	0.177	15	0.149	
196	H,B	33.468	0.475	0.18	41.4	33.464	0.467	0.177	19	0.182	
197	H,B	33.549	-0.193	0.17	48.7	33.553	-0.189	0.144	15	0.141	
198	H,B	34.002	0.867	0.25	40.2	33.964	0.870	0.209	22	0.212	
199	H,b	34.090	0.267	0.28	44.6	34.085	0.266	0.209	12	0.243	
200	B	0.000	0.000	0.00	0.0	34.666	-0.209	0.275	13	0.000	
201	B	0.000	0.000	0.00	0.0	34.675	0.114	0.275	20	0.272	
202	h,B	34.751	-0.586	0.26	30.0	34.723	-0.529	0.286	13	0.273	
203	h,B	35.139	0.468	0.31	48.8	35.137	0.468	0.286	23	0.272	
204	B	0.000	0.000	0.00	0.0	35.877	1.134	0.231	14	0.000	
205	h,B	35.957	1.039	0.18	36.0	35.980	0.978	0.220	13	0.000	
206	H,b	36.304	-1.064	0.20	45.5	36.309	-1.086	0.166	8	0.169	
207	h,B	36.687	-1.123	0.34	52.1	36.685	-1.132	0.286	19	0.000	
208	B	0.000	0.000	0.00	0.0	36.892	-0.922	0.286	13	0.000	
209	B	0.000	0.000	0.00	0.0	37.118	-0.913	0.253	14	0.300	
210	h,B	37.293	-1.124	0.25	37.1	37.284	-1.045	0.286	14	0.000	
211	h,B	38.623	-0.271	0.23	37.9	38.661	-0.296	0.231	16	0.245	
212	B	0.000	0.000	0.00	0.0	38.936	-0.947	0.220	15	0.000	
213	H,B	39.032	-1.002	0.27	47.3	39.036	-1.007	0.231	18	0.251	
214	H,b	39.084	-0.608	0.25	41.6	39.084	-0.591	0.253	7	0.244	
215	h,B	39.116	0.229	0.21	31.3	39.144	0.242	0.264	17	0.270	
216	B	0.000	0.000	0.00	0.0	39.588	0.282	0.199	13	0.000	
217	h,B	40.213	-0.930	0.18	35.2	40.213	-0.932	0.231	19	0.240	
218	h,B	40.604	-0.855	0.24	37.0	40.606	-0.865	0.220	13	0.000	
219	H,B	40.806	-1.028	0.20	45.4	40.801	-1.020	0.220	22	0.239	

Table 2—Continued

BH #	Method	α(H) (2000)	δ(H) (2000)	z_{hmf}	Λ	α(B) (2000)	δ(B) (2000)	z_{bcg}	N_{gal}	z_{spec}	Comments
220	H,b	40.935	-0.240	0.29	42.8	40.934	-0.236	0.341	19	0.377	
221	B	0.000	0.000	0.00	0.0	41.030	-0.883	0.231	14	0.000	
222	B	0.000	0.000	0.00	0.0	41.418	-0.723	0.177	25	0.182	A381
223	B	0.000	0.000	0.00	0.0	42.296	-0.057	0.177	19	0.175	
224	B	0.000	0.000	0.00	0.0	42.301	-0.835	0.264	13	0.272	
225	H,B	42.392	0.051	0.22	49.2	42.438	0.102	0.177	13	0.185	
226	H,b	43.194	1.081	0.14	40.6	43.192	1.085	0.133	10	0.137	
227	H,b	43.554	1.229	0.29	50.8	43.528	1.243	0.275	11	0.000	
228	B	0.000	0.000	0.00	0.0	43.599	0.248	0.297	17	0.361	
229	H,B	43.759	1.203	0.20	46.0	43.713	1.204	0.199	13	0.000	
230	H,b	44.644	-0.082	0.29	48.7	44.669	-0.088	0.308	6	0.000	
231	h,B	44.883	0.239	0.13	37.9	44.886	0.232	0.188	29	0.193	
232	H,b	45.750	-0.199	0.18	44.5	45.748	-0.193	0.166	9	0.158	
233	H,B	46.065	1.003	0.17	44.4	46.109	1.046	0.144	17	0.153	A411
234	H,b	46.386	-1.074	0.27	57.2	46.369	-1.039	0.340	20	0.000	
235	H,B	46.571	-0.141	0.11	42.7	46.572	-0.140	0.101	21	0.110	A412
236	h,B	47.046	1.029	0.29	38.6	47.074	0.963	0.253	13	0.000	
237	B	0.000	0.000	0.00	0.0	47.113	-0.353	0.275	13	0.000	
238	B	0.000	0.000	0.00	0.0	47.272	0.038	0.286	20	0.000	
239	B	0.000	0.000	0.00	0.0	48.011	-0.678	0.231	13	0.000	
240	B	0.000	0.000	0.00	0.0	48.020	-0.689	0.286	17	0.000	
241	h,B	48.578	-0.613	0.09	25.7	48.573	-0.610	0.101	13	0.115	
242	B	0.000	0.000	0.00	0.0	48.663	-0.879	0.242	19	0.000	
243	H	50.193	0.178	0.30	49.4	0.000	0.000	0.000	0	0.000	
244	B	0.000	0.000	0.00	0.0	50.553	0.323	0.286	13	0.305	
245	h,B	50.585	0.432	0.14	39.5	50.594	0.437	0.122	16	0.131	
246	H	50.777	0.882	0.28	40.7	0.000	0.000	0.000	0	0.000	
247	h,B	51.194	1.022	0.23	36.7	51.194	1.017	0.297	20	0.000	
248	h,B	51.277	0.080	0.26	36.6	51.234	0.068	0.220	16	0.213	
249	H,b	52.072	0.733	0.30	58.6	52.062	0.751	0.308	25	0.315	
250	H,B	52.429	0.236	0.28	52.5	52.446	0.265	0.297	21	0.320	
251	H	52.983	0.469	0.29	40.9	0.000	0.000	0.000	0	0.000	
252	H,B	53.006	-0.794	0.16	46.4	53.017	-0.799	0.144	14	0.160	
253	B	0.000	0.000	0.00	0.0	53.262	0.386	0.286	19	0.332	
254	h,B	53.685	-0.733	0.32	78.1	53.602	-0.753	0.253	21	0.267	
255	H,b	53.605	-1.166	0.25	61.7	53.571	-1.157	0.329	7	0.000	
256	B	0.000	0.000	0.00	0.0	53.918	-0.539	0.264	13	0.270	
257	B	0.000	0.000	0.00	0.0	53.993	-0.620	0.253	17	0.279	
258	H	54.295	-0.881	0.28	40.6	0.000	0.000	0.000	0	0.000	
259	H,b	54.507	0.486	0.28	46.6	54.493	0.483	0.329	18	0.323	
260	h,B	55.125	-0.100	0.25	35.9	55.114	-0.102	0.231	15	0.000	
261	B	0.000	0.000	0.00	0.0	55.124	0.063	0.242	17	0.000	
262	H	145.785	-0.212	0.29	55.6	0.000	0.000	0.000	0	0.000	

Table 2—Continued

BH #	Method	α(H) (2000)	δ(H) (2000)	z_{hmf}	Λ	α(B) (2000)	δ(B) (2000)	z_{bcg}	N_{gal}	z_{spec}	Comments
263	H	145.854	0.050	0.13	54.9	0.000	0.000	0.000	0	0.000	A861
264	h,B	146.087	0.284	0.12	28.7	146.006	0.146	0.148	20	0.127	(A861)
265	B	0.000	0.000	0.00	0.0	146.022	-0.900	0.277	13	0.000	
266	H,b	146.114	0.477	0.22	43.4	146.106	0.471	0.209	6	0.000	
267	H,b	146.147	-0.732	0.30	67.9	146.191	-0.737	0.305	6	0.000	
268	H	146.178	0.957	0.28	43.9	0.000	0.000	0.000	0	0.000	
269	H,B	146.316	0.583	0.14	55.2	146.275	0.581	0.138	19	0.121	A867
270	B	0.000	0.000	0.00	0.0	146.425	0.567	0.295	13	0.263	
271	B	0.000	0.000	0.00	0.0	146.781	0.738	0.284	19	0.262	
272	H	146.782	0.713	0.13	45.2	0.000	0.000	0.000	0	0.000	
273	H,b	147.314	0.896	0.20	42.4	147.318	0.822	0.255	12	0.225	
274	H,b	147.316	0.340	0.23	56.2	147.330	0.253	0.286	11	0.000	
275	h,B	147.710	-0.881	0.31	57.2	147.709	-0.888	0.290	21	0.271	
276	H	147.901	0.567	0.26	40.7	0.000	0.000	0.000	0	0.000	
277	B	0.000	0.000	0.00	0.0	148.179	0.757	0.273	13	0.000	
278	H	148.212	-0.728	0.24	43.2	0.000	0.000	0.000	0	0.000	
279	H,b	148.225	0.351	0.22	44.9	148.233	0.358	0.247	11	0.255	
280	B	0.000	0.000	0.00	0.0	148.293	0.204	0.153	13	0.163	
281	H,B	148.399	0.596	0.10	50.2	148.377	0.449	0.083	15	0.080	A892
282	H,B	148.622	-1.111	0.19	41.8	148.542	-1.195	0.146	15	0.138	
283	H	148.727	0.309	0.22	44.6	0.000	0.000	0.000	0	0.000	
284	H,B	149.139	-0.354	0.11	41.3	149.161	-0.358	0.077	20	0.088	
285	B	0.000	0.000	0.00	0.0	149.704	1.081	0.081	14	0.079	
286	H,B	149.747	-0.193	0.14	42.8	149.746	-0.206	0.175	25	0.170	
287	H,b	149.750	-0.976	0.24	40.5	149.768	-1.026	0.308	8	0.000	
288	H	149.849	1.240	0.21	45.2	0.000	0.000	0.000	0	0.000	
289	H	149.850	1.030	0.19	49.9	0.000	0.000	0.000	0	0.000	
290	h,B	149.875	0.325	0.14	35.5	149.867	0.287	0.188	16	0.169	
291	H,B	149.957	0.815	0.20	51.4	149.949	0.819	0.233	17	0.219	
292	B	0.000	0.000	0.00	0.0	150.108	0.234	0.216	20	0.221	
293	H,B	150.282	-0.087	0.06	55.9	150.297	-0.133	0.094	15	0.090	A912
294	h,B	150.593	-0.775	0.12	29.8	150.470	-0.878	0.124	14	0.136	
295	H,b	150.552	-1.222	0.29	43.7	150.557	-1.210	0.334	7	0.000	
296	H,B	151.261	-0.706	0.12	42.7	151.262	-0.709	0.192	28	0.196	A919
297	B	0.000	0.000	0.00	0.0	151.540	-0.740	0.166	13	0.188	
298	H,b	151.862	-1.010	0.26	43.2	151.904	-1.027	0.338	11	0.377	
299	H,B	151.927	-0.548	0.18	40.3	151.926	-0.552	0.216	13	0.221	
300	H,B	151.962	0.534	0.08	56.7	151.886	0.594	0.096	33	0.000	A933
301	h,B	152.284	-0.257	0.06	39.9	152.266	-0.280	0.066	13	0.068	
302	h,B	152.438	0.402	0.13	37.4	152.451	0.484	0.183	13	0.186	
303	B	0.000	0.000	0.00	0.0	152.463	-0.312	0.190	15	0.102	
304	H,b	152.804	-0.066	0.06	45.6	152.833	-0.023	0.061	8	0.000	
305	h,B	152.868	-0.693	0.21	37.9	152.888	-0.717	0.229	14	0.216	
306	H,B	152.973	-0.472	0.19	54.3	152.987	-0.474	0.188	25	0.000	

Table 2—Continued

BH #	Method	α(H) (2000)	δ(H) (2000)	z_{hmf}	Λ	α(B) (2000)	δ(B) (2000)	z_{bcg}	N_{gal}	z_{spec}	Comments
307	B	0.000	0.000	0.00	0.0	152.980	-0.403	0.260	25	0.000	
308	B	0.000	0.000	0.00	0.0	153.087	-0.588	0.186	19	0.000	
309	H,b	153.379	0.755	0.30	47.9	153.352	0.772	0.292	10	0.000	
310	H,B	153.426	-0.129	0.14	80.6	153.437	-0.120	0.094	21	0.101	A954
311	H	153.430	-0.907	0.07	71.6	0.000	0.000	0.000	0	0.000	
312	H,B	153.530	-0.895	0.06	58.6	153.607	-0.872	0.057	35	0.048	A957
313	H,b	153.638	0.317	0.08	43.1	153.655	0.342	0.079	11	0.071	
314	B	0.000	0.000	0.00	0.0	153.711	0.286	0.233	13	0.271	
315	H,B	153.889	-0.866	0.17	46.8	153.895	-0.879	0.181	16	0.180	
316	B	0.000	0.000	0.00	0.0	153.902	1.150	0.297	14	0.000	
317	H,b	153.976	0.011	0.09	41.9	154.015	0.047	0.109	10	0.094	
318	H,B	154.451	-0.036	0.07	45.4	154.508	0.034	0.085	17	0.071	
319	h,B	154.705	0.385	0.06	38.8	154.908	0.332	0.090	14	0.096	
320	h,B	154.964	-0.638	0.07	32.9	154.934	-0.638	0.087	15	0.094	
321	B	0.000	0.000	0.00	0.0	155.016	-0.793	0.120	13	0.127	
322	H,b	155.276	0.415	0.27	48.2	155.277	0.478	0.319	14	0.308	
323	B	0.000	0.000	0.00	0.0	155.707	-0.054	0.286	14	0.311	
324	H	156.003	-0.236	0.24	48.6	0.000	0.000	0.000	0	0.000	
325	B	0.000	0.000	0.00	0.0	156.288	-0.565	0.157	15	0.158	
326	B	0.000	0.000	0.00	0.0	156.464	-0.588	0.146	22	0.159	
327	B	0.000	0.000	0.00	0.0	156.481	-0.443	0.179	18	0.170	
328	h,B	156.577	0.706	0.05	29.9	156.589	0.488	0.101	13	0.098	
329	B	0.000	0.000	0.00	0.0	157.009	-0.485	0.199	21	0.000	
330	H,B	157.131	-0.731	0.18	51.6	157.147	-0.752	0.192	23	0.222	
331	H,b	157.383	-0.472	0.19	47.3	157.311	-0.486	0.199	8	0.000	
332	H,b	157.602	-1.136	0.23	43.3	157.675	-1.170	0.231	8	0.000	
333	H,b	157.692	-0.790	0.29	46.6	157.686	-0.792	0.273	8	0.000	
334	H	158.736	0.794	0.26	40.0	0.000	0.000	0.000	0	0.000	
335	H,b	159.355	-0.685	0.11	46.3	159.374	-0.678	0.098	12	0.096	
336	H,b	159.841	-1.097	0.27	42.5	159.837	-1.104	0.334	10	0.385	
337	H,b	159.973	0.958	0.07	40.7	159.848	1.023	0.105	12	0.111	
338	H,B	160.264	-0.729	0.10	44.0	160.257	-0.746	0.142	17	0.138	
339	B	0.000	0.000	0.00	0.0	160.371	-0.633	0.142	14	0.136	
340	H,B	160.551	-0.126	0.14	43.7	160.601	-0.138	0.129	16	0.138	
341	H	160.607	-0.955	0.28	45.1	0.000	0.000	0.000	0	0.000	
342	H,B	160.814	0.846	0.14	57.4	160.761	0.905	0.124	21	0.126	A1078
343	B	0.000	0.000	0.00	0.0	160.819	0.579	0.124	21	0.100	
344	H,b	160.892	-0.126	0.29	49.7	160.883	-0.125	0.332	8	0.383	
345	H	160.953	-0.934	0.18	42.4	0.000	0.000	0.000	0	0.000	
346	B	0.000	0.000	0.00	0.0	160.966	1.062	0.114	28	0.116	A1080
347	B	0.000	0.000	0.00	0.0	161.200	-0.136	0.290	15	0.000	
348	H,b	161.514	-0.158	0.27	45.8	161.515	-0.161	0.233	6	0.000	
349	H,b	161.607	-1.045	0.22	40.6	161.612	-1.041	0.229	6	0.000	
350	H,b	162.136	1.139	0.21	50.6	162.134	1.140	0.216	6	0.247	

Table 2—Continued

BH #	Method	α(H) (2000)	δ(H) (2000)	z_{hmf}	Λ	α(B) (2000)	δ(B) (2000)	z_{bcg}	N_{gal}	z_{spec}	Comments
351	h,B	162.092	0.844	0.12	30.8	162.219	0.853	0.070	14	0.038	
352	h,B	162.471	1.171	0.05	29.8	162.440	1.130	0.111	15	0.098	
353	H	164.514	0.403	0.09	40.3	0.000	0.000	0.000	0	0.000	
354	H,b	164.515	0.665	0.29	46.5	164.472	0.663	0.338	6	0.000	
355	B	0.000	0.000	0.00	0.0	164.593	0.338	0.273	15	0.243	
356	H,b	165.060	-0.446	0.21	44.4	165.064	-0.444	0.240	9	0.247	
357	B	0.000	0.000	0.00	0.0	165.065	-0.647	0.253	15	0.253	
358	H,b	165.240	-0.774	0.29	51.4	165.250	-0.768	0.288	8	0.000	
359	B	0.000	0.000	0.00	0.0	165.597	-0.184	0.275	18	0.254	
360	H,b	165.667	-1.128	0.14	42.9	165.656	-1.112	0.157	9	0.155	A1148
361	H,b	165.722	-0.042	0.28	52.7	165.724	-0.097	0.323	7	0.000	
362	H,b	165.901	-0.137	0.27	40.5	165.947	-0.193	0.342	6	0.385	
363	B	0.000	0.000	0.00	0.0	165.930	0.484	0.268	15	0.273	
364	B	0.000	0.000	0.00	0.0	165.964	-0.350	0.266	14	0.000	
365	H,b	166.020	1.074	0.16	42.1	165.991	1.042	0.142	6	0.153	
366	H,B	166.065	-0.237	0.30	57.8	166.081	-0.214	0.275	13	0.000	
367	h,B	166.377	0.877	0.06	38.5	166.355	0.938	0.114	13	0.123	
368	B	0.000	0.000	0.00	0.0	166.611	-0.592	0.290	14	0.279	
369	H,b	166.865	-0.466	0.30	50.8	166.876	-0.463	0.288	12	0.270	
370	H,B	166.952	0.772	0.20	46.2	166.948	0.777	0.231	18	0.000	
371	H	166.964	1.027	0.23	49.4	0.000	0.000	0.000	0	0.000	
372	H,B	167.019	0.255	0.18	59.8	167.026	0.282	0.194	21	0.203	
373	B	0.000	0.000	0.00	0.0	167.048	0.823	0.194	14	0.200	
374	H,b	167.252	0.743	0.26	56.6	167.268	0.759	0.314	14	0.000	
375	H	167.253	-0.122	0.11	41.7	0.000	0.000	0.000	0	0.000	
376	H	167.419	0.760	0.22	42.8	0.000	0.000	0.000	0	0.000	
377	B	0.000	0.000	0.00	0.0	167.629	-0.479	0.231	16	0.241	
378	H,B	167.781	1.107	0.09	63.4	167.750	1.127	0.090	17	0.097	A1189
379	H,B	167.794	0.761	0.17	76.0	167.797	0.752	0.177	27	0.185	A1191
380	B	0.000	0.000	0.00	0.0	167.882	0.891	0.177	19	0.185	
381	B	0.000	0.000	0.00	0.0	167.895	-0.672	0.275	16	0.000	
382	B	0.000	0.000	0.00	0.0	167.975	-0.583	0.253	17	0.000	
383	H,b	168.115	0.640	0.14	40.7	168.125	0.641	0.190	10	0.194	
384	H,b	168.164	-0.941	0.29	54.2	168.147	-0.940	0.321	14	0.000	
385	h,B	168.400	-0.339	0.05	25.9	168.503	-0.336	0.092	23	0.103	
386	B	0.000	0.000	0.00	0.0	168.599	-0.550	0.251	15	0.280	
387	H	168.807	0.408	0.26	43.7	0.000	0.000	0.000	0	0.000	
388	H,b	169.201	-0.612	0.22	52.5	169.177	-0.574	0.188	8	0.186	
389	B	0.000	0.000	0.00	0.0	169.376	-0.596	0.290	19	0.276	
390	H,B	169.714	-0.797	0.29	51.8	169.718	-0.792	0.249	16	0.000	
391	h,B	170.137	-0.171	0.07	23.1	170.331	-0.221	0.087	18	0.101	
392	h,B	170.239	-0.374	0.11	37.2	170.363	-0.414	0.111	16	0.068	
393	B	0.000	0.000	0.00	0.0	170.429	0.992	0.094	15	0.102	

Table 2—Continued

BH #	Method	α(H) (2000)	δ(H) (2000)	z_{hmf}	Λ	α(B) (2000)	δ(B) (2000)	z_{bcg}	N_{gal}	z_{spec}	Comments
394	H,B	170.662	0.463	0.10	58.0	170.673	0.652	0.092	31	0.071	A1236
395	H,B	170.722	1.114	0.08	58.8	170.716	1.113	0.081	20	0.073	A1238
396	H,b	170.731	0.035	0.20	45.3	170.717	0.033	0.216	6	0.209	
397	B	0.000	0.000	0.00	0.0	170.826	-0.232	0.260	13	0.000	
398	B	0.000	0.000	0.00	0.0	171.019	0.917	0.096	14	0.100	
399	H	171.518	-0.473	0.25	42.6	0.000	0.000	0.000	0	0.000	
400	H,b	171.642	-0.337	0.23	56.3	171.655	-0.431	0.159	7	0.145	
401	H,b	171.816	-0.403	0.27	48.1	171.820	-0.404	0.310	17	0.333	
402	H	171.838	-0.857	0.29	42.5	0.000	0.000	0.000	0	0.000	
403	H,B	171.874	0.147	0.11	46.5	171.844	0.136	0.120	23	0.134	
404	H,b	172.001	-0.610	0.29	43.2	171.988	-0.615	0.336	8	0.000	
405	B	0.000	0.000	0.00	0.0	172.086	-0.540	0.295	13	0.000	
406	H,b	172.318	0.638	0.14	47.8	172.322	0.650	0.118	9	0.126	
407	B	0.000	0.000	0.00	0.0	172.320	-0.712	0.299	19	0.282	
408	H,b	172.560	0.429	0.24	40.3	172.520	0.416	0.277	8	0.000	
409	H,b	172.910	0.221	0.13	42.0	172.996	0.195	0.131	8	0.129	
410	H,b	173.637	-0.301	0.29	52.8	173.630	-0.311	0.341	18	0.341	
411	H,b	174.926	0.766	0.29	47.6	174.925	0.762	0.340	21	0.357	
412	B	0.000	0.000	0.00	0.0	175.554	0.633	0.290	16	0.306	
413	H,B	175.674	0.482	0.27	56.5	175.684	0.468	0.292	19	0.000	
414	B	0.000	0.000	0.00	0.0	175.755	-0.787	0.286	14	0.000	
415	H,b	175.946	0.353	0.29	64.2	175.947	0.337	0.238	10	0.000	
416	B	0.000	0.000	0.00	0.0	176.238	0.061	0.122	13	0.093	
417	B	0.000	0.000	0.00	0.0	176.252	-0.566	0.281	14	0.259	
418	H	176.273	-0.561	0.18	42.5	0.000	0.000	0.000	0	0.000	
419	H,b	176.316	-0.834	0.20	43.7	176.244	-0.823	0.135	7	0.156	
420	H,B	176.419	0.397	0.26	47.1	176.425	0.393	0.275	14	0.261	
421	H,b	176.545	-1.096	0.12	55.1	176.534	-1.121	0.146	12	0.119	A1376
422	B	0.000	0.000	0.00	0.0	176.996	1.077	0.247	15	0.233	
423	H,B	177.585	-0.594	0.11	55.0	177.578	-0.609	0.135	28	0.138	A1392
424	H,b	177.995	-0.409	0.19	45.1	177.988	-0.391	0.244	6	0.257	
425	B	0.000	0.000	0.00	0.0	178.084	-0.508	0.236	13	0.244	
426	H,B	178.570	-0.125	0.23	50.5	178.566	-0.127	0.271	19	0.000	
427	H,B	178.774	-0.580	0.14	50.9	178.807	-0.526	0.140	17	0.132	A1411
428	B	0.000	0.000	0.00	0.0	178.824	-0.332	0.216	14	0.244	
429	B	0.000	0.000	0.00	0.0	179.003	0.004	0.098	15	0.106	
430	B	0.000	0.000	0.00	0.0	179.012	-0.495	0.264	13	0.000	
431	B	0.000	0.000	0.00	0.0	179.041	-0.326	0.253	28	0.260	
432	H,B	179.065	-0.206	0.09	49.4	179.097	-0.364	0.109	16	0.106	A1419
433	H,b	179.306	-0.486	0.22	42.2	179.276	-0.463	0.236	12	0.000	
434	H,B	179.551	-1.047	0.11	47.5	179.671	-1.067	0.111	17	0.131	
435	B	0.000	0.000	0.00	0.0	179.603	-0.067	0.251	14	0.000	
436	h,B	179.432	0.021	0.11	33.8	179.603	-0.074	0.109	14	0.107	
437	B	0.000	0.000	0.00	0.0	179.804	0.516	0.194	16	0.174	

Table 2—Continued

BH #	Method	α(H) (2000)	δ(H) (2000)	z_{hmf}	Λ	α(B) (2000)	δ(B) (2000)	z_{bcg}	N_{gal}	z_{spec}	Comments
438	H,b	179.809	-0.053	0.22	41.3	179.781	-0.023	0.225	8	0.000	
439	H,b	179.971	1.114	0.17	42.3	179.957	1.079	0.192	12	0.200	
440	B	0.000	0.000	0.00	0.0	180.041	-0.597	0.166	16	0.169	
441	B	0.000	0.000	0.00	0.0	180.186	-0.156	0.168	27	0.166	
442	B	0.000	0.000	0.00	0.0	180.194	-0.021	0.186	14	0.165	
443	B	0.000	0.000	0.00	0.0	180.363	-0.447	0.148	18	0.169	
444	H	180.411	-0.489	0.23	70.0	0.000	0.000	0.000	0	0.000	
445	H,B	180.434	-0.186	0.21	71.4	180.420	-0.202	0.162	29	0.173	A1445
446	H,b	180.453	0.635	0.30	49.9	180.417	0.701	0.260	9	0.000	
447	H,b	180.596	0.772	0.23	47.9	180.627	0.713	0.229	10	0.000	
448	H	180.924	1.037	0.17	44.6	0.000	0.000	0.000	0	0.000	
449	H,b	180.984	0.484	0.20	42.7	180.986	0.481	0.207	10	0.210	
450	H	181.654	0.300	0.27	45.1	0.000	0.000	0.000	0	0.000	
451	H,b	181.664	1.201	0.27	43.9	181.664	1.215	0.268	10	0.253	
452	B	0.000	0.000	0.00	0.0	181.686	0.529	0.262	15	0.280	
453	H	181.848	1.141	0.14	41.1	0.000	0.000	0.000	0	0.000	
454	H,b	181.872	0.238	0.23	43.7	181.877	0.223	0.297	8	0.000	
455	H,B	182.468	-0.564	0.14	55.2	182.478	-0.558	0.181	24	0.181	
456	B	0.000	0.000	0.00	0.0	182.642	-0.412	0.186	16	0.181	
457	H,b	182.652	1.076	0.30	57.3	182.615	1.064	0.284	10	0.294	
458	H	182.695	1.205	0.29	46.0	0.000	0.000	0.000	0	0.000	
459	H,b	182.833	1.181	0.25	44.4	182.831	1.086	0.188	7	0.000	
460	B	0.000	0.000	0.00	0.0	183.371	-0.113	0.295	15	0.000	
461	H,B	183.430	-0.576	0.26	54.2	183.428	-0.634	0.260	16	0.000	
462	H,B	183.568	-0.442	0.21	49.8	183.564	-0.449	0.260	19	0.245	
463	h,B	183.520	-0.895	0.08	30.5	183.607	-0.948	0.085	14	0.082	
464	B	0.000	0.000	0.00	0.0	183.643	0.791	0.223	17	0.251	
465	H,b	183.928	1.167	0.29	51.0	183.922	1.127	0.212	7	0.000	
466	H,B	183.990	0.718	0.23	40.6	183.959	0.724	0.236	16	0.000	
467	H,B	184.107	-0.069	0.22	48.2	184.103	-0.080	0.299	24	0.276	
468	B	0.000	0.000	0.00	0.0	184.125	0.692	0.299	20	0.306	
469	H,b	184.138	-0.776	0.15	41.9	184.205	-0.742	0.081	12	0.071	
470	H,B	184.387	0.396	0.26	53.6	184.428	0.339	0.290	17	0.000	
471	H	184.415	-0.525	0.23	46.4	0.000	0.000	0.000	0	0.000	
472	H,B	184.486	-0.848	0.09	43.1	184.466	-0.905	0.138	19	0.000	
473	H,B	184.685	-1.037	0.14	53.3	184.707	-1.047	0.116	13	0.116	
474	H	184.755	-0.735	0.21	51.5	0.000	0.000	0.000	0	0.000	
475	H	184.924	1.045	0.28	43.9	0.000	0.000	0.000	0	0.000	
476	B	0.000	0.000	0.00	0.0	184.937	0.216	0.260	15	0.000	
477	H,b	185.081	-0.043	0.29	47.5	185.117	-0.059	0.312	8	0.000	
478	H,b	185.253	1.143	0.21	50.1	185.235	1.036	0.177	7	0.000	
479	H,B	185.387	0.222	0.16	67.6	185.430	0.329	0.157	25	0.159	
480	H,B	185.442	-0.409	0.25	51.2	185.443	-0.412	0.268	19	0.000	

Table 2—Continued

BH #	Method	α(H) (2000)	δ(H) (2000)	z_{hmf}	Λ	α(B) (2000)	δ(B) (2000)	z_{bcg}	N_{gal}	z_{spec}	Comments
481	H,B	185.497	-1.137	0.23	79.0	185.542	-1.196	0.225	22	0.259	A1525
482	H	185.668	-0.941	0.18	43.7	0.000	0.000	0.000	0	0.000	
483	B	0.000	0.000	0.00	0.0	185.797	0.515	0.297	13	0.000	
484	H,b	186.073	-0.509	0.22	46.6	186.072	-0.519	0.251	11	0.000	
485	H,B	186.100	-0.398	0.18	40.8	186.183	-0.346	0.159	19	0.158	
486	H,B	186.141	0.936	0.21	62.4	186.119	0.927	0.238	22	0.000	A1533
487	B	0.000	0.000	0.00	0.0	186.155	0.220	0.275	13	0.263	
488	B	0.000	0.000	0.00	0.0	186.191	-0.431	0.273	15	0.257	
489	H,b	186.299	-0.442	0.22	63.1	186.354	-0.554	0.155	8	0.155	
490	H,B	186.302	-0.013	0.23	40.2	186.248	-0.070	0.275	13	0.000	
491	H,B	186.359	0.704	0.22	60.3	186.364	0.710	0.240	18	0.236	
492	B	0.000	0.000	0.00	0.0	186.533	-0.604	0.168	17	0.157	
493	H,B	186.706	-0.645	0.17	42.0	186.687	-0.622	0.159	25	0.159	
494	H	186.830	1.135	0.21	41.2	0.000	0.000	0.000	0	0.000	
495	B	0.000	0.000	0.00	0.0	187.345	-0.012	0.295	13	0.303	
496	B	0.000	0.000	0.00	0.0	187.742	-1.198	0.292	13	0.000	
497	H,b	187.854	0.143	0.20	40.2	187.860	0.142	0.138	10	0.135	
498	H,B	188.078	-0.707	0.27	68.1	188.082	-0.710	0.196	17	0.192	
499	B	0.000	0.000	0.00	0.0	188.415	0.326	0.181	13	0.000	
500	H,b	188.571	0.660	0.23	50.6	188.598	0.573	0.199	8	0.205	
501	B	0.000	0.000	0.00	0.0	188.738	-0.794	0.255	14	0.248	
502	H	188.746	-0.815	0.17	53.8	0.000	0.000	0.000	0	0.000	
503	H	188.977	1.200	0.28	45.6	0.000	0.000	0.000	0	0.000	
504	H,b	189.259	-0.810	0.18	43.6	189.289	-0.814	0.216	12	0.234	
505	B	0.000	0.000	0.00	0.0	189.325	1.096	0.255	14	0.242	
506	H,b	189.432	-0.674	0.16	44.4	189.414	-0.623	0.140	9	0.138	
507	H,B	189.479	-0.280	0.14	64.2	189.481	-0.275	0.142	32	0.139	A1577
508	H,B	189.655	-0.860	0.17	42.9	189.653	-0.858	0.233	13	0.231	
509	H,b	189.773	0.597	0.26	40.4	189.708	0.619	0.323	10	0.344	
510	H,B	189.842	0.171	0.22	42.1	189.847	0.169	0.247	15	0.249	
511	H,b	189.943	-1.164	0.24	42.0	189.921	-1.226	0.170	6	0.188	
512	H,b	190.040	0.555	0.25	42.3	190.104	0.583	0.203	7	0.216	
513	H,b	190.185	1.186	0.25	41.3	190.243	1.117	0.207	7	0.000	
514	H,b	190.660	0.119	0.27	83.8	190.627	0.177	0.329	16	0.000	
515	H,B	190.682	-1.224	0.12	44.1	190.684	-1.232	0.153	23	0.172	
516	H,b	190.781	-0.757	0.13	44.6	190.790	-0.784	0.131	11	0.143	
517	h,B	190.896	-1.230	0.14	36.8	190.858	-1.177	0.157	31	0.168	
518	B	0.000	0.000	0.00	0.0	190.911	0.547	0.074	18	0.064	
519	B	0.000	0.000	0.00	0.0	191.082	0.747	0.081	20	0.082	
520	h,B	191.195	-1.016	0.11	39.2	191.192	-1.020	0.157	19	0.147	
521	B	0.000	0.000	0.00	0.0	191.573	-0.283	0.133	14	0.127	
522	B	0.000	0.000	0.00	0.0	191.643	-0.228	0.249	14	0.242	
523	H,B	191.720	0.306	0.05	43.1	191.713	0.297	0.096	32	0.089	
524	B	0.000	0.000	0.00	0.0	191.927	-0.137	0.111	24	0.091	

Table 2—Continued

BH #	Method	α(H) (2000)	δ(H) (2000)	z_{hmf}	Λ	α(B) (2000)	δ(B) (2000)	z_{bcg}	N_{gal}	z_{spec}	Comments
525	h,B	191.996	-0.349	0.06	24.2	192.071	-0.261	0.087	19	0.089	
526	H,B	192.391	-0.763	0.17	41.0	192.390	-0.765	0.201	14	0.194	
527	H,b	193.413	0.067	0.29	46.7	193.450	0.101	0.358	9	0.000	
528	H	194.003	0.466	0.27	44.1	0.000	0.000	0.000	0	0.000	
529	H	194.113	-0.209	0.29	44.2	0.000	0.000	0.000	0	0.000	
530	H,B	195.172	1.052	0.09	46.3	195.169	1.069	0.090	19	0.082	
531	H	195.582	0.233	0.20	43.9	0.000	0.000	0.000	0	0.000	
532	H,b	195.818	-0.757	0.23	55.1	195.900	-0.821	0.186	10	0.208	
533	H,b	195.974	0.074	0.25	45.3	195.956	0.138	0.292	8	0.000	
534	H	196.455	-0.589	0.29	49.0	0.000	0.000	0.000	0	0.000	
535	B	0.000	0.000	0.00	0.0	196.591	-0.828	0.186	13	0.190	
536	H	196.780	1.204	0.25	50.4	0.000	0.000	0.000	0	0.000	
537	H,b	196.963	1.185	0.29	47.7	196.977	1.155	0.251	6	0.000	
538	B	0.000	0.000	0.00	0.0	197.659	-0.657	0.087	14	0.086	
539	H	197.826	-1.234	0.20	49.3	0.000	0.000	0.000	0	0.000	
540	H,b	197.830	0.070	0.16	42.1	197.770	-0.046	0.094	8	0.096	
541	B	0.000	0.000	0.00	0.0	197.903	-0.483	0.096	13	0.090	
542	H,B	198.049	-0.988	0.09	54.0	198.057	-0.975	0.090	30	0.083	A1692
543	H,b	198.223	1.016	0.07	46.1	198.228	1.036	0.063	8	0.072	
544	h,B	198.403	0.563	0.31	60.3	198.395	0.567	0.251	14	0.000	
545	B	0.000	0.000	0.00	0.0	198.576	0.363	0.251	13	0.264	
546	B	0.000	0.000	0.00	0.0	198.638	-0.466	0.271	14	0.273	
547	H,b	198.676	0.051	0.20	41.8	198.658	0.156	0.268	7	0.000	
548	H,b	198.706	1.046	0.29	44.0	198.698	1.034	0.321	8	0.000	
549	H	198.709	1.177	0.26	40.1	0.000	0.000	0.000	0	0.000	
550	B	0.000	0.000	0.00	0.0	198.777	-0.677	0.279	13	0.292	
551	h,B	198.897	1.100	0.11	29.3	198.848	0.959	0.148	14	0.142	
552	B	0.000	0.000	0.00	0.0	198.887	-0.645	0.277	16	0.000	
553	B	0.000	0.000	0.00	0.0	198.916	-1.075	0.275	14	0.000	
554	H,b	199.049	-0.930	0.10	48.5	199.057	-0.913	0.090	7	0.111	
555	B	0.000	0.000	0.00	0.0	199.078	-0.948	0.249	19	0.000	
556	H,b	199.106	0.863	0.08	41.0	199.136	0.870	0.090	11	0.080	
557	B	0.000	0.000	0.00	0.0	199.130	-1.087	0.275	19	0.274	
558	B	0.000	0.000	0.00	0.0	199.298	-0.923	0.279	14	0.290	
559	H,b	199.475	1.085	0.14	41.3	199.510	1.114	0.077	9	0.110	
560	B	0.000	0.000	0.00	0.0	199.528	-1.179	0.203	16	0.000	
561	h,B	199.661	-0.810	0.07	38.6	199.557	-0.626	0.094	18	0.110	
562	H,b	199.702	0.692	0.16	46.2	199.697	0.680	0.209	11	0.220	
563	H,B	199.813	-0.932	0.06	59.3	199.820	-0.995	0.068	27	0.082	
564	H,b	200.031	-0.264	0.23	42.8	200.046	-0.269	0.303	14	0.284	
565	B	0.000	0.000	0.00	0.0	200.094	-0.402	0.220	14	0.000	
566	B	0.000	0.000	0.00	0.0	200.218	-0.516	0.209	14	0.000	
567	h,B	200.152	1.237	0.09	30.8	200.224	1.220	0.142	13	0.148	
568	B	0.000	0.000	0.00	0.0	200.329	-1.150	0.236	15	0.224	

Table 2—Continued

BH #	Method	α(H) (2000)	δ(H) (2000)	z_{hmf}	Λ	α(B) (2000)	δ(B) (2000)	z_{bcg}	N_{gal}	z_{spec}	Comments
569	B	0.000	0.000	0.00	0.0	200.356	-0.693	0.109	17	0.108	
570	H,B	200.374	-1.031	0.13	40.2	200.228	-0.941	0.063	14	0.048	
571	H,B	200.936	1.052	0.09	45.5	200.952	1.113	0.109	23	0.105	
572	B	0.000	0.000	0.00	0.0	201.068	0.808	0.092	13	0.108	
573	B	0.000	0.000	0.00	0.0	201.128	1.018	0.286	13	0.000	
574	H	201.131	-1.195	0.29	45.5	0.000	0.000	0.000	0	0.000	
575	B	0.000	0.000	0.00	0.0	201.478	-0.306	0.181	13	0.189	
576	H,B	201.515	-0.427	0.18	53.1	201.517	-0.442	0.183	21	0.181	
577	H	201.569	0.229	0.13	44.1	0.000	0.000	0.000	0	0.000	RXC 1326.2
578	B	0.000	0.000	0.00	0.0	201.602	0.036	0.098	13	0.083	(RXC 1326.2)
579	B	0.000	0.000	0.00	0.0	201.899	-0.945	0.183	23	0.184	
580	B	0.000	0.000	0.00	0.0	202.046	-1.005	0.214	15	0.200	
581	B	0.000	0.000	0.00	0.0	202.084	0.438	0.244	15	0.260	
582	H,b	202.086	0.436	0.13	43.0	202.093	0.472	0.148	6	0.000	
583	H,b	202.605	0.735	0.21	51.6	202.613	0.748	0.192	10	0.217	
584	H	202.691	1.197	0.16	48.3	0.000	0.000	0.000	0	0.000	
585	h,B	202.801	1.005	0.32	79.7	202.796	1.083	0.299	15	0.000	
586	H	202.833	-1.168	0.29	45.2	0.000	0.000	0.000	0	0.000	
587	H	203.115	1.153	0.09	40.9	0.000	0.000	0.000	0	0.000	
588	H,B	203.505	1.196	0.26	59.8	203.511	1.216	0.233	15	0.248	
589	H,b	203.536	0.798	0.26	47.5	203.483	0.728	0.253	9	0.000	
590	H,b	203.573	-0.951	0.15	45.7	203.682	-0.898	0.083	10	0.000	
591	B	0.000	0.000	0.00	0.0	203.577	-0.957	0.262	17	0.270	
592	B	0.000	0.000	0.00	0.0	203.596	-0.216	0.271	21	0.267	
593	h,B	203.601	-0.299	0.34	59.8	203.596	-0.310	0.292	20	0.245	
594	H	203.605	0.994	0.29	62.1	0.000	0.000	0.000	0	0.000	
595	H,b	203.640	0.352	0.27	46.5	203.659	0.303	0.332	10	0.000	
596	H,b	204.201	-0.215	0.25	41.6	204.217	-0.144	0.251	6	0.000	
597	H,b	204.390	0.796	0.29	43.0	204.393	0.769	0.255	9	0.000	
598	B	0.000	0.000	0.00	0.0	204.515	-0.317	0.236	14	0.233	
599	H,b	204.591	0.035	0.26	47.1	204.630	-0.042	0.251	12	0.249	
600	H,B	204.602	0.252	0.28	47.6	204.578	0.301	0.227	13	0.000	
601	H,B	204.887	-0.283	0.14	56.8	204.859	-0.267	0.140	17	0.146	
602	H,b	205.064	0.032	0.14	46.9	205.074	0.032	0.144	12	0.145	
603	B	0.000	0.000	0.00	0.0	205.122	-0.212	0.268	15	0.000	
604	H	205.137	-0.616	0.20	55.5	0.000	0.000	0.000	0	0.000	
605	B	0.000	0.000	0.00	0.0	205.155	-0.633	0.297	19	0.285	
606	H,B	205.350	-1.013	0.23	42.5	205.356	-1.042	0.286	14	0.287	
607	H	205.853	-0.190	0.20	40.2	0.000	0.000	0.000	0	0.000	
608	H,B	205.949	0.973	0.17	52.4	205.943	0.979	0.233	13	0.229	
609	H,b	205.958	0.757	0.16	41.7	205.984	0.722	0.231	6	0.000	
610	B	0.000	0.000	0.00	0.0	206.154	-0.120	0.290	14	0.000	
611	H,B	206.291	0.123	0.05	40.7	206.377	0.343	0.096	13	0.089	

Table 2—Continued

BH #	Method	α(H) (2000)	δ(H) (2000)	z_{hmf}	Λ	α(B) (2000)	δ(B) (2000)	z_{bcg}	N_{gal}	z_{spec}	Comments
612	h,B	206.410	-0.160	0.08	30.9	206.315	-0.142	0.083	15	0.087	
613	B	0.000	0.000	0.00	0.0	206.345	0.206	0.271	20	0.256	
614	B	0.000	0.000	0.00	0.0	206.451	0.226	0.271	22	0.276	
615	H,b	206.633	0.129	0.27	55.5	206.639	0.117	0.249	7	0.000	
616	H	207.483	0.625	0.18	45.6	0.000	0.000	0.000	0	0.000	
617	B	0.000	0.000	0.00	0.0	207.640	-0.412	0.299	14	0.360	
618	H	207.780	-0.515	0.28	47.1	0.000	0.000	0.000	0	0.000	
619	H	207.901	0.110	0.30	44.1	0.000	0.000	0.000	0	0.000	
620	H	208.005	0.435	0.26	48.5	0.000	0.000	0.000	0	0.000	
621	h,B	208.169	-1.050	0.12	35.9	208.193	-1.027	0.129	13	0.151	
622	h,B	208.178	0.134	0.11	30.7	208.359	0.047	0.107	15	0.116	
623	H,b	208.414	0.965	0.24	41.8	208.415	0.969	0.303	9	0.000	
624	B	0.000	0.000	0.00	0.0	208.508	0.242	0.229	14	0.251	
625	H,B	208.591	-1.025	0.14	58.8	208.600	-1.044	0.146	21	0.146	
626	H,b	209.250	-0.904	0.21	42.6	209.245	-0.894	0.172	11	0.196	
627	B	0.000	0.000	0.00	0.0	209.426	1.003	0.162	13	0.168	
628	H,b	209.975	-1.127	0.24	42.0	209.971	-1.192	0.297	6	0.000	
629	B	0.000	0.000	0.00	0.0	210.024	0.361	0.164	14	0.167	
630	H,B	210.058	0.245	0.15	42.5	210.064	0.230	0.181	14	0.188	
631	B	0.000	0.000	0.00	0.0	210.065	0.280	0.244	13	0.253	
632	B	0.000	0.000	0.00	0.0	210.091	-0.149	0.170	13	0.190	
633	H	210.168	-1.023	0.28	45.0	0.000	0.000	0.000	0	0.000	
634	H,b	210.184	-0.515	0.18	47.1	210.128	-0.464	0.177	12	0.132	
635	H,b	210.382	0.056	0.19	49.3	210.380	0.058	0.168	12	0.188	
636	H,B	210.719	1.231	0.23	47.0	210.775	1.216	0.253	16	0.255	
637	H,b	210.769	-0.237	0.29	60.0	210.772	-0.192	0.297	6	0.000	
638	H,B	210.789	0.415	0.20	43.0	210.787	0.413	0.181	16	0.182	
639	H,B	210.829	0.096	0.15	51.0	210.873	0.112	0.162	19	0.189	
640	H,B	210.964	-0.519	0.19	42.6	210.915	-0.446	0.177	13	0.000	
641	H,b	211.284	-0.149	0.25	53.6	211.310	-0.129	0.247	12	0.000	
642	B	0.000	0.000	0.00	0.0	211.774	0.258	0.277	13	0.258	
643	B	0.000	0.000	0.00	0.0	212.733	0.613	0.155	23	0.178	
644	B	0.000	0.000	0.00	0.0	212.946	0.406	0.251	13	0.262	
645	H,B	213.086	0.060	0.12	52.5	213.091	0.077	0.105	15	0.127	
646	B	0.000	0.000	0.00	0.0	213.099	0.640	0.205	19	0.262	
647	B	0.000	0.000	0.00	0.0	213.191	0.783	0.227	15	0.000	
648	H	213.265	0.356	0.30	44.8	0.000	0.000	0.000	0	0.000	
649	H,b	213.460	0.855	0.29	45.1	213.452	0.805	0.273	9	0.000	
650	H,B	213.616	-0.376	0.10	87.2	213.740	-0.350	0.144	66	0.139	A1882
651	h,B	213.815	0.184	0.07	26.9	213.736	0.206	0.129	18	0.127	
652	H,b	213.778	1.015	0.27	45.2	213.837	0.994	0.260	7	0.000	
653	H,b	213.906	1.022	0.26	42.0	213.837	0.994	0.260	7	0.000	
654	B	0.000	0.000	0.00	0.0	213.944	-0.992	0.122	14	0.149	
655	H,B	213.963	0.256	0.13	49.4	213.954	0.260	0.129	15	0.126	RXC 1415.8

Table 2—Continued

BH #	Method	α(H) (2000)	δ(H) (2000)	z_{hmf}	Λ	α(B) (2000)	δ(B) (2000)	z_{bcg}	N_{gal}	z_{spec}	Comments
656	h,B	214.025	-0.723	0.05	20.3	214.022	-0.586	0.114	20	0.000	
657	H,b	214.096	0.765	0.23	41.7	214.082	0.812	0.301	7	0.000	
658	H,b	214.197	0.602	0.26	42.1	214.196	0.607	0.292	11	0.000	
659	H,b	214.391	-0.495	0.11	40.7	214.477	-0.521	0.116	10	0.148	
660	H,b	214.620	0.791	0.28	47.1	214.618	0.785	0.341	27	0.343	
661	H,b	214.914	-0.450	0.10	41.8	214.796	-0.469	0.120	11	0.134	
662	H,b	215.017	0.997	0.16	51.7	215.036	0.990	0.157	9	0.171	
663	H,B	215.111	-0.103	0.20	50.3	215.117	-0.109	0.262	13	0.000	
664	B	0.000	0.000	0.00	0.0	215.257	0.196	0.275	17	0.278	
665	B	0.000	0.000	0.00	0.0	215.310	-0.035	0.238	14	0.000	
666	H,b	215.403	-0.346	0.06	44.6	215.423	-0.338	0.068	7	0.052	
667	H,b	215.410	0.848	0.14	52.2	215.417	0.780	0.142	11	0.146	
668	B	0.000	0.000	0.00	0.0	215.831	-0.539	0.299	20	0.278	
669	H,b	216.038	0.517	0.19	49.7	216.014	0.499	0.133	6	0.125	
670	H	216.078	-0.211	0.15	45.1	0.000	0.000	0.000	0	0.000	
671	H,b	216.103	-0.682	0.16	41.0	216.111	-0.685	0.201	6	0.176	
672	H,b	216.241	1.155	0.23	57.3	216.243	1.154	0.238	6	0.304	
673	H,b	216.318	-1.050	0.09	41.0	216.281	-1.128	0.127	6	0.134	
674	H,B	216.376	0.340	0.11	45.8	216.365	0.338	0.140	15	0.134	
675	H,b	216.624	0.839	0.11	51.6	216.568	0.838	0.138	12	0.125	
676	B	0.000	0.000	0.00	0.0	216.639	-0.109	0.271	15	0.000	
677	B	0.000	0.000	0.00	0.0	216.643	1.103	0.288	15	0.281	
678	B	0.000	0.000	0.00	0.0	216.841	0.946	0.299	20	0.291	
679	B	0.000	0.000	0.00	0.0	216.843	-0.202	0.284	15	0.000	
680	H,B	216.849	-0.200	0.19	60.6	216.754	-0.175	0.242	13	0.000	
681	H,b	216.976	0.479	0.23	44.3	216.979	0.453	0.203	6	0.000	
682	H	216.980	-1.234	0.17	42.1	0.000	0.000	0.000	0	0.000	
683	H,b	217.073	0.730	0.23	44.7	217.190	0.708	0.159	8	0.103	
684	H,b	217.210	-0.357	0.26	51.7	217.203	-0.406	0.312	15	0.279	
685	h,B	217.669	0.245	0.05	36.2	217.419	0.366	0.061	18	0.056	
686	B	0.000	0.000	0.00	0.0	217.644	1.069	0.131	14	0.132	
687	H,b	217.688	0.802	0.18	63.9	217.673	0.825	0.188	7	0.205	
688	B	0.000	0.000	0.00	0.0	217.745	0.405	0.133	15	0.131	
689	H	217.956	-0.289	0.27	48.0	0.000	0.000	0.000	0	0.000	
690	B	0.000	0.000	0.00	0.0	218.347	-0.794	0.214	14	0.229	
691	B	0.000	0.000	0.00	0.0	218.439	-0.632	0.227	17	0.000	
692	H,b	218.597	-0.615	0.20	54.2	218.629	-0.572	0.205	10	0.221	
693	H,B	218.789	-0.293	0.20	42.5	218.797	-0.293	0.216	14	0.221	
694	B	0.000	0.000	0.00	0.0	218.895	-0.709	0.251	14	0.257	
695	H,B	219.055	-0.251	0.18	66.2	219.057	-0.269	0.207	16	0.219	
696	H,b	219.168	1.164	0.30	46.2	219.134	1.125	0.329	7	0.000	
697	B	0.000	0.000	0.00	0.0	219.212	-0.700	0.218	16	0.215	
698	H,b	219.241	-1.072	0.10	43.3	219.084	-1.130	0.090	8	0.106	
699	H,B	219.396	-0.333	0.13	58.9	219.371	-0.267	0.144	26	0.135	A1938

Table 2—Continued

BH #	Method	α(H) (2000)	δ(H) (2000)	z_{hmf}	Λ	α(B) (2000)	δ(B) (2000)	z_{bcg}	N_{gal}	z_{spec}	Comments
700	B	0.000	0.000	0.00	0.0	219.489	-0.708	0.271	13	0.000	
701	B	0.000	0.000	0.00	0.0	219.566	1.013	0.227	13	0.260	
702	B	0.000	0.000	0.00	0.0	219.662	-0.595	0.266	13	0.000	
703	B	0.000	0.000	0.00	0.0	219.762	-0.188	0.177	13	0.181	
704	B	0.000	0.000	0.00	0.0	219.775	-0.581	0.281	17	0.298	
705	H,b	219.888	0.539	0.12	46.3	219.917	0.498	0.146	8	0.138	
706	H,b	219.947	-0.130	0.22	42.9	220.030	-0.104	0.225	7	0.000	
707	H,b	220.040	0.717	0.21	42.3	220.046	0.724	0.249	7	0.259	
708	H,b	220.324	-0.984	0.17	40.5	220.324	-0.988	0.148	10	0.184	
709	h,B	220.542	-0.748	0.11	37.0	220.436	-0.827	0.148	20	0.143	
710	H,b	220.440	0.559	0.27	48.1	220.476	0.600	0.340	13	0.321	
711	h,B	220.826	-0.667	0.14	39.6	220.862	-0.721	0.144	14	0.150	
712	H	220.866	-0.330	0.19	45.9	0.000	0.000	0.000	0	0.000	
713	B	0.000	0.000	0.00	0.0	220.897	-0.352	0.275	16	0.291	
714	H	220.989	-1.141	0.22	40.6	0.000	0.000	0.000	0	0.000	
715	h,B	220.962	-0.954	0.19	37.3	221.009	-0.947	0.133	15	0.149	
716	B	0.000	0.000	0.00	0.0	221.038	0.178	0.299	33	0.296	
717	B	0.000	0.000	0.00	0.0	221.227	0.142	0.277	25	0.000	
718	H	221.236	-1.173	0.23	46.8	0.000	0.000	0.000	0	0.000	
719	H,B	221.328	0.115	0.29	70.3	221.334	0.115	0.297	22	0.294	
720	H,B	221.632	0.739	0.20	40.2	221.750	0.752	0.162	15	0.171	
721	H,b	221.649	-1.023	0.26	52.2	221.651	-1.015	0.183	10	0.000	
722	H,B	221.856	-1.210	0.19	47.4	221.848	-1.196	0.138	13	0.145	
723	B	0.000	0.000	0.00	0.0	222.918	-0.779	0.297	14	0.000	
724	B	0.000	0.000	0.00	0.0	223.554	-0.237	0.238	16	0.000	
725	H,b	224.130	0.424	0.29	48.3	224.130	0.431	0.295	7	0.000	
726	H,B	224.282	0.119	0.21	48.0	224.283	0.121	0.251	18	0.000	
727	H,B	224.889	-0.019	0.29	52.1	224.896	-0.006	0.255	13	0.000	
728	B	0.000	0.000	0.00	0.0	225.001	-0.025	0.244	13	0.000	
729	H	225.070	-1.225	0.26	41.9	0.000	0.000	0.000	0	0.000	
730	H,B	225.983	-0.129	0.22	43.1	225.984	-0.128	0.231	20	0.000	
731	B	0.000	0.000	0.00	0.0	226.090	-0.090	0.231	18	0.000	
732	H,B	226.419	0.657	0.19	41.8	226.361	0.617	0.229	19	0.225	
733	H,b	226.594	0.464	0.22	40.1	226.580	0.468	0.218	9	0.218	
734	H,b	226.726	0.589	0.27	43.0	226.724	0.583	0.279	8	0.000	
735	B	0.000	0.000	0.00	0.0	226.729	-0.136	0.207	16	0.234	
736	B	0.000	0.000	0.00	0.0	226.740	0.114	0.220	15	0.000	
737	h,B	226.765	1.120	0.16	36.8	226.761	1.114	0.203	15	0.185	
738	B	0.000	0.000	0.00	0.0	226.783	-0.280	0.223	16	0.237	
739	H,B	226.901	0.035	0.19	74.0	226.906	0.040	0.249	34	0.232	
740	H,B	227.114	-0.266	0.08	54.0	227.107	-0.266	0.077	16	0.090	A2026
741	B	0.000	0.000	0.00	0.0	227.216	0.686	0.236	16	0.233	
742	H,B	227.217	0.021	0.22	58.4	227.207	0.037	0.244	21	0.000	

Table 2—Continued

BH #	Method	α(H) (2000)	δ(H) (2000)	z_{hmf}	Λ	α(B) (2000)	δ(B) (2000)	z_{bcg}	N_{gal}	z_{spec}	Comments
743	H,B	227.259	0.385	0.22	71.0	227.250	0.391	0.238	28	0.247	
744	H,b	227.279	-1.202	0.28	67.4	227.275	-1.207	0.348	19	0.342	
745	B	0.000	0.000	0.00	0.0	227.290	1.141	0.247	21	0.000	
746	B	0.000	0.000	0.00	0.0	227.330	-0.239	0.275	20	0.000	
747	B	0.000	0.000	0.00	0.0	227.367	0.899	0.268	17	0.000	
748	B	0.000	0.000	0.00	0.0	227.388	-0.333	0.212	16	0.000	
749	B	0.000	0.000	0.00	0.0	227.421	1.154	0.273	15	0.000	
750	B	0.000	0.000	0.00	0.0	227.596	-0.760	0.284	13	0.000	
751	B	0.000	0.000	0.00	0.0	227.613	0.021	0.236	13	0.000	
752	B	0.000	0.000	0.00	0.0	227.619	1.029	0.292	17	0.000	
753	H,B	227.822	-0.111	0.08	65.5	227.821	-0.130	0.101	42	0.092	A2030
754	B	0.000	0.000	0.00	0.0	227.846	0.983	0.286	14	0.287	
755	B	0.000	0.000	0.00	0.0	227.870	0.472	0.288	13	0.302	
756	B	0.000	0.000	0.00	0.0	227.898	0.098	0.218	19	0.217	
757	H,b	227.977	0.621	0.16	47.0	227.971	0.620	0.120	12	0.123	
758	H	227.980	-1.247	0.25	58.5	0.000	0.000	0.000	0	0.000	
759	B	0.000	0.000	0.00	0.0	228.073	0.723	0.216	14	0.219	
760	H,B	228.102	-0.953	0.22	59.4	228.003	-0.948	0.207	21	0.212	
761	H,b	228.109	0.159	0.23	45.8	228.132	0.122	0.214	7	0.215	
762	B	0.000	0.000	0.00	0.0	228.118	-0.073	0.194	14	0.215	
763	B	0.000	0.000	0.00	0.0	228.126	-0.251	0.203	13	0.215	
764	H,B	228.196	0.936	0.25	64.0	228.204	0.938	0.223	19	0.218	
765	B	0.000	0.000	0.00	0.0	228.206	0.814	0.129	14	0.000	
766	H,b	228.232	-0.673	0.27	46.3	228.281	-0.674	0.314	8	0.000	
767	B	0.000	0.000	0.00	0.0	228.306	1.156	0.238	13	0.000	
768	H,B	228.324	0.273	0.20	50.1	228.247	0.228	0.218	17	0.223	
769	B	0.000	0.000	0.00	0.0	228.381	1.073	0.251	13	0.218	
770	H,b	228.397	-0.442	0.25	49.9	228.398	-0.458	0.277	11	0.251	
771	H,b	228.421	-0.201	0.29	42.8	228.391	-0.226	0.312	9	0.000	
772	h,B	228.195	0.381	0.05	23.0	228.457	0.359	0.090	14	0.092	
773	h,B	228.588	1.179	0.11	36.0	228.597	1.192	0.148	15	0.125	
774	H,b	228.677	0.271	0.11	40.8	228.669	0.271	0.122	12	0.138	
775	B	0.000	0.000	0.00	0.0	229.053	-0.801	0.122	28	0.118	
776	H,B	229.082	0.111	0.13	79.5	229.083	0.060	0.120	39	0.117	A2050
777	H	229.137	-0.381	0.14	41.8	0.000	0.000	0.000	0	0.000	
778	B	0.000	0.000	0.00	0.0	229.242	-1.111	0.116	22	0.117	
779	h,B	229.497	0.227	0.05	19.2	229.290	0.129	0.114	20	0.119	
780	H,B	229.326	-0.708	0.11	73.2	229.351	-0.738	0.120	44	0.116	A2053
781	H,b	229.537	1.099	0.25	41.5	229.589	1.065	0.247	6	0.000	
782	H	229.736	-0.331	0.27	50.1	0.000	0.000	0.000	0	0.000	
783	H,b	229.811	-0.086	0.24	49.7	229.816	-0.066	0.212	6	0.205	
784	H,b	230.476	-0.396	0.26	46.3	230.466	-0.389	0.240	10	0.000	
785	H	230.556	1.024	0.21	43.7	0.000	0.000	0.000	0	0.000	
786	H,b	230.611	-0.733	0.30	47.7	230.589	-0.661	0.288	9	0.000	

Table 2—Continued

BH #	Method	α(H) (2000)	δ(H) (2000)	z_{hmf}	Λ	α(B) (2000)	δ(B) (2000)	z_{bcg}	N_{gal}	z_{spec}	Comments
787	H,B	230.991	1.035	0.14	77.3	230.979	1.064	0.138	16	0.077	A2066
788	H,B	231.280	1.168	0.26	59.3	231.282	1.160	0.277	13	0.279	
789	H,b	231.694	0.814	0.12	44.3	231.675	0.891	0.135	10	0.116	
790	H,b	231.885	-0.856	0.13	41.1	231.853	-0.704	0.129	10	0.000	
791	H,B	232.308	-0.250	0.06	48.9	232.303	-0.252	0.087	16	0.089	
792	H	232.329	0.927	0.27	52.0	0.000	0.000	0.000	0	0.000	
793	H,b	232.641	-0.803	0.06	41.7	232.639	-0.809	0.070	10	0.077	
794	B	0.000	0.000	0.00	0.0	232.764	-0.201	0.288	15	0.000	
795	H,B	233.274	-0.766	0.13	82.6	233.265	-0.771	0.148	53	0.149	
796	H,B	233.367	-0.378	0.20	49.2	233.359	-0.386	0.257	16	0.261	
797	h,B	234.891	0.590	0.05	34.1	234.877	0.853	0.109	14	0.085	
798	H	235.196	0.924	0.09	40.2	0.000	0.000	0.000	0	0.000	
799	H	235.544	1.180	0.26	47.0	0.000	0.000	0.000	0	0.000	

*Comments:

1. z_{est} = 0.05-0.3; 379 deg^2; α(2000) = 355° to 56° and 145.3° to 236.0°, δ(2000) = -1.25° to 1.25°.

2. All HMF clusters with $\Lambda \geq$ 40, maxBCG clusters with $N_{gal} \geq$ 13, and their matches are included (see #4 below).

3. Some detections are false-positives, i.e., non-real clusters (§5); all are included in order to avoid unquantitative visual selection.

4. Cluster matches are algorithmically defined as B and H clusters separated by $\leq 1h^{-1}$ Mpc (projected) and $\Delta z_{est} \leq$ 0.08 (3-σ). All matching clusters with $N_{gal} \geq$ 6 and $\Lambda \geq$ 20 are included.

5. The same cluster is sometimes listed as two separate H and B clusters (i.e., 'un-matched') if the separation is $\Delta z_{est} > 0.08$ or $> 1h^{-1}$ Mpc (due to uncertainties in z_{est} and the different definitions of cluster 'center'). (If one of the 'un-matched' clusters is below the catalog richness or redshift cuts, it will not be listed in the catalog.)

6. Occasionally, a single H or B cluster may be split by the detection algorithm into two separate clusters; this may represent sub-structure in larger systems.

7. HMF clusters are typically centered on a mean high overdensity region of galaxies; maxBCG clusters center on a galaxy with a color and magnitude estimated as likely to be a BCG. Some B clusters thus center on a bright galaxy or small group of red galaxies in the outskirts of clusters. (This can cause splitting of a cluster match into two or more separate listings; #5). This may also represent sub-structure in or near clusters.

8. Some systems may represent parts of extended large-scale structure rather than condensed virialized clusters.

9. The catalog is not volume limited. Selection functions as a function of redshift and richness are provided in §5.

Table 3. Cluster Catalog Statistics

Λ	N_{cl}(HMF)* (z=0.05-0.3)	N_{gal}	N_{cl}(maxBCG)* (z=0.05-0.3)
40-50	297	13-20	402
50-60	97	20-30	103
60-70	25	30-40	15
$\geq$70	17	$\geq$40	4
Total($\Lambda\geq$40)	436	Total($N_{gal}\geq$13)	524

z_{hmf}	N_{cl}(HMF)* ($\Lambda\geq$40)	z_{bcg}	N_{cl}(maxBCG)* ($N_{gal}\geq$13)
0.05-0.1	45	0.05-0.1	52
0.1-0.2	150	0.1-0.2	173
0.2-0.3	241	0.2-0.3	299
Total(z=0.05-0.3)	436	Total(z=0.05-0.3)	524

*N_{cl} is the number of clusters observed, uncorrected for selection function and false-positive detections. Survey area = 379 deg^2.

Table 4. Comparison to NORAS X-ray clusters

NORAS cluster	$\alpha(2000)$	$\delta(2000)$	z	L_x^{44}	z_{bcg}	N_{gal}	z_{hmf}	Λ
RXC J0020.1+0005	5.044	0.092	0.212	1.08	0.220	33	—	—
RXC J0106.8+0103	16.709	1.055	0.253	8.65	0.286	25	0.22	50.9
RXC J0114.9+0024	18.740	0.406	0.044	0.92	0.068	12	0.05	42.6
RXC J0121.9+0021	20.493	0.358	0.175	1.85	0.166	32	0.16	46.7
RXC J0152.7+0100	28.182	1.016	0.227	9.37	0.264	29	0.23	73.4
RXC J1326.2+0013	201.573	0.225	0.082	1.65	0.098	13	0.13	44.1
RXC J1415.8+0015	213.965	0.259	0.125	0.83	0.129	15	0.13	49.4
RXC J2341.1+0018	355.276	0.315	0.110	1.03	0.140	8	0.09	45.1